UNCLASSIFIED

AD NUMBER
ADB115252
LIMITATION CHANGES

TO:

Approved for public release; distribution is unlimited.

FROM:

Distribution authorized to U.S. Gov't. agencies and their contractors; Critical Technology; SEP 1987. Other requests shall be referred to Air Force Wright Aeronautical Laboratories, Wright-Patterson AFB, OH 45433-6533. This document contains export-controlled technical data.

AUTHORITY
AFSC/DOCS(Arnold AFB) ltr dtd 2 July 1991

THIS PAGE IS UNCLASSIFIED

Surface Effects of Satellite Outgassing Products

B. E. Wood, W. T. Bertrand,
R. J. Bryson and B. L. Seiber
Calspan Corporation
and
Lt. Patrick M. Falco and Capt. Ray A. Cull
Air Force Wright Aeronautical Laboratories
Wright-Patterson AFB, Ohio 45433

September 1987

Final Report for Period October 1, 1984 − October 31, 1986

ARNOLD ENGINEERING DEVELOPMENT CENTER
ARNOLD AIR FORCE BASE, TENNESSEE
AIR FORCE SYSTEMS COMMAND
UNITED STATES AIR FORCE

NOTICES

DESTRUCTION NOTICE

APPROVAL STATEMENT

This report has been reviewed and approved.

JULIUS D. HOLT, Capt, USAF
Facility Technology Division
Directorate of Technology
Deputy for Operations

Approved for publication:

FOR THE COMMANDER

MARION L. LASTER
Director of Technology
Deputy for Operations

REPORT DOCUMENTATION PAGE

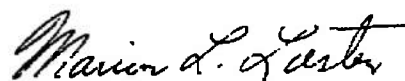| 1a. REPORT SECURITY CLASSIFICATION UNCLASSIFIED		1b. RESTRICTIVE MARKINGS			
2a. SECURITY CLASSIFICATION AUTHORITY		3 DISTRIBUTION/AVAILABILITY OF REPORT Approved for public release; distribution unlimited. SEE REVERSE OF THIS PAGE			
2b. DECLASSIFICATION/DOWNGRADING SCHEDULE					
4. PERFORMING ORGANIZATION REPORT NUMBER(S) AEDC-TR-87-8		5. MONITORING ORGANIZATION REPORT NUMBER(S)			
6a. NAME OF PERFORMING ORGANIZATION Arnold Engineering Development Center	6b. OFFICE SYMBOL (If applicable) DOT	7a. NAME OF MONITORING ORGANIZATION			
6c. ADDRESS (City, State and ZIP Code) Air Force Systems Command Arnold Air Force Base, TN 37389-5000		7b. ADDRESS (City, State and ZIP Code)			
8a. NAME OF FUNDING/SPONSORING ORGANIZATION Air Force Wright Aeronautical Laboratories	8b. OFFICE SYMBOL (If applicable)	9. PROCUREMENT INSTRUMENT IDENTIFICATION NUMBER			
8c. ADDRESS (City, State and ZIP Code) Wright-Patterson AFB, OH 45433-6533		10. SOURCE OF FUNDING NOS			
		PROGRAM ELEMENT NO	PROJECT NO.	TASK NO	WORK UNIT NO.
11. TITLE (Include Security Classification) SEE REVERSE OF THIS PAGE		62102F			

12. PERSONAL AUTHOR(S) Wood, B. E., Bertrand, W. T., Bryson, R. J., and Seiber, B. L., Calspan (cont)				
13a. TYPE OF REPORT Final	13b. TIME COVERED FROM 10/1/84 TO 10/31/86	14 DATE OF REPORT (Yr., Mo., Day) September 1987		15 PAGE COUNT 115
16. SUPPLEMENTARY NOTATION Available in Defense Technical Information Center (DTIC).				

17	COSATI CODES		18. SUBJECT TERMS (Continue on reverse if necessary and identify by block number)
FIELD	GROUP	SUB. GR.	solar absorptance measurements cryogenic degradation
20	06		outgassing products reflectance measurements
20	05		optical systems

19. ABSTRACT (Continue on reverse if necessary and identify by block number)

The Air Force Wright Aeronautical Laboratories (AFWAL) and the Arnold Engineering Development Center (AEDC) have initiated a program for measuring optical and radiative effects of satellite material outgassing products on thermal-control and cryo-optic surfaces. Two systems were required for making the measurements, (1) an optical properties chamber for measuring the optical properties such as the complex refractive indices and bidirectional reflectance distribution function (BRDF) of condensed contaminants on cryo-optic surfaces, and (2) a solar absorptance chamber for making reflectance/absorptance measurements on thermal-control materials. This report identifies and describes the operation of these systems and presents optical property data for condensed contaminants on cryogenic surfaces. Refractive and absorptive index data are presented for the adhesives DC93-500, DC6-1104, RTV566, RTV-732 Silastic®, for Kapton® film, and S13G/LO paint. This program is continuing and properties for other materials will be available in the future. Measurements (cont)

20. DISTRIBUTION/AVAILABILITY OF ABSTRACT	21. ABSTRACT SECURITY CLASSIFICATION	
UNCLASSIFIED/UNLIMITED ☐ SAME AS RPT ☒ DTIC USERS ☐	UNCLASSIFIED	
22a. NAME OF RESPONSIBLE INDIVIDUAL C. L. Garner	22b. TELEPHONE NUMBER (Include Area Code) (615) 454-7813	22c. OFFICE SYMBOL DOCS

DD FORM 1473, 83 APR   EDITION OF 1 JAN 73 IS OBSOLETE.

3. DISTRIBUTION/AVAILABILITY OF REPORT

    Distribution authorized to U. S. Government Agencies and their contractors; critical
    technology; September 1987. Other requests for this document shall be referred to
    Air Force Wright Aeronautical Laboratories, Wright-Patterson AFB, OH 45433-6533.

11. TITLE

    Surface Effects of Satellite Outgassing Products

12. PERSONAL AUTHORS (Concluded)

    Corporation, AEDC Division, and Falco, Lt. Patrick M. and Cull, Capt. Ray A.,
    Air Force Wright Aeronautical Laboratories

19. ABSTRACT (Concluded)

    of BRDF data on contaminated cryogenic optical components and solar absorptance
    data on contaminated thermal-control surfaces will begin in FY87.

PREFACE

CONTENTS

ILLUSTRATIONS

Figure   Page

3

4

5

6

TABLES

1.0 INTRODUCTION

As satellite applications become more sophisticated and satellite lifetimes are extended, the roles of contamination prediction and control become increasingly important. Contamination can end a mission because of (1) cryogenically cooled optical systems becoming coated or (2) thermal-control surfaces becoming contaminated, thereby increasing the solar absorptance and causing the spacecraft to overheat. These are the two most important ways contamination can adversely affect the mission.

A spacecraft designer must predict effects of contamination with a very limited amount of data. Previously, the American Society for Testing and Materials (ASTM) 595 has been the industry standard for screening materials. The total mass loss (TML) and the collected volatile condensable material (CVCM) are used as guides. From the ASTM 595 criteria, a material, to be space rated, must have a TML of less than 1 percent and a CVCM of less than 0.1 percent. These parameters are determined by heating a sample to 125°C for 24 hr under vacuum. The TML is found from the measurements of the sample weight before and after heating. The CVCM is determined by weighing a 25°C collector surface, which was positioned above the heated sample before and after the 24-hr heating cycle. Neither the time history nor the identification of outgassed species are available from the ASTM 595 test.

The Air Force Wright Aeronautical Laboratories (AFWAL) is pursuing a plan to determine the outgassing properties of materials and the effects of condensed gases on critical surfaces such as thermal-control and cryogenically cooled optical components. An improved test method for determining material outgassing characteristics has been developed by Lockheed (Ref. 1). This method uses quartz crystal microbalances (QCM's) maintained at 77 K to measure the mass loss by outgassing and a time history of each outgassed species. This test method can be used to indicate how much of a given satellite material may be lost in space by outgassing, but it cannot determine what effect the outgassed material will have on an optical or thermal radiative surface. The surface effects of these products are being studied at the Arnold Engineering Development Center (AEDC) under another program sponsored by AFWAL.

Two chambers were assembled for determining (1) optical properties (refractive and absorptive indices) of condensed contaminant films on cryogenically cooled optical components and (2) the solar absorptance change in an optical solar reflector (OSR) as a function of contaminant thickness. Bidirectional reflectance distribution function (BRDF) measurements and solar cell degradation measurements will also be made in these systems.

Infrared (IR) transmittance measurements of contaminants condensed from satellite materials have begun in the AEDC 2- by 3-ft chamber (Fig. 1), and these results will be

9

discussed in this report. The materials were heated to 125°C under vacuum, and the outgassed products were frozen as thin films on a 77 K germanium window. A scanning Michelson-type interferometer was used to measure the transmittance over the 4,000- to 450-cm^{-1} wavenumber range. These data were input into the TRNLIN computer program to determine the refractive (n) and absorptive (k) indices of the contaminants. These n and k values can then be used to calculate the transmittance or reflectance of other optical components contaminated with the outgassing products of the same satellite material and for any film thickness. Measurements were made for the adhesives RTV-732 Silastic® , DC6-1104, DC93-500, RTV566, and RTV560, for KAPTON® film, and for S13G/LO paint (a developmental coating for thermal control).

Contamination measurements are being made in the solar absorptance measurements (SAM) chamber (Fig. 2) and will be made for the list of materials established by AFWAL. These measurements will be made on thermal-control surfaces, either OSR's or paints, maintained at 25°C. Solar cell degradation measurements will also be made in the SAM chamber.

BRDF measurements will also begin soon in the 2- by 3-ft chamber. A He-Ne laser will be used initially to determine the scatter effects of contaminants originating from the same materials being tested for cryogenic degradation and solar absorptance effects. Similar tests are planned later using a CO_2 laser as an irradiation source.

2.0 EXPERIMENTAL TEST APPARATUS

2.1 CRYOGENIC CONTAMINATION CHAMBER

IR transmittance measurements were made of satellite material outgassing contamination products on cryogenic surfaces in the AEDC 2- by 3-ft chamber (Fig. 1). The pumping system consists of a turbomolecular pump with a mechanical forepump and a liquid nitrogen-(LN_2)-cooled chamber liner. The turbopump and the cryopanels are necessary to provide a near contaminant-free vacuum. Base pressures before contamination deposition are generally in the mid-10^{-7}-torr range. Thermocouple and ion gauges are used to monitor the chamber pressure. A quadrupole mass spectrometer (QMS) is used to identify gas species in the chamber. An effusion cell heats the test materials to 125°C, which provides the source of contamination.

The test surface is a germanium window mounted in the center of the chamber. It can be cooled to near 77 K with a constant flow of LN_2. The germanium window temperature is monitored by platinum resistors embedded in the surrounding housing. The thin-film interference model on which the optical property determinations are based requires that only the front surface be coated by the contaminant material. Therefore, special precautions are

taken to insure that nothing deposits on the rear surface. Two LN$_2$-cooled baffles are located behind the rear surface to scavenge any gases that otherwise would be incident on it. One is a rectangular, flat plate located directly behind the germanium surface when it is in position for film deposition. The other is a hollow LN$_2$-cooled cylinder that shields the rear surface when it is rotated into IR transmittance-measurement position. The IR beam used in making the transmittance measurements passes through the center of the hollow tube.

2.1.1 Effusion Cell

The outgassing products for contaminating the sample surface are generated using an effusion cell, shown schematically in Fig. 3. The effusion cell has a cylindrical aluminum body 3.5 in. (8.89 cm) long with an internal bore diam of 1.75 in. (4.45 cm). A replaceable orifice plate covers one end, while the other end is closed. The material used to produce the outgassing flux is loaded into the closed end of the effusion cell. Three band heating elements cover most of the outside surface of the cylinder. A temperature-controlled power supply is used to maintain the temperature of the cell at a constant value (usually 125°C). Cell temperatures are sensed by a platinum resistance temperature detector (RTD). The effusion cell has a shutter to interrupt the contamination flux if required. The entire effusion cell assembly is mounted on a vacuum feed-through for positioning in or out relative to the chamber centerline.

The temperature of the effusion cell is maintained at 125°C by a proportional-temperature controller. This controller keeps the effusion cell temperature within ±1 K of the set point and provides an analog output for recording the cell temperature. This controller uses a platinum RTD embedded in the effusion cell wall as the temperature-sensing element. If desired, the controller-sensor-heater combination will function at other temperatures (from 0 to 200°C). The effusion cell exit is positioned at 2 in. (5.08 cm) from the germanium window and QCM. The centerline of the effusion cell is located midway between the centers of the germanium window and the QCM so that the deposition rates on the two are equal. This allows film-density measurements to be made.

The effusion cell is lined with disposable aluminum foil liners. The liners and aluminum foil sample boat are baked out at 125°C for 24 hr prior to each material test. This insures that the deposited contaminants come from the material being tested and not the peripheral components. New aluminum foil liners and boats are installed after each material test.

2.1.2 Germanium Window Deposition Surface

Germanium was picked for the deposition surface because it has good thermal conductance and a flat transmittance spectrum over the 700- to 4,000-cm^{-1} (2.5- to 14-μm) wavenumber

range. The window is 2.75 in. (6.99 cm) square and is 0.157 in. (4 mm) thick. Nominally, the transmittance of the window (at room temperature) is 47 to 48 percent over most of the wavenumber range. At 77 K the transmittance increases to about 49 percent in the flat portion of the spectrum and increases considerably more for wavenumbers less than 700 cm^{-1} where the germanium becomes absorbing.

The refractive index of germanium (Ref. 2) is given by

$$ng(\nu) = A + BL + CL^2 + D\nu^{-2} + E\nu^{-4} \tag{1}$$

where

ν = wavenumber,

A = 3.88,

B = 0.391707,

C = 0.163492,

D = −0.000006,

E = 0.000000053, and

L = $(\nu^{-2} − 0.028)^{-1}$

2.1.3 IR Transmittance Measurement Equipment

A commercially made Michelson-type interferometer is used in making IR transmittance measurements of the deposited contaminant film on the germanium window. A graphite radiation source is located inside the interferometer housing. The interferometrically modulated IR beam is collimated and allowed to pass through a housing port. The exit beam is then passed through a KBr window on the chamber port, through the germanium test window, through another KBr window on the opposite side of the chamber, and finally to a box containing the detector optics and detector. The detector is a type C Hg-Cd-Te, which is sensitive to wavelengths from 4,000 to 450 cm^{-1} (2 to 22 μm). Typically, 32 scans are co-added for both the sample and reference measurements with a resolution of 2 cm^{-1}. A reference measurement is made before each sample measurement. Data are initially stored on the system hard disk and later transferred to flexible disks.

12

2.1.4 QCM Configuration

For measuring the mass deposition, a quartz crystal microbalance is used. The QCM has a sensitivity of 4.43×10^{-9} gm/cm^2 • Hz. The unit is made up of two crystals, (1) the reference surface and (2) the sensing surface. They have AT-cut crystals of 39 deg + 40 min to minimize temperature effects at near LN$_2$ temperature. One of the crystals serves as the sensing surface, whereas the other is not exposed to mass flux and is the reference. The sensing crystal is optically polished and is overcoated with aluminum. Any material that adheres to the sensing crystal will alter the oscillator operating frequency. This change in frequency is proportional to the mass of material condensed on the crystal surface.

Since the crystals used in a QCM are sensitive to temperature changes, a method of compensating for temperature effects is required. This compensation is accomplished using the second, identical reference crystal-oscillator. It is placed in close proximity to the sensing crystal but shielded from any contamination. The output frequency change of this reference system is then a measure of the temperature variation only. The signals of these two systems are mixed electronically. The difference frequency is a temperature-compensated measurement of the mass accumulation on the active crystal. An exploded view of the QCM is shown in Fig. 4.

The QCM has a platinum resistance device (the RTD) placed between the sensing and reference crystals that functions as both a temperature sensor and a low-power (2-w) heater through a time-sharing electronics circuit. In this way, the temperature of the crystals may be monitored and small temperature changes made.

The QCM electronic controller is set up such that four outputs from the QCM are possible. They are mass, temperature, frequency, and mass rate. The signal representing the mass accumulation is differentiated with respect to time to furnish a mass build-up rate. Knowing the rate and temperature at which mass accumulates (or evaporates) can aid in interpreting the QCM data and identifying the species condensed or evaporated.

The mass deposited on the sensing crystal is determined by recording the change in mass directly or by monitoring the frequency of the sensing crystal. The relation between the frequency change (df) and the deposited mass (dm) can be expressed as (Ref. 3)

$$dm = 1.4 \times 10^{-9} \, df \text{ gm/Hz} \tag{2}$$

or

$$dm/S \ = \ 4.43 \ \times \ 10^{-9} \ df \ gm/cm^2 \bullet Hz \qquad (3)$$

where S $=$ surface area of the sensing crystal electrode, $0.316 \ cm^2$. If a density of $1.0 \ gm/cm^3$ is assumed for the condensed film, then the change in film thickness (dt) can be calculated from the frequency change (df) using the equation

$$dt \ = \ 4.43 \ \times \ 10^{-9} \ \times \ df \qquad (4)$$

where dt is given in cm and df is given in Hertz.

QCM cooling to LN_2 temperature is accomplished by conduction as it is mounted directly to the LN_2-cooled housing holding the germanium window. The QCM cooling rate is less than that of the germanium window. Temperature equilibrium is established for both QCM and germanium window before testing can begin.

2.2 SOLAR ABSORPTANCE MEASUREMENTS CHAMBER

The solar absorptance measurements (SAM) chamber measures changes in the absorption of solar radiation by thermal control or optical surfaces contaminated by outgassing products at vacuum conditions. The equipment also allows generation of the outgassing material within the chamber, and the determination of the amount of material deposited on the sample surface. If desired, the outgassing material can be irradiated by simulated solar radiation, either during deposition or after. The chamber atmospheric contents can be monitored with a 200 atomic mass units (amu) range quadrupole mass spectrometer (QMS). The chamber and associated contamination equipment are shown in Fig. 2. The details of each of these systems are discussed separately in the following sections.

The SAM vacuum is maintained by a 400-ℓ/sec turbomolecular pump. The chamber is also outfitted with an LN_2-cooled liner that can be used when test conditions dictate. Pressure in the chamber is measured with a Bayard-Alpert ion gauge and can be maintained at 4×10^{-6} torr.

2.2.1 Effusion Cell

The effusion cell used for contaminating thermal-control surfaces is identical to the one shown in Fig. 3 and discussed previously in Section 2.1.1. It too will operate over the temperature range from 0 to 200°C and was positioned such that the test surface and QCM are exposed to the same contaminant flux.

14

2.2.2. Solar Simulation

The characteristics of a contaminant are sometimes modified extensively if it is exposed to solar radiation. The changes that occur in the contaminant as a result of irradiation may be dependent on whether it occurs during or after coating deposition. The SAM is equipped to allow sample surfaces to be irradiated with simulated solar radiation, either during or after deposition. In Fig. 2, the solar radiation source is shown in the after-deposition position. The sample surface is first exposed to contamination from the effusion cell and then rotated 180 deg to expose it to simulated solar radiation. Ports are available on the effusion cell side of the SAM so that the source can be moved there and the sample irradiated at a 45-deg angle while being contaminated.

The portion of the solar radiation spectrum that has the most effect on contamination characteristics is thought to be ultraviolet (UV) (Ref. 4). The source used to irradiate sample surfaces is a 1,000-w xenon lamp. This lamp produces continuum radiation in the region of interest from 0.2 to 0.4 μm. The remainder of the radiation outside this region of interest will tend to heat the sample surface. To minimize this heating, a water-filled and water-cooled filter cell is used to remove the IR wavelengths that produce this effect.

2.2.3 Solar Absorptance Measurement Equipment

The solar absorptance measurement equipment consists of a modified Beckman DK-2A ratio-recording spectroreflectometer, an 8-in.-diam integrating sphere, and focusing mirrors to direct the spectroreflectometer's light beams into the integrating sphere. As the name of the spectroreflectometer implies, the measurement actually made with this equipment is the reflectivity of the sample surface. It is assumed that the absorptivity of the sample is equal to one minus the reflectivity.

The Beckman spectroreflectometer is designed to use its own internal integrating sphere to measure the spectral reflectance of samples placed in an access port on the sphere. The instrument generates a light beam that is sent through a quartz prism to be dispersed, and then the monochromatic beam is focused on an exit slit. The light beam then goes through a chopper wheel, which chops it at 480 Hz and on to a 15-Hz oscillating mirror that separates it into a reference and sample beam. Next, focusing mirrors direct these beams into the integrating sphere where the sample beam strikes the sample and the reference beam strikes the sphere wall. A detector on the sphere, along with an electronics package, records the ratio of the two light beam intensities to determine the reflectivity of the sample. For this measurement program, the instrument's internal integrating sphere is replaced with one attached to the SAM (See Fig. 2). This allows the sample reflectance to be measured in the sphere while under vacuum. External focusing mirrors direct the light beams into the integrating

15

sphere through a quartz window. Detection and comparison of light intensities is the same for both spheres.

The integrating sphere used for this program is 8 in. (20.3 cm) in diam and has three ports. A 2-in.-diam (5.08-cm) port connects the sphere to the SAM and is the path used to insert the sample. The second port is 1.25 in. (3.18 cm) in diam, perpendicular to the first, and is covered with a quartz window through which the light beams pass. The third port is also 1.25 in. (3.18 cm) in diam, is perpendicular to both of the others, and is used to mount the detector. The inside of the sphere is coated with a barium sulfate paint giving it a diffuse and highly reflective surface. A baffle is placed between the sample and the detector to prevent a direct line of sight between them.

The reflectivity of the sample is recorded as a function of wavelength. As noted previously, the light beam is dispersed by a prism before being split into two beams. To record the wavelength dependency of the reflectivity, the prism is rotated so that the dispersed light beam is swept past the exit slit. The position of the prism is monitored with an encoder. The encoder position is calibrated with the wavelength of the light beam so that the recording detector output, as a function of encoder position, yields the wavelength-dependent reflectivity.

The wavelength range capability of the reflectivity instrument is 0.2 to 2.5 μm. Two sets of light source and detector combinations are required to cover this range. The 0.2- to 0.5-μm portion of the spectrum is covered with a hydrogen lamp source and a 1P28 photomultiplier tube. The portion between 0.5 and 2.5 μm is covered with a tungsten lamp and a lead sulfide (PbS) detector.

2.2.4 QCM Configuration

Contaminant mass that is deposited on a 25°C sample surface in the SAM is measured with a QCM of the same type as discussed previously in Section 2.1.4. Major differences are that it is optimized for 25°C operation and uses crystals with an AT-cut of 35 deg + 12 min. Temperatures of the QCM and sample are regulated by flowing 25°C water through the circulation passages. The sensing quartz crystal is optically polished and overcoated with aluminum. Location of the QCM is below the optical solar reflector sample as shown in Fig. 2. The QCM and sample are located symmetrically about the effusion cell centerline to insure equal deposition rates on the two surfaces. The QCM mass deposition rate is used to calculate the film thickness deposited on the OSR by assuming the contaminant density is 1 gm/cm^3. (The density of films condensed at 77 K have varied from 0.8 to 1.1 gm/cm^3.)

2.2.5 Deposition Surfaces

The sample surface to be tested is mounted on the end of an actuator arm that can move axially as well as rotate 360 deg. The axial motion carries the sample surface from the center of the SAM, where the contamination is deposited, into the integrating sphere of the solar absorptance measurement system. The sample surface holder on the end of the actuator will accept samples that are 1.0 in. (2.54 cm) in diam by 0.125 in. (0.32 cm) thick. A retaining ring holds the sample in place. By attaching the sample to an adaptor that screws into the actuator, other shapes can be accommodated. The temperature of the sample end of the actuator is stabilized by water cooling.

Provision is made in the SAM for testing the effects of contamination on solar cell operation. A vacuum feed-through positioner, in the top of the SAM, allows a solar cell array to be contaminated and then turned to be irradiated by the solar simulation lamp (Fig. 2). There are other ports available so that an auxiliary lamp could be placed to irradiate the solar cells at a 45-deg angle while they are being contaminated.

2.2.6 Mass Spectrometer

The SAM is equipped with a QMS to allow continuous monitoring of the contents of the chamber while a test is being conducted. The mass range of the QMS is 1 to 200 amu, and detection is accomplished by a Faraday cup or an electron multiplier.

The QMS mass scan data are recorded with a microcomputer. Software is available that will subtract previously recorded SAM background mass scan data from that recorded during a test and plot the resulting differences as a function of mass number. This allows the removal of any chamber background contamination from the test data. The mass range of 1 to 200 amu prevents detection of high mass number species such as some of the hydrocarbons.

3.0 EXPERIMENTAL TEST PROCEDURE

3.1 INTRODUCTION

The objective of this study was to examine the surface effects of condensed outgassing products from satellite materials. Lockheed (Ref. 1) has established a test method for determining the expected mass loss of the same materials. It is desirable that both companies make these measurements on similar sample materials under similar conditions. Therefore, some of the samples have come from a common source provided and/or procured by Lockheed. In some instances this was not possible. A considerably larger quantity of material was required for the surface effects studies than for the outgassing measurements. Generally,

a quantity of 50 to 100 gm of material was required to get a sufficiently large contaminant thickness for determining the optical constants. An amount of only 10 gm or less was required for most of the Lockheed outgassing studies.

The thin-film thickness measurement technique has been described previously (Refs. 5 and 6) and will only be reviewed here. In order to make accurate n,k measurements, the transmittance must be measured for carefully determined film thicknesses. The thin-film interference technique provides a method for calculating these discrete thicknesses. As a thin film forms on a reflecting (or transmitting) substrate, a reflected or transmitted beam of radiation will exhibit a sinusoidally varying signal. From the interference equations, the maxima and minima locations can be used to accurately calculate the thin-film thickness

$$t = m\lambda/2n \, [1 - (\sin^2\theta/n^2)]^{1/2} \tag{5}$$

where

t = film thickness, μm,

$\lambda.$ = wavelength, μm,

n = real part of refractive index at wavelength, λ,

θ = incidence angle deg, and

m = order of interference

However, in order to make these calculations, the film refractive index n must be known for the incident wavelength. Usually, the He-Ne laser wavelength of 0.6328 μm is used. Since germanium does not transmit this wavelength, the technique is used in the reflective mode. Two He-Ne laser beams are incident at two angles (24.0 and 67.5 deg), and interference fringes are observed as the contaminant film is deposited. The refractive index at 0.6328 μm is determined from the interference patterns observed on a strip chart recorder trace for the two laser-solar cell outputs. This is done by fringe (interference maxima or minima) counting for each of the incidence angles and using the equation (Ref. 7)

$$n = [\sin \theta_1^2 - (m_1/m_2)^2 \bullet \sin \theta_2^2] \, / \, [1 - (m_1/m_2)^2]^{1/2} \tag{6}$$

18

where θ_1 and θ_2 are the two incidence angles, and m_1 and m_2 are the numbers of interference peaks counted for the angles θ_1 and θ_2, respectively.

Knowing the refractive index at 0.6328 μm, the film thicknesses at the interference maxima and minima peaks are easily calculated using Eq. (5). Either incidence angle can be used, but the smaller angle provides smaller thickness increments. For a sample thickness calculation, let n = 1.4, θ = 24 deg, λ = 0.6328 μm, and m = 1 (for the first interference maxima). From Eq. (5) then, t = 0.2474 μm. Similarly, calculations for the first minima (m = 1/2) yield a film thickness of 0.1237 μm.

Film densities are determined from the calculated thickness and from the surface density (gm/cm^2) that is obtained from the QCM. This assumes that the surface density determined by the QCM is the same as that experienced by the germanium window. The density, d, (gm/cm^3) is determined from

$$d = (dM/S)/t \qquad (7)$$

where

dM = the change in mass detected by the QCM,

S = the surface area of the QCM element (0.316 cm^2), and

t = the film thickness in cm determined from Eq. (5)

The mass accumulated for each thickness is recorded, and thus, provides a means of determining film density. Frequency changes up to 100,000 Hz are assumed reliable. Densities calculated for frequencies above 100 kHz usually were somewhat higher than for the smaller film thicknesses.

3.2. MATERIAL TEST SAMPLE REQUIREMENTS

3.2.1 Material Documentation and Preparation

At a joint meeting of government agencies and contractors, a list of satellite materials that should be tested for contamination potential was compiled. This list is shown in Table 1 and is being used as an initial guideline for determining the materials to be investigated.

Sample material time of preparation, cure time, mixture ratio, batch number, and preconditioning time were all carefully documented (See Table 2). In some instances, the

19

cure time recommended was seven days or longer. Tests on these materials sometimes could not be completed because of insufficient mass deposited on the germanium window to obtain enough transmittance measurements to make reliable n,k measurements. In these cases, tradeoffs had to be made in that shorter cure times were used so that a greater contaminant flux could be obtained. Generally, the longer the material cures, the less will be its outgassing rate.

3.2.2 Material Sample Configuration and Preconditioning

The adhesives were prepared by pouring them into an aluminum foil boat that was 3 by 1.5 by 1.5 in. (7.62 by 3.81 by 3.81 cm) and allowed to cure. The empty aluminum foil boat was outgassed for 24 hr prior to filling with material. The TML for the foil boat was found to be 0.03 percent. Even though this is small compared to the material outgassing, the effusion cell was still outgassed prior to each set of material measurements. For the S13G/LO paint tests, seven strips of aluminum foil were painted, allowed to cure, and then rolled up and inserted in the effusion cell. The Mylar® film tested was simply cut to the correct length, rolled up, and placed inside the effusion cell.

Where possible, the materials tested were checked in Ref. 8 to determine the approximate total outgassing expected so that enough outgassed products could be gotten to test at least ten film thicknesses (interference maxima). Test materials were preconditioned by placing the boat and material in a 50-percent (± 5 percent) relative humidity cell for 24 hr prior to chamber installation.

3.3 CRYOGENIC CONTAMINATION CHAMBER TEST PROCEDURES

After the test material had been preconditioned, the boat containing the sample material was inserted in the effusion cell and installed in the 2- by 3-ft chamber. He-Ne laser alignment checks were carried out to insure that the laser beams reflected from the germanium window were incident on the solar cell detectors. Also, the transmittance of the germanium window was inspected to insure that no contaminant film had remained after cleaning. The housekeeping data program was started for monitoring the QCM frequency, mass, temperature, and mass deposition rate. Also monitored were the effusion cell temperatures, the shutter temperature, the laser-solar cell outputs for the two incidence angles, and the germanium window temperatures. Pumpdown of the chamber then began using a mechanical pump and a turbomolecular pump. Once the chamber pressure had been reduced to the 10^{-5}-torr level, the chamber liner was cooled to LN_2 temperature. After the liner reached LN_2 temperature, the LN_2 flow to the germanium window and QCM was started. The germanium window cooled down much quicker than the QCM because of its better thermal conductivity. At this point, the chamber pressure was usually in the mid- to high-10^{-7}-torr

20

range, and testing was begun. The effusion cell heater was turned on, and the laser-solar cell outputs were observed with time on a strip chart recorder. The effusion cell was thermostatically controlled to 125°C, and the outgassed components were condensed on the germanium window and the QCM. The centers of the germanium window and the QCM were aligned equidistant from the effusion cell centerline so that the two surfaces would see the same flux rate. As the outgassed products condensed on the germanium window, the thin-film interference caused the laser-solar cell outputs to exhibit sinusoidally varying outputs. Deposition continued until the first interference minimum (quarter wavelength) occurred. The transmittance of the germanium window with the deposited film was then measured. This required rotating the germanium out of the deposition position into the transmittance-measurement position. In making the transmittance measurement, a set of 32 scans was taken with the germanium rotated out of the IR interferometer beam. This was the 100-percent or reference beam. The germanium window was next rotated into position so that the interferometer beam was incident normal to it, and again 32 scans were taken. The transmittance was determined by ratioing the Fourier transforms of the two sets of interferograms.

Once the transmittance measurements were completed, the germanium was rotated back into deposition position, and the film build-up and transmittance measurements continued. This procedure was repeated for as many thicknesses as could be obtained before the deposition rate decreased to a minimal value. For some materials, films up to 25 interference maxima thick were obtained. Transmittance measurements were made for as many thicknesses as possible to maximize the accuracy of the n,k calculations.

After transmittance measurements were completed, the effusion cell heater was maintained at 125°C for a period of 24 hr. This allowed a direct comparison of the present TML values, the values given in Ref. 8 using the ASTM 595 method (125°C for 24 hr), and the values obtained with the new Lockheed technique (QCM method).

In some cases, transmittance measurements were made during warmup of the germanium window. This helped to determine at what temperature the individual contaminant species were re-evaporated and to aid in their identification. Unfortunately, because the QCM and the germanium window warmup rates were different, the QCM could not be used to correlate mass loss with the transmittance spectra. The spectral dependence on temperature, however, was obtained.

After the effusion cell had returned to room temperature, the 2- by 3-ft chamber was pressurized to atmospheric pressure, and the sample material removed and weighed. The TML (percent) value was determined by dividing the mass lost attributable to outgassing

(at 125°C under vacuum) by the original mass. The original mass was determined after removal from the 50-percent relative humidity chamber and prior to installation in the effusion cell.

The germanium window was observed after warmup and a transmittance spectrum was taken. Often there was a film left on the germanium. It was easily removed using alcohol, Freon®, or acetone. Transmittance measurements of the film showed evidence of hydrocarbons and silicones. The QCM also had a contaminant film left on it, as the frequency was generally 5 to 10,000 Hz higher than that observed prior to the beginning of the test. Both the germanium window and QCM were cleaned before the next test.

3.4 SOLAR ABSORPTANCE MEASUREMENTS CHAMBER

The amount of solar irradiance that is absorbed by a thermal-control, optical, or solar cell surface affects the performance of that surface in space. Knowing how the absorption changes with exposure to a contaminant is necessary to predict the useful lifetime of the surface. An experimental program to catalog surface solar irradiance absorption as a function of exposure to various contaminants is to be accomplished in the SAM. The chamber and associated equipment have been assembled and vacuum pump-down and leak-checking accomplished. Tentative procedures for conducting the experimental solar absorptance measurements program are discussed in the following sections.

3.4.1 Effusion Cell

The effusion cell generates the contamination products for surface deposition. To prepare the effusion cell for a test period, the bore of the cell is cleaned with a solvent and then dried. The bore is then lined with aluminum foil, which can be removed to aid clean-up for a future test. The material from which the contaminants are to be derived is placed in an aluminum boat and placed in the effusion cell. The effusion cell and contents are then installed in the SAM and positioned for the test. Heater electrical connections and temperature sensing RTD connections are made to complete the effusion cell set-up.

The contamination material is used in approximately 100-gm quantities. The exposed surface area is maximized to get the most contaminant flux possible. For solids, this means that the material is cut into small pieces; nonsolids are spread out as much as possible.

A test period is begun by closing the shutter on the effusion cell and turning on heater power. The temperature-controlled heater power supply maintains the effusion cell temperature at the set point. When the temperature set point is reached, the shutter is opened and contamination of the test surface begins.

3.4.2 Solar Irradiation Procedure

As stated previously, the xenon solar-simulation lamp can irradiate the sample surface during or after contamination. The lamp also has built-in focusing optics to allow the light beam to be focused on surfaces within short distances of the lamp.

For the case where irradiation is to be done after contamination, the lamp is placed opposite the effusion cell orifice (Fig. 2). The sample surface is turned toward the lamp, and the light beam is focused on the sample. The lamp is then turned off, and the sample surface is turned back toward the effusion cell to be contaminated. When contamination is complete, the surface is turned back toward the lamp, and the lamp is turned on to irradiate the sample.

If irradiation is to be accomplished while the contaminant is being deposited, the lamp is moved to a window on the side with the effusion cell. The light beam is again focused on the sample surface, and the lamp is left on while the surface is contaminated.

3.4.3 Solar Absorptance Measurement

The absorptance of a sample surface is determined as a function of the amount of contaminant deposited on that surface. The amount of contaminant on the surface is monitored with the QCM. The surface is contaminated to a predetermined level, moved into the integrating sphere, and its absorptance measured. This procedure is repeated as many times as necessary to build the contaminant to the desired final thickness.

The absorptance of a sample surface is measured at each contamination level as a function of wavelength, over the range of the spectroreflectometer (0.2 to 2.5 μm). Thus, the sample surfaces tested will have wavelength dependent absorptances cataloged for them as functions of contaminant mass and level of simulated solar irradiation.

3.4.4 Monitoring of Contaminant Deposition

The contaminant thickness on the sample surface is assumed to be the same as that on the QCM since the two surfaces are maintained at the same temperature and are exposed to the same contaminant flux. The operating frequency of the QCM oscillator circuit is monitored continuously during a test. Care is taken that the QCM and sample surface are equally exposed by assuring that the effusion cell shutter is closed before moving the sample into the integrating sphere. The QCM thus furnishes a continuous record of the sample surface contamination build-up.

4.0 EXPERIMENTAL DATA

4.1 INTRODUCTION

4.1.1 Housekeeping Data

The housekeeping data were monitored and stored by a computer during material testing in the 2- by 3-ft chamber. An example of a typical set of data is shown in Figs. 5 through 12 for the QCM parameters, the laser-solar cell outputs, the effusion cell temperature, and the germanium window temperature. The data presented in Figs. 5 through 12 were obtained during testing of RTV566 and are typical of that recorded for each material tested. Usually, housekeeping data were recorded every 5 min, but the time interval could be varied.

Figure 5 shows the QCM temperature versus test time. Initially, the temperature was 25°C before cooldown and leveled off at -190°C after LN_2 cooldown. The QCM temperature remained constant at -190°C during the entire test time. Warmup of the QCM began after 29 hr of test time. This was accomplished by flowing warm helium gas through the cryogen supply line until the QCM reached -20°C. After the helium flow was shut off, the QCM cold soaked because of the LN_2 liner, and the temperature decreased again before finally warming up as the liner warmed up.

The cryocondensed QCM mass values are depicted in Fig. 6 as a function of test time. There was a gradual build-up with time until the mass reached 140 μgm. Further build-up saturated the QCM causing the signal to drop to zero after nearly 15 hr of testing. During warmup, the QCM began functioning again when the mass level reached 80 μgm, and it finally levelled off at 20 μgm. This level indicated a mass increase of 17 μgm over that measured prior to the beginning of the test.

The QCM frequency plot versus time is shown in Fig. 7. The QCM controller reset to zero frequency when 100,000 Hz was reached. This can be observed in Fig. 7 at the 11-hr mark. Again, the QCM stopped functioning at the 29-hr mark. The frequency versus time plot should track the mass versus time plot as they are directly related.

The mass rate of condensed material is shown in Fig. 8. The maximum condensation rate occurred at about 5 hr into the test, reaching an approximate value of 8×10^{-9} gm/sec. The negative values observed at the 30-hr mark were attributable to the QCM losing mass during warmup.

The temperature history of the effusion cell is shown in Fig. 9. The initial decrease is caused by the LN_2 liner being cooled prior to heating of the effusion cell. This is seen as

24

the initial decrease from 25°C down to 0°C before heating began. For this particular case, there was an instrument noise problem as can be seen in the figure. The temperature normally was between 125 and 130°C. The effusion cell heater was shut off after 24 total hr of heating.

The germanium window temperature is shown in Fig. 10. Usually, the germanium window was 3 to 4 deg colder than the QCM, evidently as a result of better thermal conduction. Figures 11 and 12 show the laser-solar cell outputs for the incidence angles of 24 and 67.4 deg, respectively. The thin-film interference patterns can be observed as the sinusoidally varying functions. The voltage values near zero are the result of rotating the germanium window out of the deposition position and into the transmittance-measurement position. The film refractive index at 0.6328 μm was determined by fringe counting for each angle.

4.1.2 Preliminary Bare Germanium Tests

Prior to testing any contaminant, the transmittance of the bare, clean germanium window was measured. If there were evidence of any contaminant film on the surface, then the germanium was recleaned with acetone or Freon. Figure 13 shows the germanium window IR transmittance at 25°C. It is seen that the transmittance is essentially flat over the wavenumber region from 4,000 to 700 cm^{-1}. It is nonabsorbing in this range and transmits only about 47 percent because of its high refractive index value (n = approximately 4.0).

4.2 DOW CORNING® SILASTIC RTV-732 SEALANT

The first material tested was Dow Corning Silastic RTV-732. This is a one-component material, 100-percent silicone rubber, and is used as an adhesive or sealant. This material is not space rated, but was used for checking out the system and components to be used in materials testing. According to the manufacturer, the TML should be close to that of RTV-731 as given in Ref. 8 (1.39 percent when cured for 24 hr). For this test, a quantity of 20 gm of the material was allowed to cure for only 1 hr before testing began. The refractive index at 0.6328 μm was calculated to be 1.44 for the 77 K films. This was based on thicknesses up to 15 interference maxima or 3.44 μm thick. Transmittance spectra are shown in Figs. 14, 15, and 16 for thicknesses of 0.23, 1.15, and 2.29 μm.

For the 0.23-μm thickness (first interference maximum), Fig. 14, absorption bands can be seen for wavenumbers less than 1,800, but the transmittance is not reduced by more than 2 or 3 percent. For a thickness of 1.15 μm, the absorption bands are well defined as shown in Fig. 15. The hydrocarbon band near 2,960 cm^{-1} can now be seen as well as the silicone bands below 1,800 cm^{-1}. The CO$_2$ band at 2,340 cm^{-1} shows up only as a trace constituent. No H$_2$O bands were observed for this material. The maximum mass deposition rate observed with the QCM was 95 × 10^{-10} gm/sec, which occurred 2 hr after warmup began.

25

Figure 17 shows the transmittance of the germanium window with remaining contaminant film after warmup to 10° C. There is considerable contaminant still on the germanium window as evidenced by the presence of the absorption bands. Upon opening the chamber, there was a strong odor similar to vinegar (acetic acid). After removing the sample from the effusion cell and weighing it, a TML value of 4.5 percent was calculated. This is considerably higher than the 1.6 percent determined after 24 hr of curing (Ref. 8). The intent of this test was not to duplicate the curing conditions, but to get a material that would provide enough outgassing to check out the system and deposition techniques. The 4.5-percent TML value should not be used as an indication of the outgassing characteristics of cured RTV-732.

A transmittance spectrum was made for the RTV-732 smeared on a sodium chloride window at standard temperature and pressure (See Fig. 18). The reference measurement for this case was the uncoated NaCl window to accentuate the absorption bands of the RTV-732. Comparing Figs. 16, 17, and 18 shows that the spectra of the material outgassed from the sample is very similar to the spectra of the parent material. Two prominent absorption bands observed in Fig. 16 at 950 and 1,820 cm^{-1} are much weaker or do not exist at all in the warmup data (Fig. 17) or for the parent material (Fig. 18).

4.3 DOW CORNING DC93-500 SPACE-GRADE ENCAPSULANT

Dow Corning 93-500 is a space-grade encapsulant and has a TML between 0.1 and 0.2 percent (Ref. 8), depending on the lot number, for a cure time of seven days. It is prepared by mixing encapsulant and curing agent in the ratio of ten to one. When cured, it is a firm, colorless, clear silicone rubber. For this test, the sample was taken from Lot GA115893 and mixed as prescribed. An amount of approximately 67 gm of the material was allowed to cure for four days before testing began. The maximum QCM deposition rate observed was 16×10^{-10} gm/sec occurring 2.5 hr after heatup began. Note that this mass rate is a factor of six less with three times the mass as was obtained with the uncured RTV-732. A thickness of only 5.5 interference maxima was obtained before the deposition rate became undetectable. The refractive index at 0.6328 μm was 1.44.

The transmittance spectra of the DC93-500 outgassing components condensed on germanium are shown in Figs. 19, 20, and 21 and are for film thicknesses of 0.23, 0.69, and 1.26 μm, respectively (corresponding to 1.0, 3.0, and 5.5 interference maxima). For a thickness of 0.23 μm, only traces of contaminant absorption bands are observable. For the largest thickness, 1.26 μm, the broad H_2O band centered near 3,290 cm^{-1}, the C-H band near 2,935 cm^{-1}, a trace of CO_2 at 2,340 cm^{-1}, and silicone bands between 800 and 2,200 cm^{-1} are observed (Fig. 21). After the germanium was warmed back up to -1.5°C, a transmittance measurement was made to determine if any material remained (Fig. 22). Considerable deposit

remained on the germanium as can be seen by the absorption bands. The absorption band locations are similar to those in Fig. 21, except the broad H_2O band centered near 3,290 cm^{-1} is no longer present. The H_2O evaporated during warmup when the surface temperature was between 160 and 170 K.

Transmittance spectra of the two DC93-500 components, the encapsulant and the catalyst, are shown in Figs. 23 and 24, respectively. The background reference was the bare germanium window to accentuate the absorption bands. The transmittance values of Figs. 23 and 24 are, therefore, not indicative of the true transmittance of the gernamium window and material films. The wavenumber locations of the absorption bands are given in the figures. Both encapsulant and catalyst have similar absorption spectra. The main difference is that the catalyst shows a band located at 2,162 cm^{-1}. All other bands are very similar. Figure 21 shows for films deposited during the test, the 2,162 cm^{-1} is present, indicating that the catalyst was the source of part of the outgassing. On warmup, there was still a trace of the band, but the location of the absorption peak is now at 2,154 cm^{-1} (Fig. 22).

4.4 DOW CORNING DC6-1104 CONTROLLED VOLATILITY SEALANT

DC6-1104 is a controlled volatility sealant designed for systems that operate in hard vacuums. The one component sealant cures at room temperature by reacting with the moisture in the air, and has a TML between 0.13 and 0.26 (Ref. 8). It is designed for sealing, bonding, and adhering components and equipment used in space environments. Curing proceeds inward from the surface at a rate dependent on relative humidity and sealant thickness. After curing, the material is a flexible silicone rubber.

A sample of DC6-1104 material was prepared by placing about 100 gm into an aluminum boat and curing for four days (final 24 hr in 50-percent relative humidity chamber). After the test, it was observed that the innermost part had not completely cured. Therefore, the outgassing rate was greater than normal. No TML values were determined during the test because some of the mass became attached to the foil liner.

Transmittance measurements were made for thicknesses up to 24 interference maxima thick (5.43 μm). The refractive index at 0.6328 μm was found to be 1.46. Transmittance spectra are shown in Figs. 25, 26, and 27 for film thicknesses of 0.23, 2.26, and 4.53 μm, respectively (corresponding to 1, 10, and 30 interference maxima). One of the major outgassing constituents is H_2O, which is seen in Fig. 27 as the broad band centered at 3,233 cm^{-1}. The CO_2 band at 2,339 cm^{-1} also is present. Neither of these bands were seen in the transmittance of the parent material at 25°C (Fig. 28) nor was the sharp band at 1,192 cm^{-1}. The C-H band is very prominent in the condensed film (Fig. 27) but much less noticeable in the parent material.

Also, the location of the C-H bands differ as the weaker low-wavenumber band appears at 2,904 cm^{-1} for the parent material and at 2,837 cm^{-1} for the condensed film. Relatively strong bands are seen at 1,466 and 844 cm^{-1} for the condensed films, which are not observed for the parent material. The strong Si-O bands that occur at 1,080 and 1,032 cm^{-1} for the condensed films are seen at the same locations in the parent material.

After the deposition measurements were completed, the germanium window was warmed up to $-88°C$ (185 K), and a transmittance spectrum was made of the condensate remaining on the window. The results are shown in Fig. 29. Notice that the CO_2 band at 2,340 cm^{-1} and most of the H_2O band centered near 3,290 cm^{-1} have vanished. The intensities of the bands at 1,466 and 800 cm^{-1} have been greatly reduced after warmup (Fig. 29). Much of the absorption in these bands can be attributed to H_2O. The Si-O double band at 1,080 and 1,032 cm^{-1} seen in Fig. 27 is now observed as a single band at 1,087 cm^{-1} in Fig. 29.

A transmittance spectrum taken after germanium window warmup to room temperature showed no residual contaminant remaining on the window. This was in sharp contrast to warmup transmittance data that had been observed for the previous two materials. Visually, the germanium window appeared to be slightly contaminated, but no IR absorption was seen.

4.5 GENERAL ELECTRIC RTV566

RTV566 is a low-volatile content RTV compound, based on a phenyl silicone polymer and cures to a tough silicone rubber. It is designed to meet the ASTM standards of less than 1-percent TML and less than 0.1-percent CVCM. TML values of between 0.08 and 0.36 are given in Ref. 8, depending on the preparation technique. According to the manufacturer's data sheet, optimizing all material properties requires a catalyst to silicone rubber ratio (RTV566B:RTV566A) of 0.7 percent by weight. This was the ratio used in the preparation of RTV566 for the optical properties test. A quantity of 95 gm of the sample was allowed to cure for 44 hr before testing began.

The RTV566 was heated to 125°C and the outgassed products were condensed on the germanium for films up to 25 interference maxima thick. The refractive index at 0.6328 μm was 1.43. Transmittance curves are shown in Figs. 30, 31, and 32 for film thicknesses of 0.23, 2.29, and 4.59 μm corresponding to 1, 10, and 20 interference maxima. The band locations are labeled for the largest thickness in Fig. 32. These can be compared with bands seen in Figs. 33 and 34 for the silicone base RTV566A and for the catalyst RTV566B measured at 25°C.

After 24 hr of heating at 125°C, the sample was removed and weighed. The TML was found to be 0.57 percent, which is a little higher than the values reported in Ref. 8. This

is considered to be in good agreement since the cure time was only two days as compared to seven days for the data in Ref. 8.

4.6 GENERAL ELECRIC RTV560

RTV560 is a silicone polymer and a polydimethylsiloxane. It is very versatile but is generally not regarded as a space-rated material. It has a relatively high TML value, between 0.4 and 3.3 percent, depending on the preparation technique and cure time. The sample was prepared by mixing the catalyst (dibutyl tin dilaurate or DBT) with the RTV silicone rubber base compound in the ratio of 0.5 percent by weight. An amount of about 78 gm of the mixed material was used in the test. The total cure time before testing was 45 hr.

Transmittance spectra were obtained for film thicknesses up to 25 interference maxima thick. Figs. 35, 36, and 37 are transmittance curves for thicknesses of 0.23, 2.32, and 4.69 μm, respectively, corresponding to 1, 10, and 20 interference maxima. The band locations are given in Fig. 37 with the most noticeable being H_2O at 3,231 cm^{-1}, the C-H band at 2,971 and 2,897 cm^{-1}, the methyl bands at 1,260 and 810 cm^{-1}, and the Si-O band at 1,053 cm^{-1}. CO_2 shows up only as a trace compound at 2,338 cm^{-1}. There are many other weaker bands between 500 and 1,500 cm^{-1}. After warmup to 5°C, there was still a noticeable film remaining on the window, as indicated in the transmittance spectra shown in Fig. 38. The C-H band at 2,962 cm^{-1} and the characteristic methyl silicone bands at 843, 1,062, and 1,260 cm^{-1} are still present, although the structure has changed somewhat. Many of the weaker bands seen in Fig. 37 have disappeared. After removal from the chamber, the germanium window had a thin, translucent film that was easily visible.

The spectra of RTV560A (base) and RTV560B (catalyst) are shown in Figs. 39 and 40. The outgassing spectra condensed at 77 K (Fig. 37) is very similar to that of RTV560A (Fig. 39). No evidence of the catalyst was observed in the condensed spectra.

The RTV560 refractive index at 0.6328 was 1.42, and the density was 0.96 gm/cm^3 for the condensed film. The TML was found to be 2.0 percent, which is close to the value of 2.22 percent for a seven-day cured sample (Ref. 8).

4.7 S13G/LO PAINT

Illinois Institute of Technology Research Institute (IITRI) in Chicago prepared a developmental coating for AFWAL to determine the surface effects of the condensed outgassing in the IR. The coating was mixed according to the manufacturer's specifications, which was 0.6-percent catalyst by weight. The S13G/LO used V-10 resin as a binder. After mixing, the coating was applied to seven aluminum foil strips, with 53 gm of paint remaining

29

(after drying). Prior to painting the strips, there were 100 gm of the paint; an amount of approximately 47 gm of mass was lost by evaporation. The seven strips were allowed to cure and were preconditioned for 24 hr in a 50-percent relative humidity environment. Total cure time before testing was 45 hr. The strips were all rolled together and placed inside the effusion cell. Transmittance data of the condensed outgassed products were obtained for 14 film thicknesses up through the 12th interference maxima.

The results of the outgassing studies are shown in Figs. 41, 42, and 43 for condensed film thicknesses of 0.25, 1.78, and 2.96 μm (corresponding to 1 interference maxima, 7 maxima, and 12 maxima). Only for the thickest film was there evidence of anything other than H_2O or CO_2. The transmittance of the paint-binder and the catalyst are shown in Figs. 44 and 45. No evidence is seen for the catalyst in Fig. 43. Therefore, essentially all of the outgassing came from the S13G/LO base. This is not unexpected since the ratio of catalyst to base was very small.

After the test measurements were completed, a transmittance measurement was made with the germanium window warmed up to 203 K. All of the deposit had evaporated, except for a very small absorption in the C-H absorption band region near 2,900 to 3,000 cm^{-1}. After weighing the seven strips of painted aluminum foil following the test, a TML of 0.16 percent was obtained. The refractive index at 0.6328 μm was 1.34, and the film density was 1.11 gm/cm^3.

4.8 KAPTON®

A roll of Kapton film was obtained from Lockheed in Sunnyvale. This same sample is also being tested in the outgassing apparatus by Lockheed. For the surface properties measurements, an amount of 126 gm of material was placed inside the effusion cell. It also was preconditioned at 50-percent relative humidity for 24 hr prior to the test.

Transmittance measurements for 15 thicknesses were made for films up to 13 interference maxima thick. Transmittance spectra for the condensed outgassing products on the germanium window are presented in Figs. 46, 47, and 48 for film thicknesses of 0.28, 1.66, and 3.59 μm. H_2O is the only major identifiable component. Again, CO_2 shows up as only a trace. Although the deposit appears to be predominantly H_2O, the refractive index at 0.6328 μm was found to be 1.21, which is considerably lower than for pure H_2O films ($\sim$1.31). The density measured (0.91 gm/cm^3) was essentially the same as for H_2O films. The reason for the low refractive index at 0.6328 μm is presently unknown. Figure 49 shows the transmittance of a 5-mil thick Kapton film measured at 25°C and atmospheric pressure. The outgassed products condensed and measured (Fig. 48) show little resemblance to the pure Kapton spectra

(Fig. 49). It appears that the source of H_2O is chemical decomposition of the Kapton. After testing, the sample was removed and weighed. The TML determined was 1.26 percent.

5.0 OPTICAL PROPERTIES DETERMINATION

Most contaminant problems encountered in space involve contaminant thicknesses of a few micrometers or less. Therefore, thin-film interference equations are generally used to predict contaminant effects on the reflectance or transmittance of an optical element. These calculations require knowledge of the optical properties of the contaminant film—the refractive and absorptive indices, n and k. They are components of the more general expression for the complex refractive index given by $n^* = n - ik$. In order to determine the complex refractive index of the thin, solid, contaminant films, an analytical model of film plus substrate transmittance has been developed (Refs. 5, 6, 9, and 10). Most of the model follows the expressions given in Ref. 11 for thin-film transmittance and reflectance. The model assumes the germanium window is a thick film, and there is no phase coherence between multiple, internally reflected rays. All interference occurs within the thin contaminant film. An expression is derived for the normal transmittance of a thin film on a nonabsorbing substrate. Expressions for the partially absorbing substrate case are also available but were not used in this study.

The optical constants of the contaminant films were determined using the experimentally determined transmittance values over the 4,000 to 700 wavenumber range and for as many film thicknesses as possible. These were input into the analytical transmittance model TRNLIN that uses a nonlinear least-squares convergence routine for determining n and k. In some instances, the program did not converge upon a unique value of n. This usually occurred in regions of strong absorption or low wavenumber, where it was only possible to form a few thicknesses of contaminant. The n value appears to be primarily defined by the period of the transmittance versus thickness curve at each wavenumber. At small thicknesses, high absorption, or low wavenumbers, the transmittance versus thickness (for each wavenumber) curve is not well defined; i.e., the period of the interference as a function of thickness is not well defined. The k value, which is primarily defined by the magnitude of the transmittance, was well defined over the whole spectral region (700 to 4,000 cm^{-1}). Therefore, for some cases where the n values were not uniquely defined, the k values were used with the Subtractive Kramers-Kronig relationship to compute n. The Subtractive Kramers-Kronig expression is given by

$$n(\nu_m) + \frac{2}{\pi} P \int_0^\infty \left[\frac{k(\nu')\nu - k(\nu)\nu}{(\nu')^2 - (\nu)^2} - \frac{k(\nu')\nu' - k(\nu_m)\nu_m}{(\nu')^2 - (\nu_m)^2} \right] d\nu' \qquad (8)$$

where ν_m is a reference frequency, and P is the Cauchy principal integral value. The $k(\nu')$

31

values used in Eq. (8) were those determined using TRNLIN. These new n values were then used in the analytical model (along with the k values) to see if good agreement with the transmittance data was obtained. Generally, the Kramers-Kronig n values yielded good agreement when the analytical model results and actual transmittance data were compared.

5.1 MATERIAL'S REFRACTIVE AND ABSORPTIVE INDICES

The refractive and absorptive indices determined from the transmittance data are shown in Figs. 50 through 56 for RTV-732, DC93-500, DC6- 1104, RTV566, RTV560, S13G/LO, and Kapton, respectively. The refractive indices are shown at the top with the absorptive indices directly below.

The refractive index for a material was first calculated using TRNLIN. Values were obtained for both n and k. Using the Kramers-Kronig relationship [Eq. (8)], the TRNLIN k values were used to calculate n's. These were compared with the TRNLIN n values. Generally, there was good agreement between the two. The n values, derived using TRNLIN, were usually larger in areas of strong absorption than the Kramers-Kronig values. This may be attributable to the Subtractive Kramers-Kronig integration being carried out over the wavenumber range (700 to 4,000 cm^{-1}) instead of from zero to plus infinity as specified in the integration limits of Eq. (8). All of the refractive and absorptive indices reported were obtained using the TRNLIN program.

The transmittance experimental data were taken using 2 cm^{-1} resolution. The n's and k's then were determined at every 2 cm^{-1} in the range from 700 to 4,000 cm^{-1}. An example of the tabulated n,k data obtained for each of the materials mentioned previously is given in Table 3. Results presented in Table 3 are for RTV566. Similar tables are available for each of the other materials investigated.

6.0 TRANSMITTANCE AND REFLECTANCE CALCULATIONS USING CALCRT

To realize the maximum utility of the data (n's and k's) generated from the experimental and analytical studies, it was necessary to develop another computer program, CALCRT (calculations of reflectance and transmittance). CALCRT, written in FORTRAN IV, calculates the reflectances and transmittances of a radiation beam that strikes a film and substrate system that has planar interfaces that are, ideally, infinite in extent. The film and substrate are sandwiched between semi-infinite vacuums, so that the refractive indices on each side of the film-substrate are identically equal to one.

The user must supply the optical constants and thicknesses of the film and substrate and the incident angle of the beam. Also, the user must indicate which beam coherence case applies

and choose either an output format that gives the reflectances and transmittances as functions of wavenumber or wavelength at a constant film thickness or an output format that displays the transmittances and reflectances versus film thickness at a constant wavenumber or wavelength. The calculations can be repeated on the same optical data for incremented values of the film and substrate thicknesses and the angle of incidence.

6.1 CALCRT TRANSMITTANCE CALCULATIONS

To show how CALCRT can be used, examples of transmittance versus wavenumber and transmittance versus thickness were calculated for RTV566 material, using the n's and k's previously determined. Figure 57 shows three curves of transmittance versus wavenumber. The curves are for (1) the actual experimental data obtained for an RTV566 contaminant film 2.30 μm thick (10th interference maxima), (2) the same film thickness but calculated using the n,k values determined from TRNLIN, and (3) the same film thickness but calculated using TRNLIN k values and n values derived from the Subtractive Kramers-Kronig expression [Eq. (8)]. As seen in Fig. 57, there is excellent agreement between the three sets of data. Maximum transmittance variations were about 2 percent.

CALCRT can also be used to calculate the transmittance dependence on film thickness; an example is shown in Fig. 58 that is for RTV560 contaminant films condensed on 77 K germanium. The three curves presented are for 1,070, 1,960, and 3,250 cm^{-1}. These represent no absorption (n = 1.40, k = 0.00) for 1,960 cm^{-1}, strong absorption (n = 0.336, k = 0.3843) for 1,070 cm^{-1}, and intermediate absorption (n = 1.284, k = 0.0707) for 3,250 cm^{-1}. The solid curves for each of the three show the analytical results calculated using the TRNLIN-derived n's and k's. The data points are for the actual experimental values. As can be seen in the figure, the analytical and experimental results agree very well.

6.2 CALCRT REFLECTANCE CALCULATIONS

Figures 59 and 60 show calculated reflectance curves using CALCRT based on the TRNLIN-determined n's and k's for RTV566 contaminant films condensed near 77 K. For these calculations, the substrate is assumed to be a specular metal surface, such as a gold mirror, with a complex refractive index of n* = 1.8 + 18.i and independent of wavelength/wavenumber. This yields a bare surface reflectance of 97.8 percent for all wavelengths/wavenumbers. The symbols on the curves in Figs. 59 and 60 do not represent experimental data points, but are included to facilitate curve identification. Figure 59 shows calculated reflectances versus wavenumber for three film thicknesses, 0.23, 2.30, and 4.59 μm. For the thinnest film, 0.23 μm, degradation of a few percent is observed between 2,800 to 3,400 cm^{-1}, with little or no change for other wavenumbers. However, for the two thicker films, considerable reflectance decrease is observed. These three thicknesses were picked to

33

show typical results that can be obtained using CALCRT. The important point is that once the contaminant n's and k's have been determined, transmittances and reflectances can be calculated for any desired film thickness and for any substrate whose refractive index is known.

Figure 60 presents reflectance versus film thickness for the three wavenumbers 1,070, 1,960, and 3,250 cm^{-1}. The thin-film interference is vividly displayed for all three wavenumbers. These curves give a good indication of how little contaminant thickness it takes to cause a large decrease in a mirror's reflectance. These three wavenumbers, again, represent regions of strong, intermediate, and weak absorption.

7.0 SUMMARY

The Air Force Wright Aeronautical Laboratories (AFWAL) and the Arnold Engineering Development Center (AEDC) have initiated a program to measure optical properties of outgassing products on cryo-optic and thermal-control surfaces. Two systems have been established for surface effects studies, (1) an optical properties chamber for measuring the complex refractive index components, n and k, of contaminants condensed on a cryogenic surface and (2) a solar absorptance chamber for determining the degradation in solar reflectance of optical solar reflectors or thermal-control coatings as a function of contaminant film thickness for surfaces maintained at 25°C.

The basic optical properties used in determining surface effects of contaminants on cryogenic optical components are the real (n) and imaginary (k) portions of the complex refractive index n* = n + ik. These properties, generally, are unavailable to designers who must predict long-term contamination effects. In this study, the n's and k's were determined from IR transmittance measurements of several contaminant film thicknesses condensed on a cryogenic germanium window. The transmittance data were then input into an analytical thin-film interference model, called TRNLIN, which determined the best n,k fit for all of the data using a nonlinear least-squares convergence routine. In some instances, the subtractive Kramers-Kronig technique was used to determine n, if the TRNLIN program did not converge on a unique n value.

The contaminant films were formed by placing a sample of the material to be studied in an effusion cell, heating and controlling the material at 125°C, and condensing the outgassed products under vacuum (10^{-7} to 10^{-6} torr) on a germanium window cooled to 80 K. The film thicknesses were measured using a dual-angle interference technique with two helium-neon lasers. IR transmittance measurements were made using an interferometer for the wavenumber range from 4,000 to 450 cm^{-1}. Calculations for n,k were made only for the 4,000 to 700 cm^{-1} range since beyond 700 cm^{-1} the germanium becomes absorbing. Materials that have been tested include the adhesives DC93-500, DC6-1104, RTV566, RTV560,

RTV-732, S13G/LO paint, and Kapton. These materials provided enough outgassed products to determine the n's and k's. Table 3 gives the n,k values determined for RTV566 as an example of the property values that are now available.

A computer program, CALCRT, has been written that calculates the transmittance and reflectance values for the following parameters: substrate refractive index and thickness, contaminant refractive index and film thickness, incidence angle, wavenumber, and wavelength. The program calculates both parallel and perpendicular polarization components as well as the degrees of polarization for the reflected and transmitted beams. This provides a potential optical property user with the program for using the n's and k's generated for the materials mentioned previously.

The solar absorptance chamber was designed, and fabrication was completed. This system is just now becoming operational and will provide a means of (1) contaminating an optical solar reflector (OSR), maintained at 25°C, with outgassing products from the satellite material heated to 125°C in an effusion cell, (2) translating the OSR to an integrating sphere refectometer, where the spectral solar absorptance of the contaminated surface will be measured for the 0.25- to 2.5-μm wavelength range, and (3) irradiating the contaminated film with UV from a solar simulator. A QCM, maintained at 25°C, will provide a method for determining condensed contaminant mass on the surface and, hence, film thickness. Solar cell array output can be monitored to determine contaminant effects on solar cell efficiencies. The array can be contaminated using the same effusion cell, and the solar irradiance can be provided by the xenon lamp used for UV studies.

7.1 FUTURE EFFORTS

Future plans call for investigations of the following areas:

1. Continue n,k measurements of outgassed products from satellite materials on AFWAL's list (Table 1), heated to 125°C and condensed on LN_2-cooled germanium.

2. Reduce the effusion cell temperature to 75°C or below and compare results with that obtained for the 125°C temperature.

3. Begin BRDF measurements on cryogenic optical surfaces that have been contaminated with the outgassed products of satellite materials. Measurements will be made, initially, using a He-Ne laser for the scattering source, and it will later be replaced with a CO_2 laser.

4. Begin solar absorptance measurements in the SAM chamber for OSR's at 25°C contaminated with satellite material outgassing products. Determine UV effects on the contaminant by irradiation with a xenon lamp and measuring reflectance changes.

. 5. Determine degradation of solar cells attributable to deposited contaminants.

REFERENCES

1. Glassford, A. P. M. and Garrett, J. W. "Characterization of Contamination Generation Characteristics of Satellite Materials Phase II—Test Method Development." AFWAL-TR-85-4118, December 1985.

2. Herzberger, M. and Salzberg, C. D. "Refractive Indices of Infrared Optical Materials and Color Correction of Infrared Lenses." *Journal of the Optical Society of America,* Vol. 52, Number 4, April 1962, pp. 420-427.

3. Operation and Service Manual for Quartz Crystal Microbalance, QCM Sensor Mark 9, QCM Research, Laguna Beach, California.

4. Hall, D. F. and Stewart, T. B. "Photo-Enhanced Spacecraft Contamination Deposition." AIAA Paper No. 85-0953, Presented at the AIAA 20th Thermophysics Conference, June 19-21, 1985.

5. Wood, B. E. and Roux, J. A."Infrared Optical Properties of Thin H_2O, NH_3, and CO_2 Cryofilms." *Journal of the Optical Society of America,* Vol. 72, No.6, June 1982, pp. 720-728.

6. Roux, J. A. et al. "IR Optical Properties of Bipropellant Cryocontaminants." *Proceedings of the USAF/NASA International Spacecraft Contamination Conference,* Edited by Capt. J. M. Jemiola, AFML-TR-78-190 and NASA-CP-2039, March 1978, pp.412-455.

7. Wood, B. E. and Smith, A. M. "Infrared Reflectance of Condensed Gas Films." *Progress in Astronautics and Aeronautics: Thermophysics and Thermal Control,* Vol. 65, Edited by Raymond Viskanta, 1979, pp. 22-38.

8. Campbell, William A., Jr., Marriott, Richard S., and Park, John J. "Outgassing Data for Selecting Spacecraft Materials." NASA RP 1124, June 1984.

9. Roux, J.A., Wood, B.E., and Smith, A.M. "IR Optical Properties of Thin H_2O, NH_3, and CO_2 Cryofilms." AEDC-TR-79-57 (AD-A074913), September 1979.

10. Wood, B.E. and Roux, J.A. "Infrared Optical Properties of Thin CO, NO, CH_4, HCl, N_2O, O_2, and Ar Cryofilms." *AIAA Progress in Astronautics and Aeronautics; Spacecraft Contamination: Sources and Prevention,* Vol. 91, Edited by J.A. Roux and T.D. McCay, 1984, pp. 139-161.

11. Heavens. O.S. *Optical Properties of Thin Films,* Dover Publications, Inc., New York, 1965.
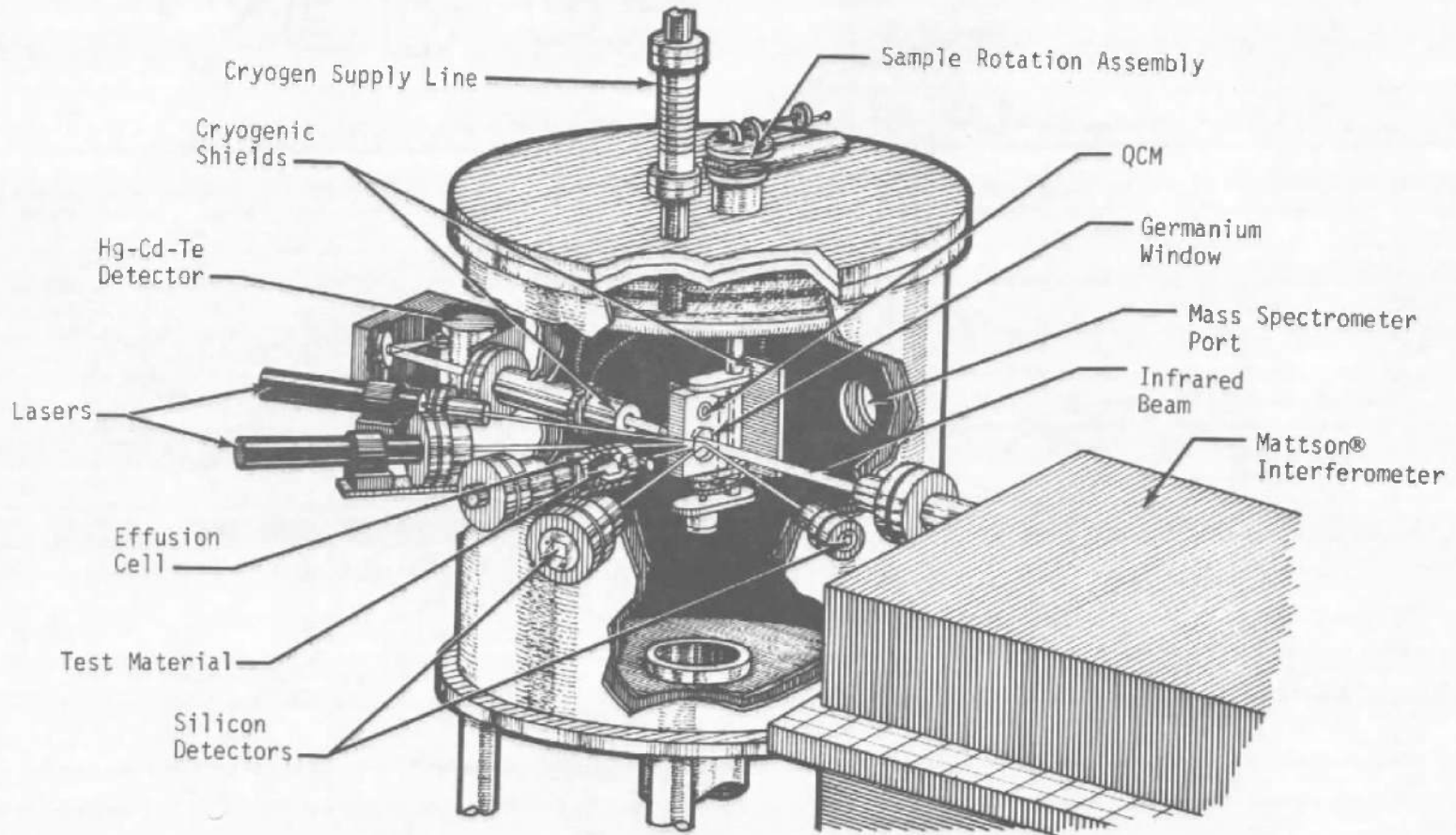
Figure 1. Schematic of 2-by 3-ft cryogenic optics degradation chamber.
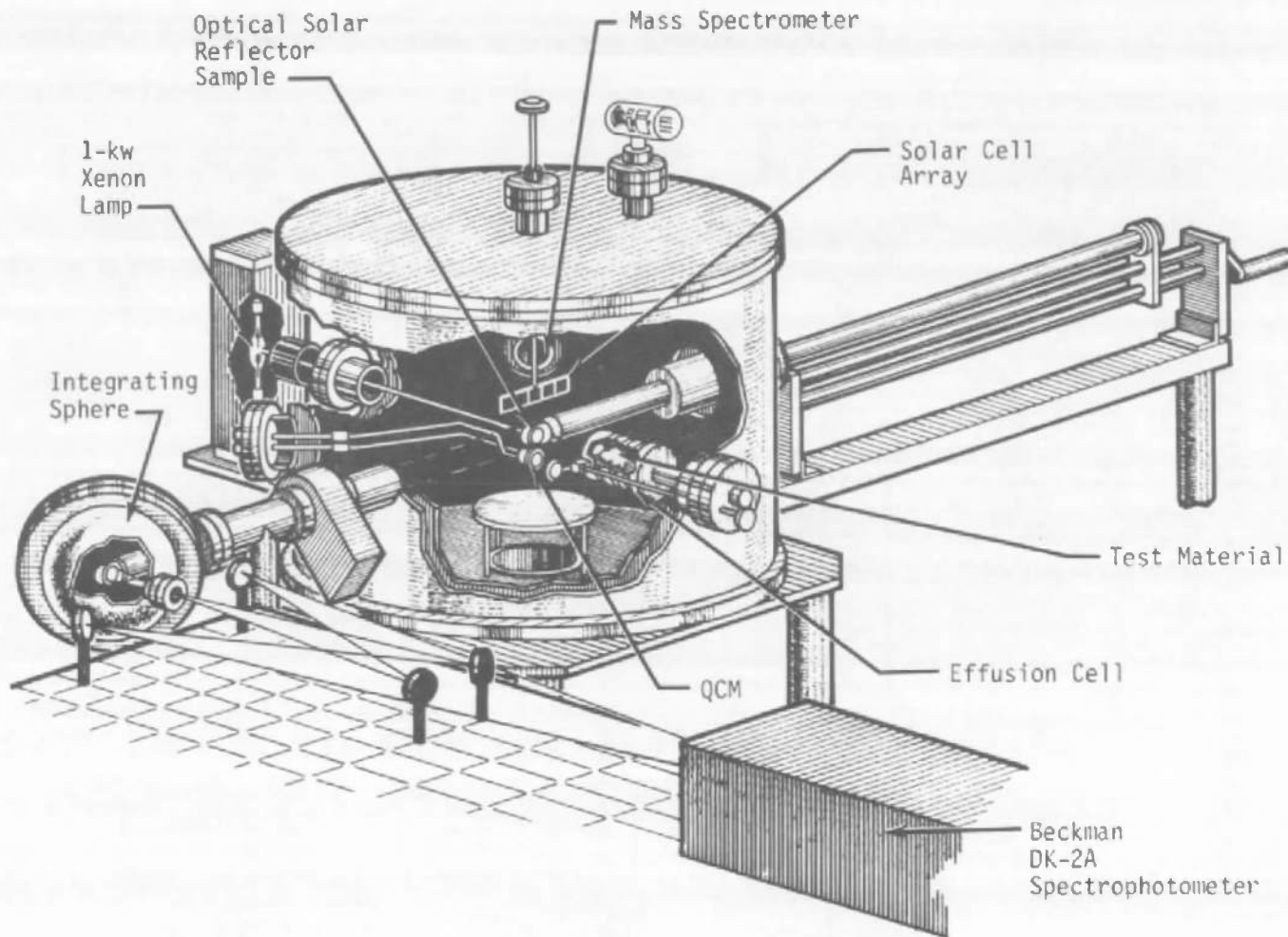
Figure 2. Solar absorptance measurements facility.

Figure 3. Effusion cell.

Labels in figure:
- Mounting Rod
- Shutter Assembly
- Heat-Transfer Isolator
- RTD
- Heater (3 Places)
- Aluminum Body
- Orifice Plate
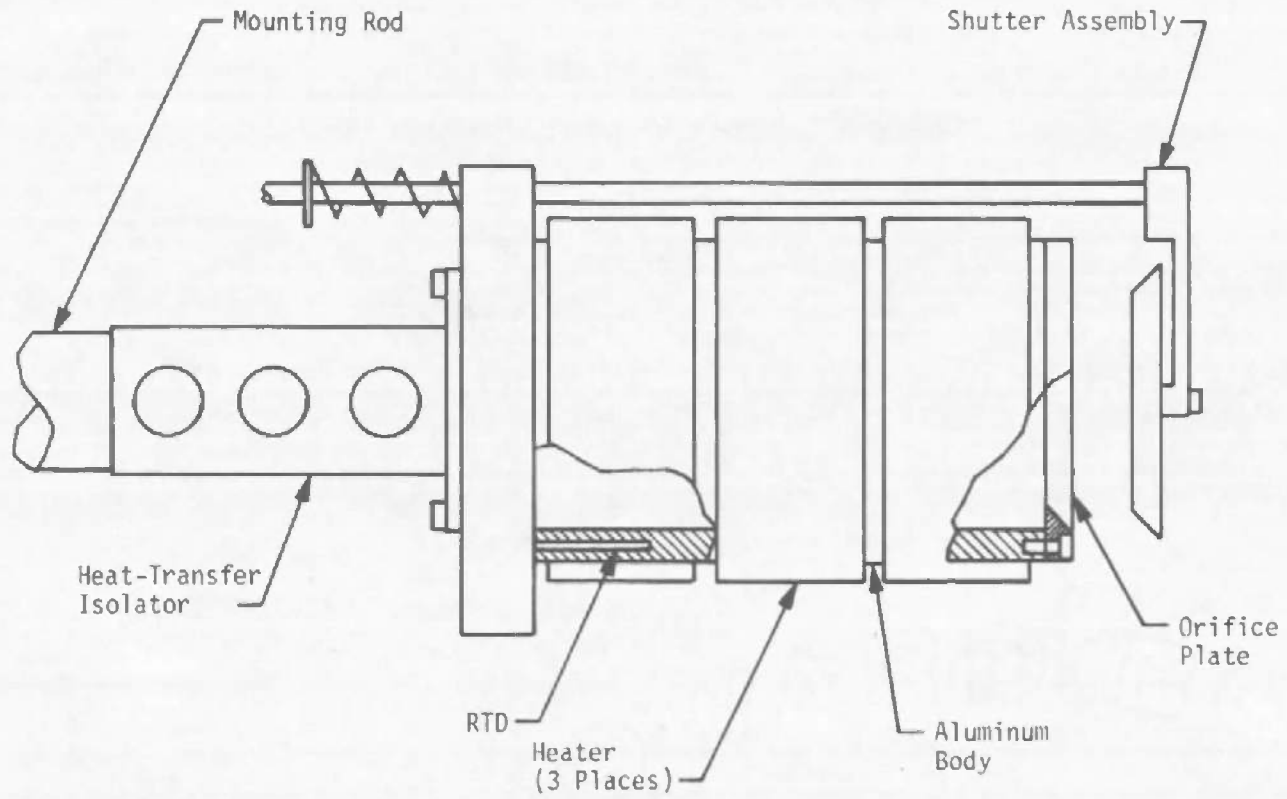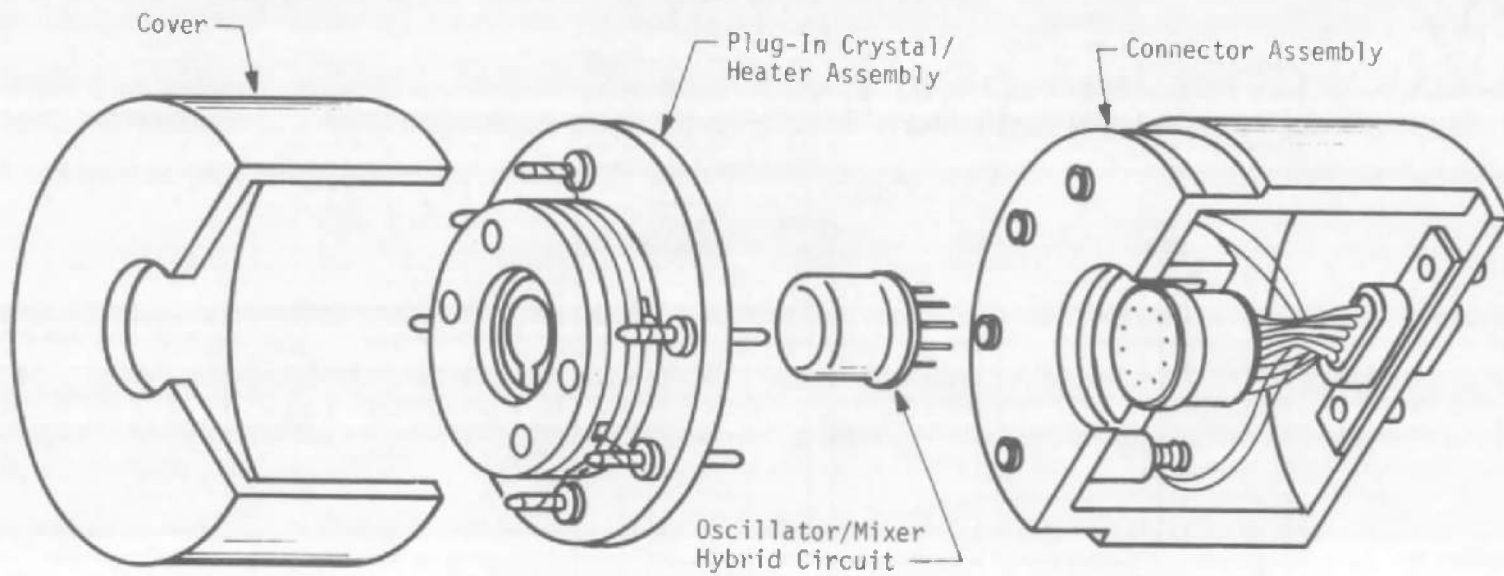
Figure 4. Quartz crystal microbalance, exploded view.
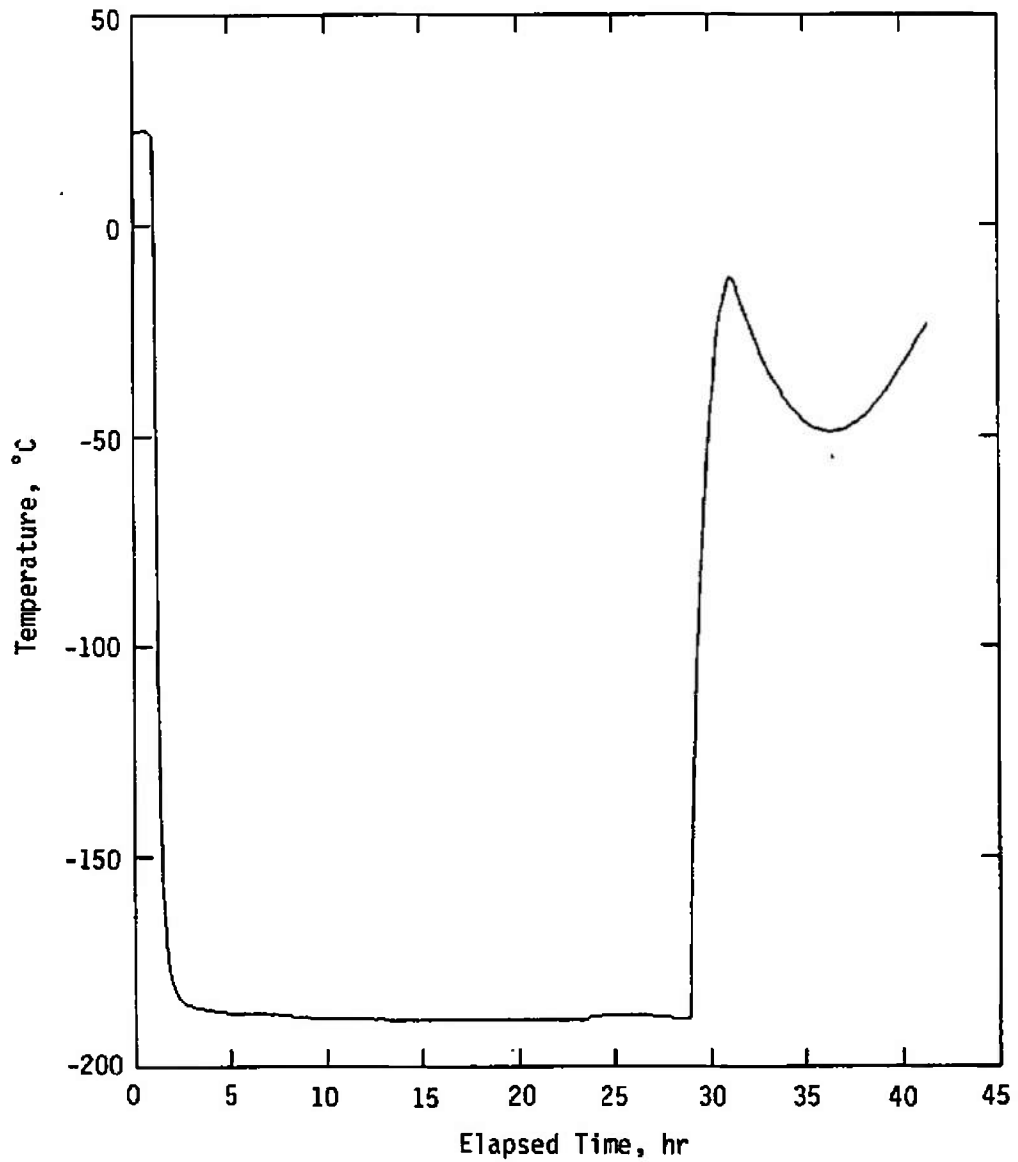
Figure 5. Housekeeping data, QCM temperature versus time for RTV566.
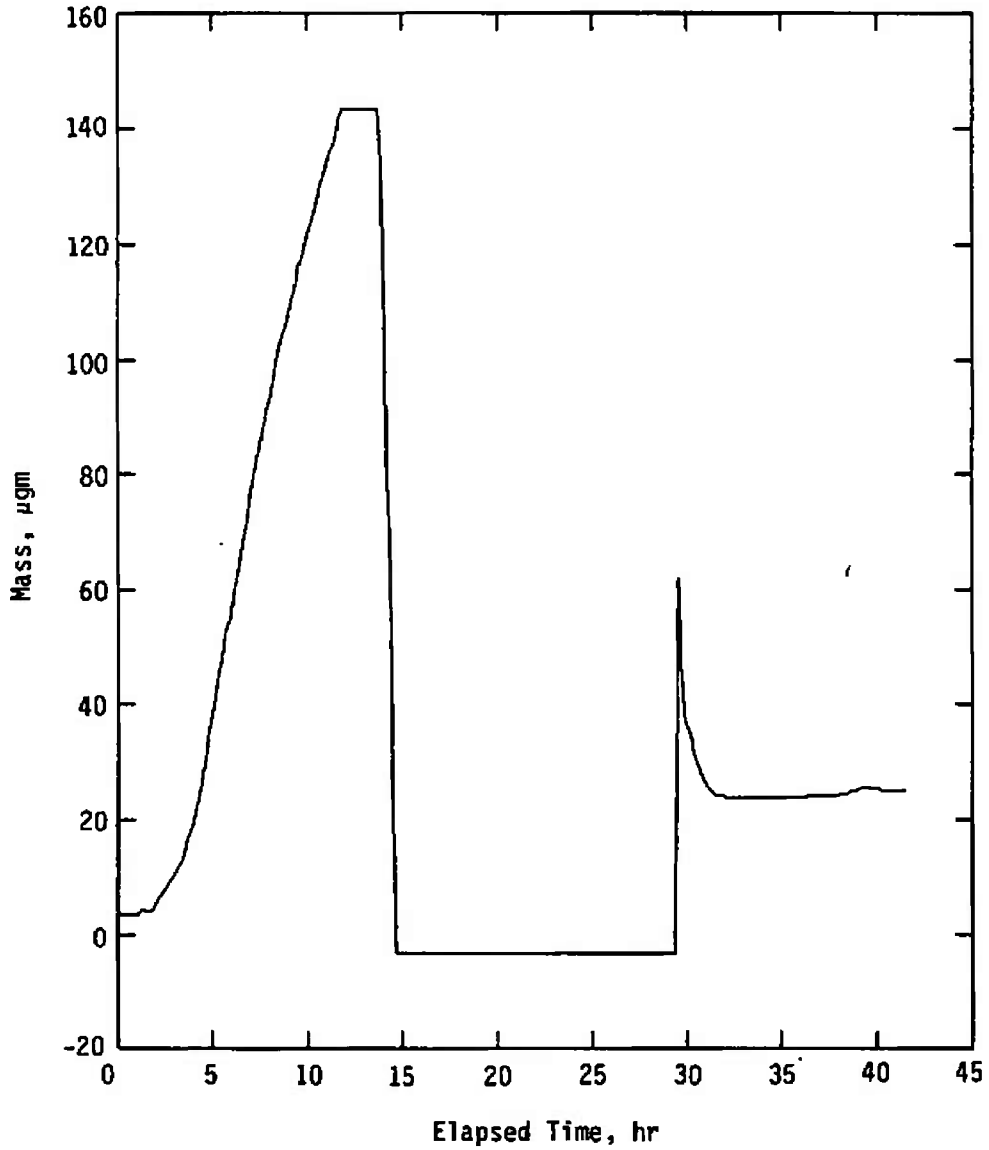
Figure 6. Housekeeping data, QCM mass versus time for RTV566.
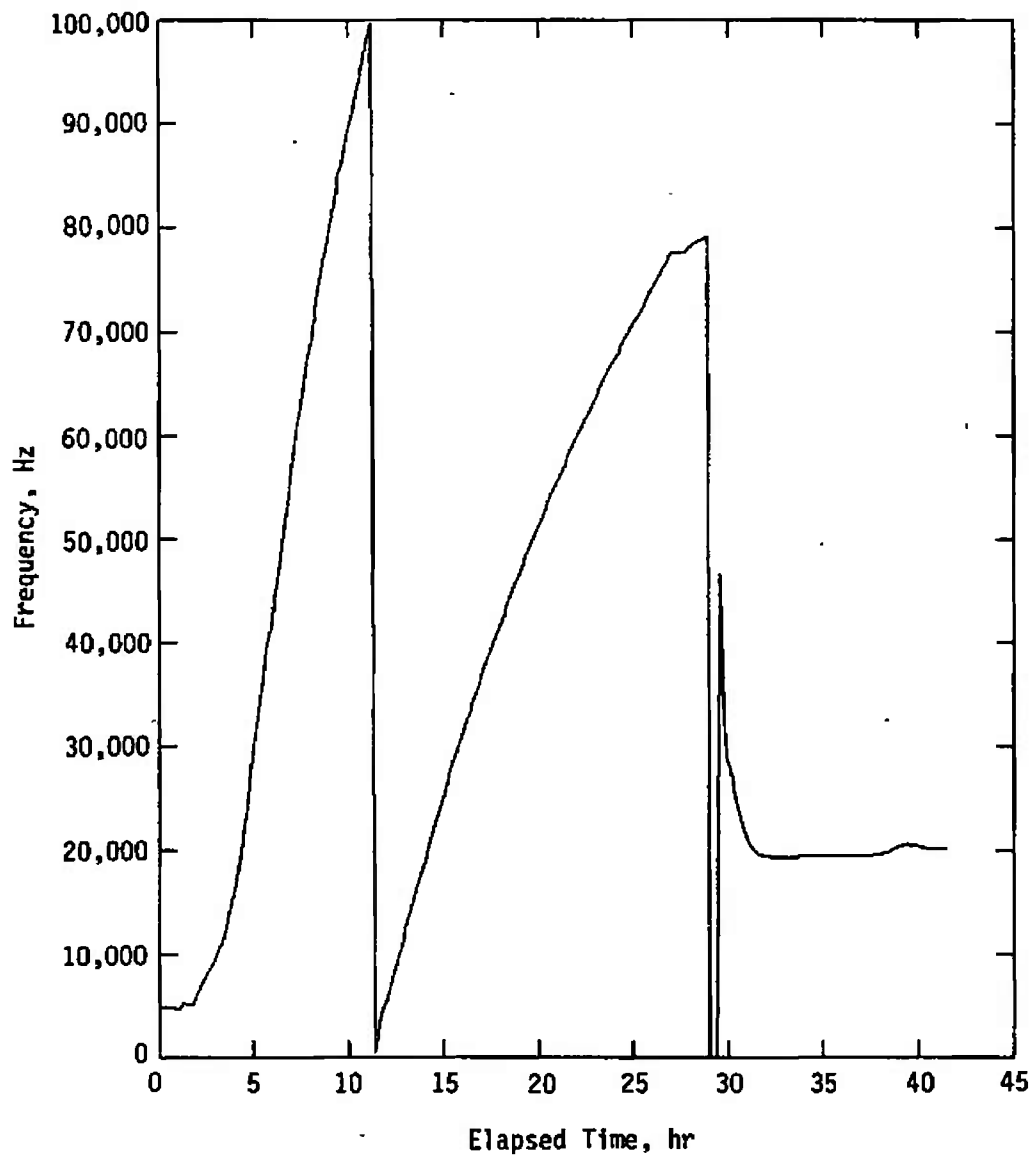
Figure 7. Housekeeping data, QCM frequency versus time for RTV566.
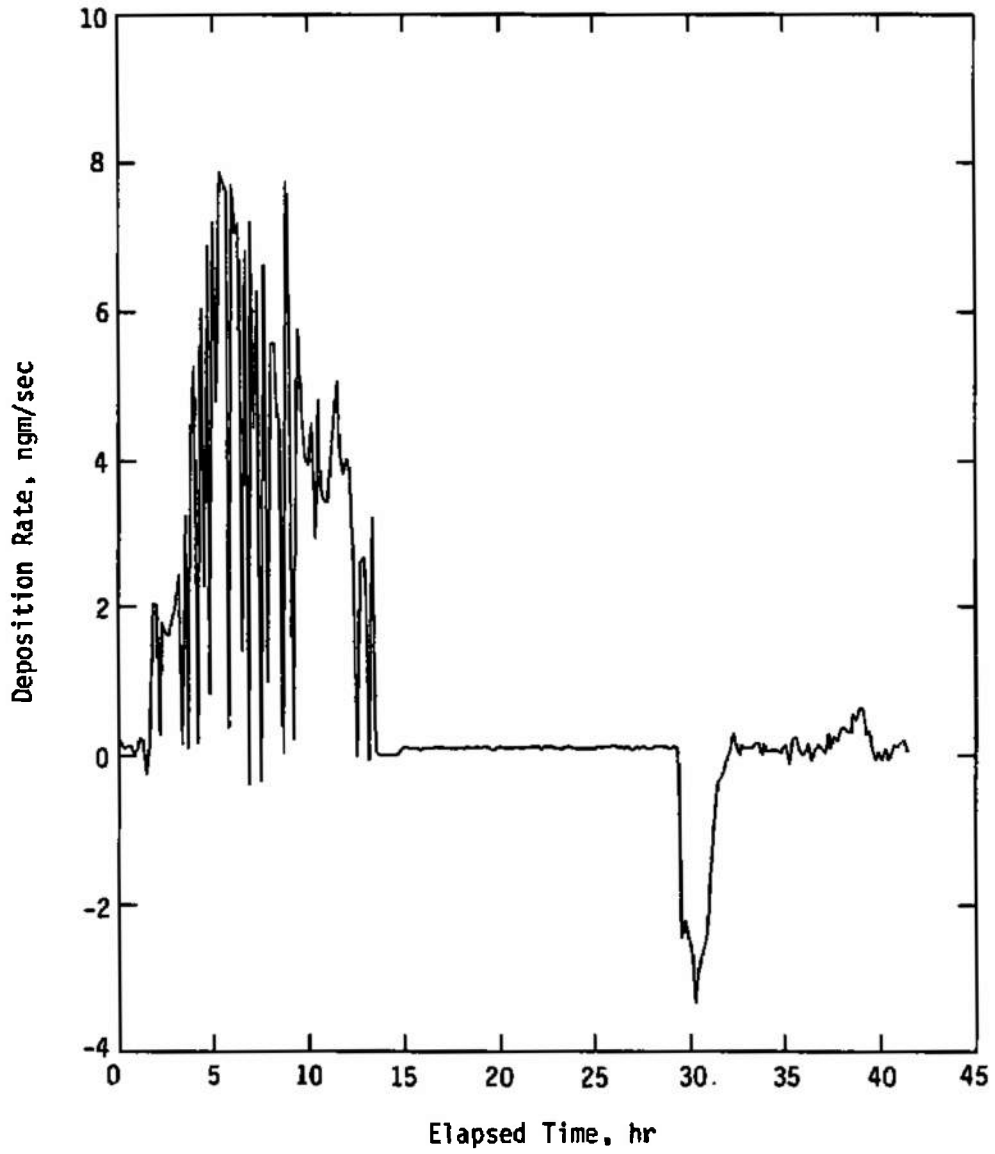
Figure 8. Housekeeping data, QCM mass deposition rate versus time for RTV566.
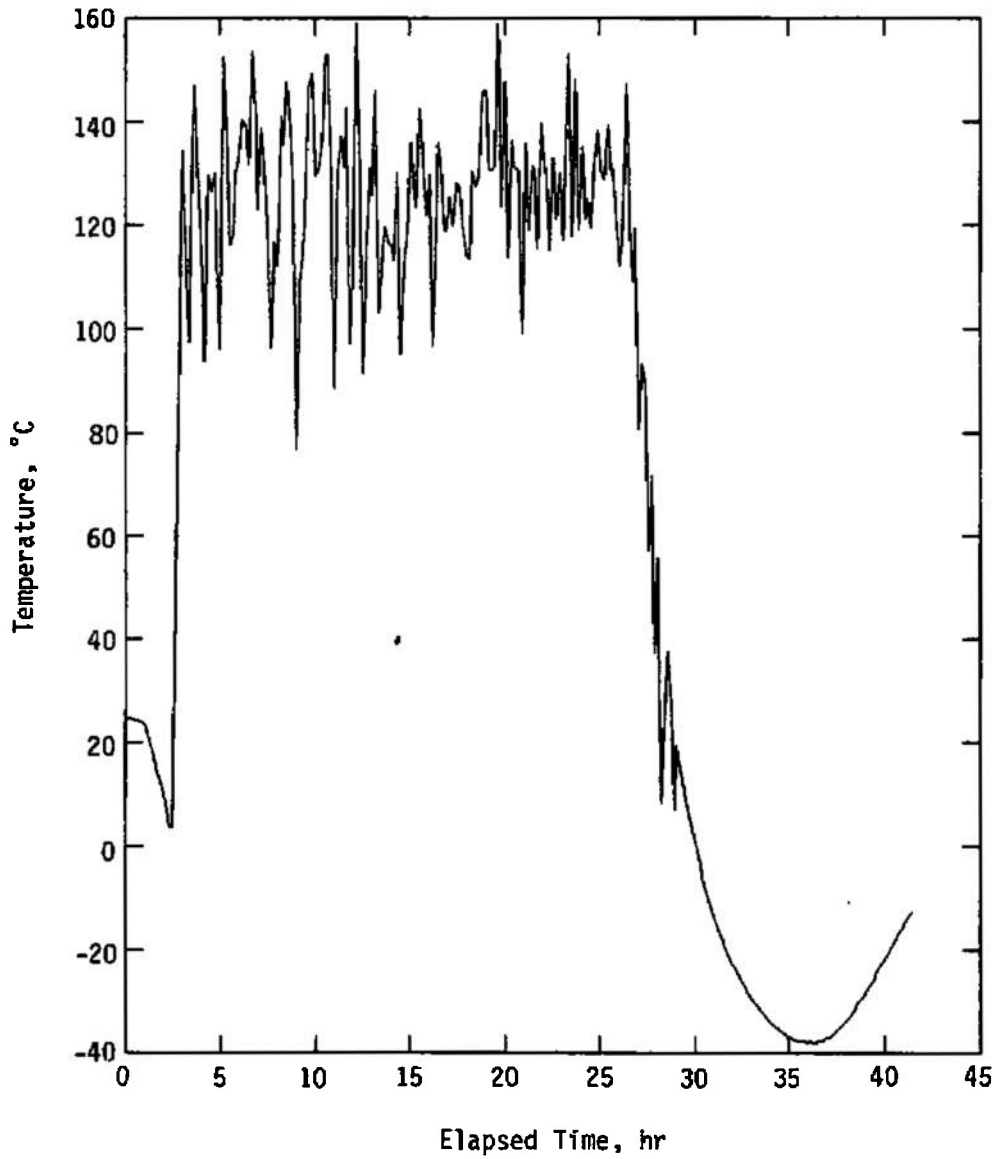
Figure 9. Housekeeping data, effusion cell temperature versus time for RTV566.
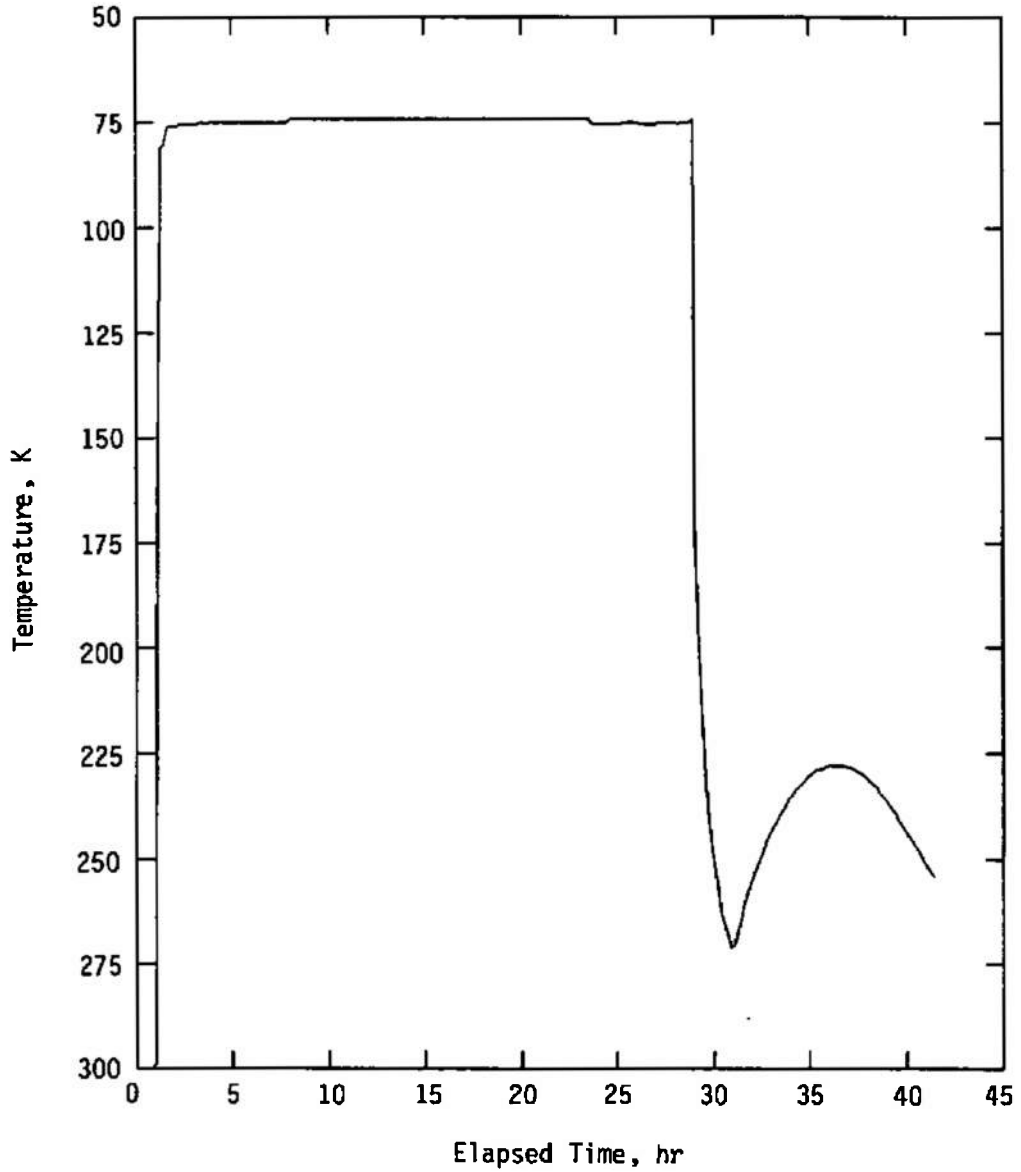
Figure 10. Housekeeping data, germanium window temperature versus time for RTV566.
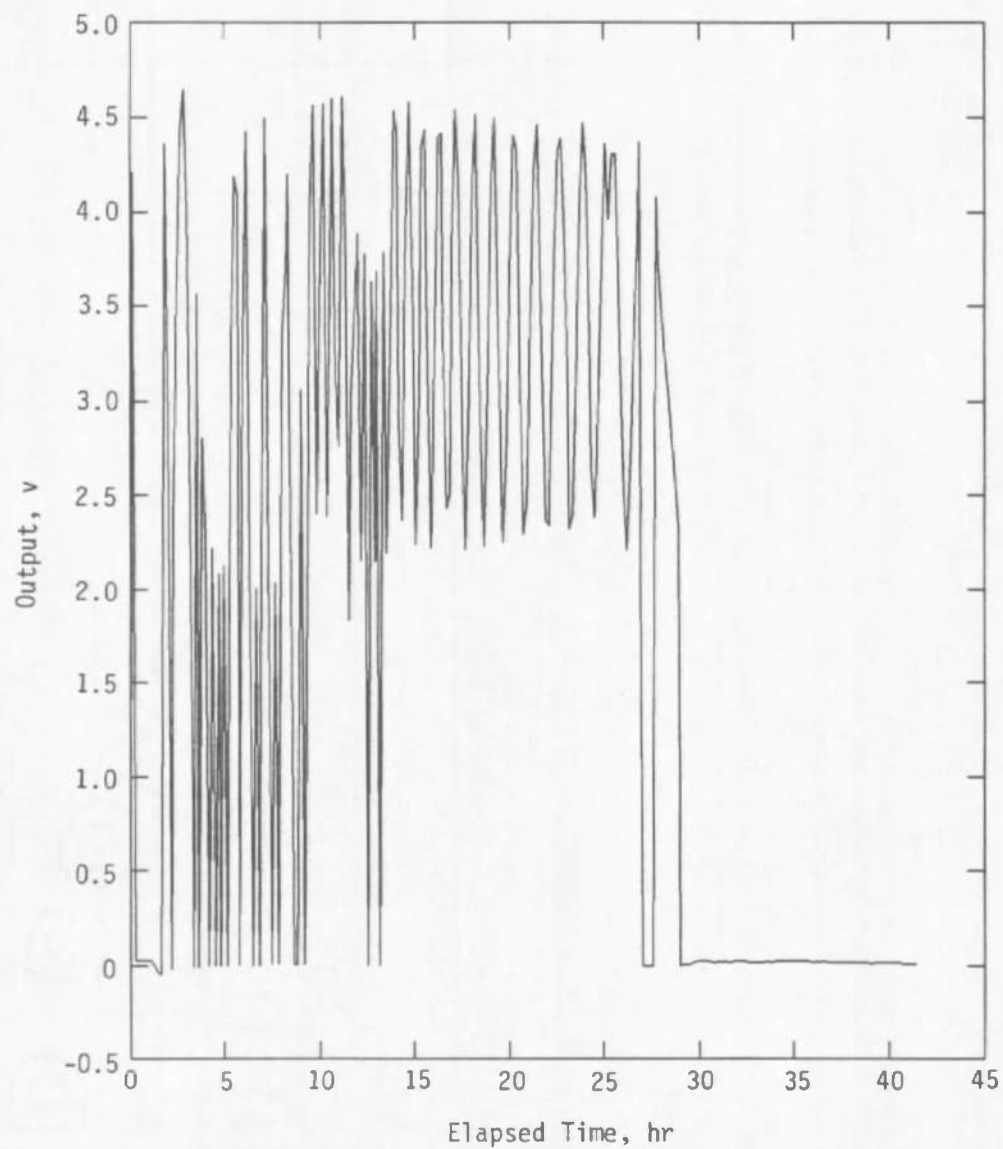
Figure 11. Housekeeping data, low-angle laser-solar cell output versus time for RTV566.
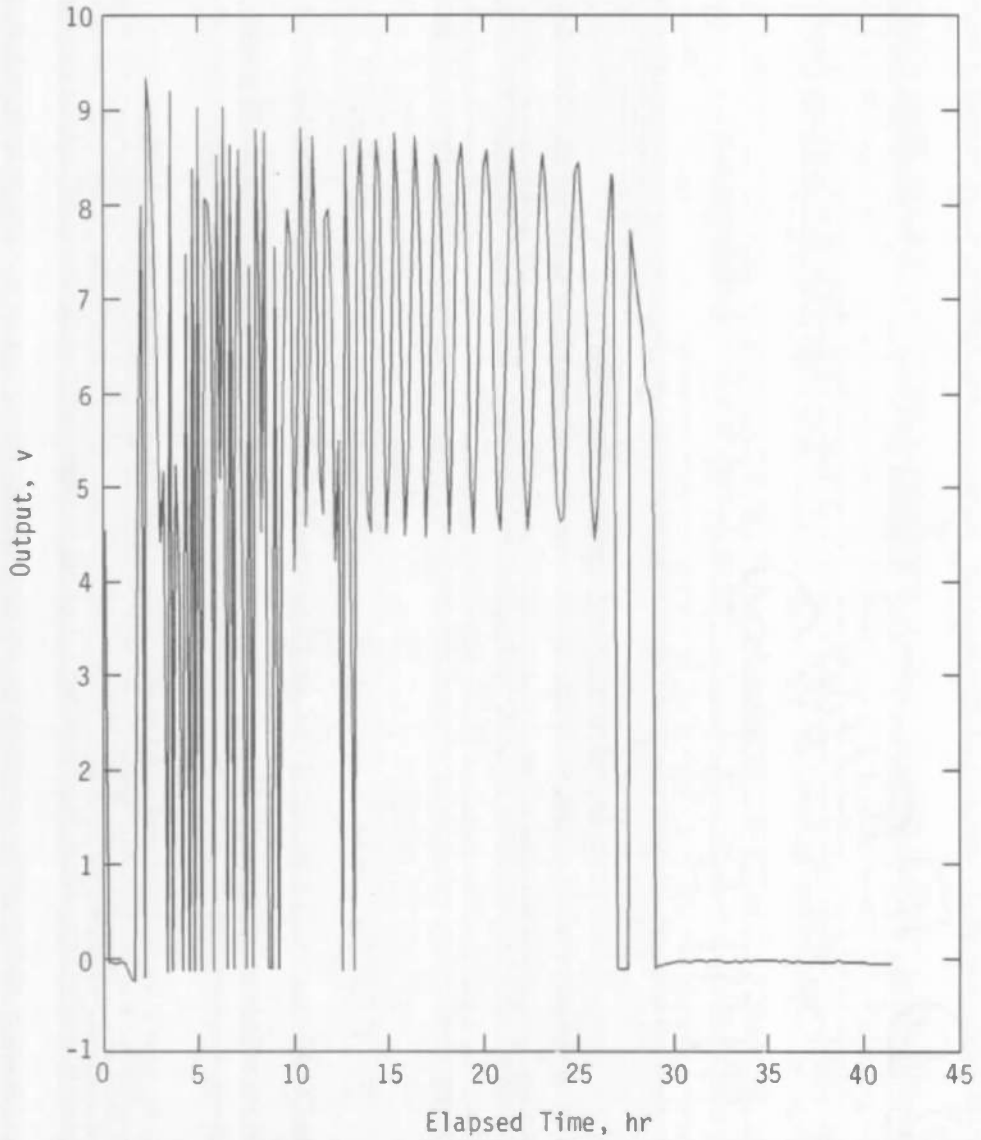
Figure 12. Housekeeping data, high-angle laser-solar cell output versus time for RTV566.
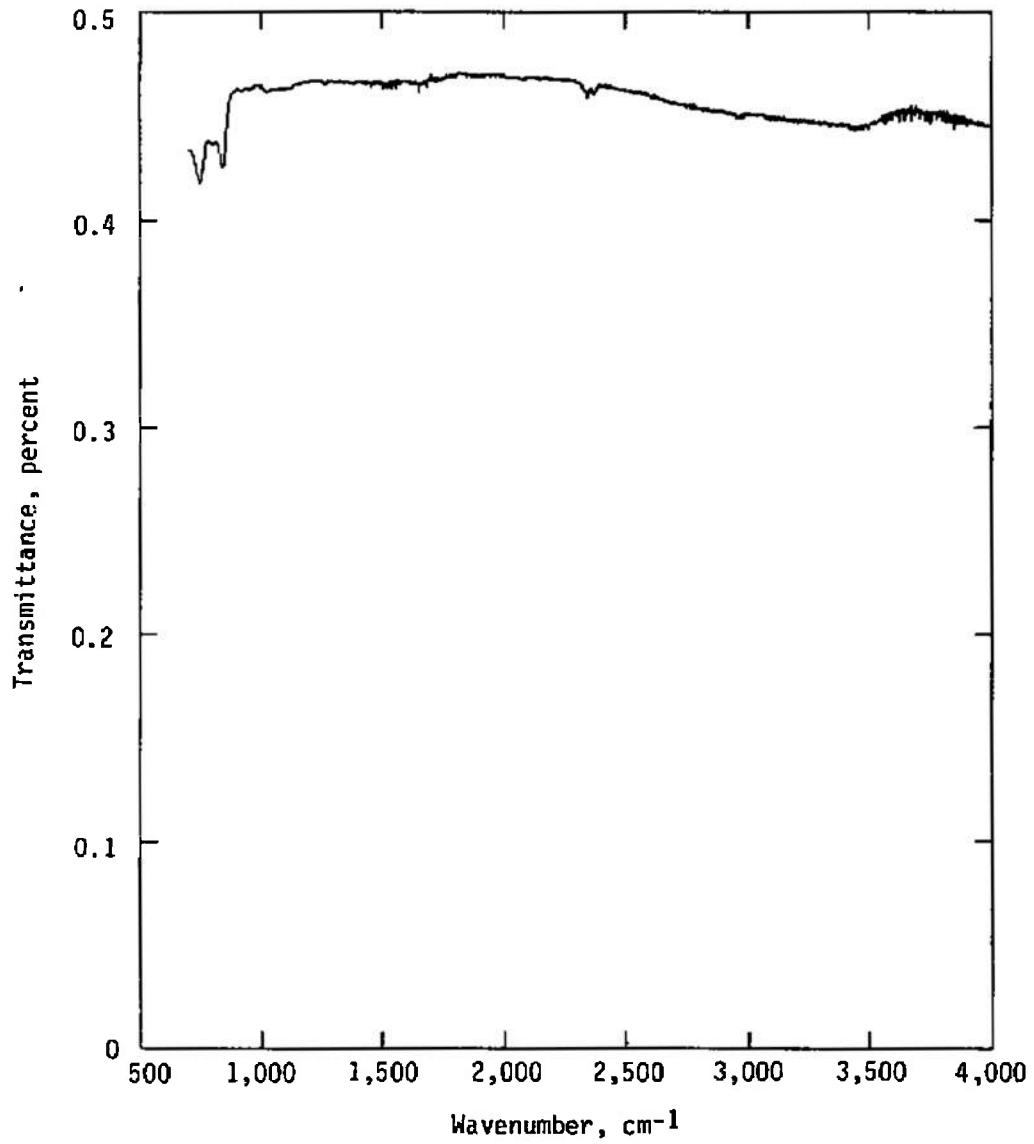
Figure 13. Transmittance of clean germanium window at 25°C.
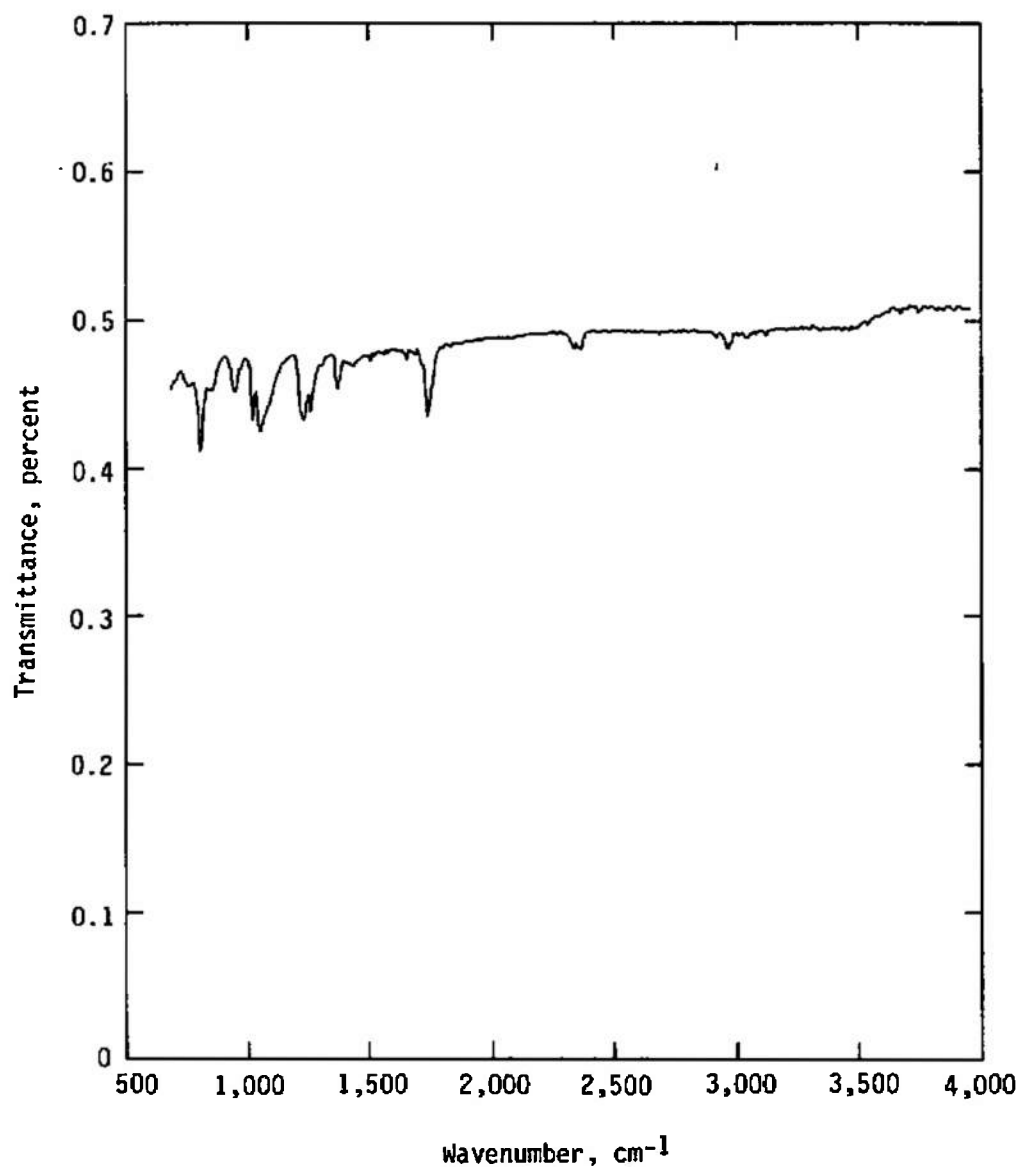
Figure 14. Transmittance of 0.23-μm-thick contaminant film condensed on 77 K germanium window, material RTV-732.
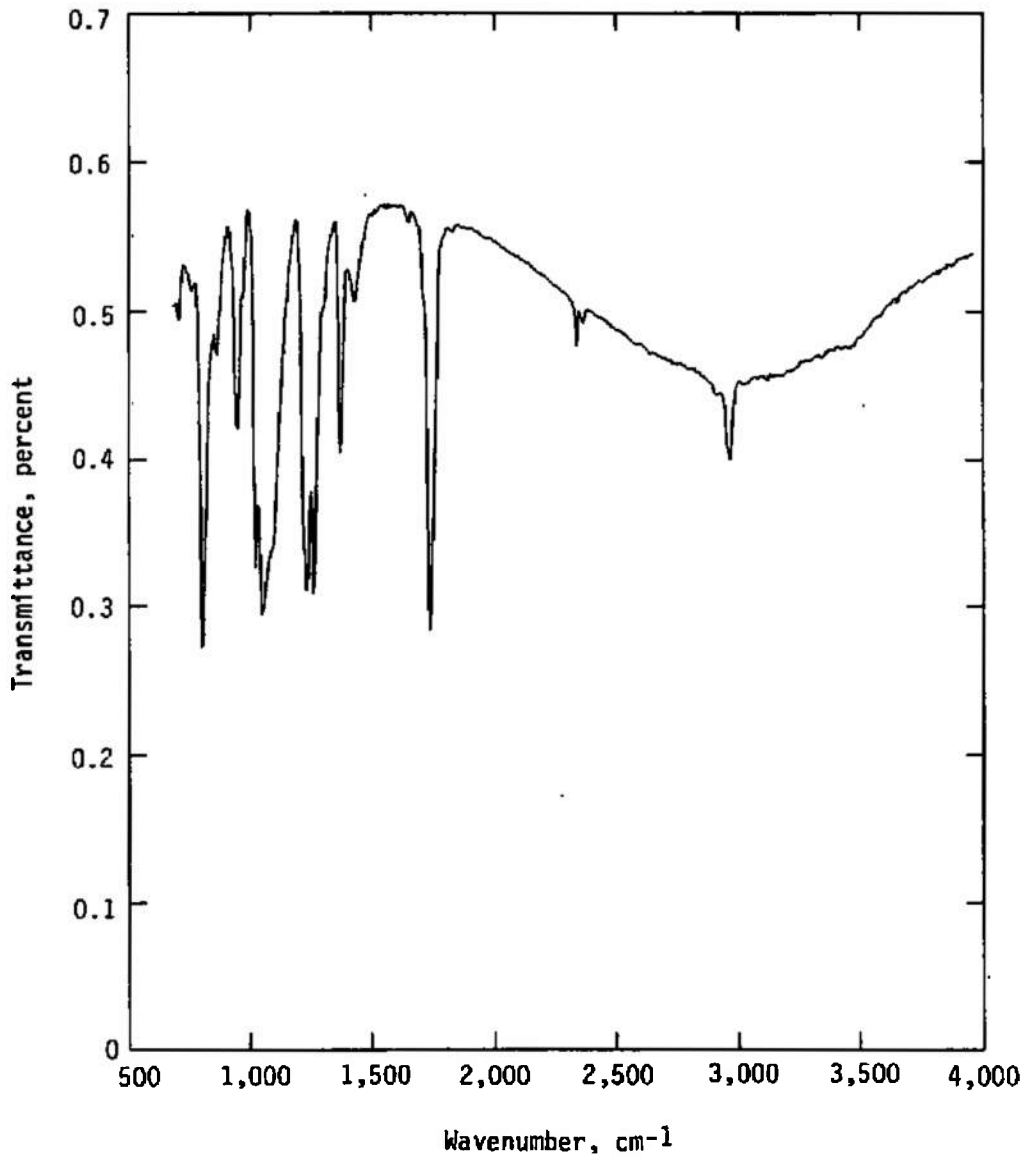
Figure 15. Transmittance of 1.15-μm-thick contaminant film condensed on 77 K germanium window, material RTV-732.
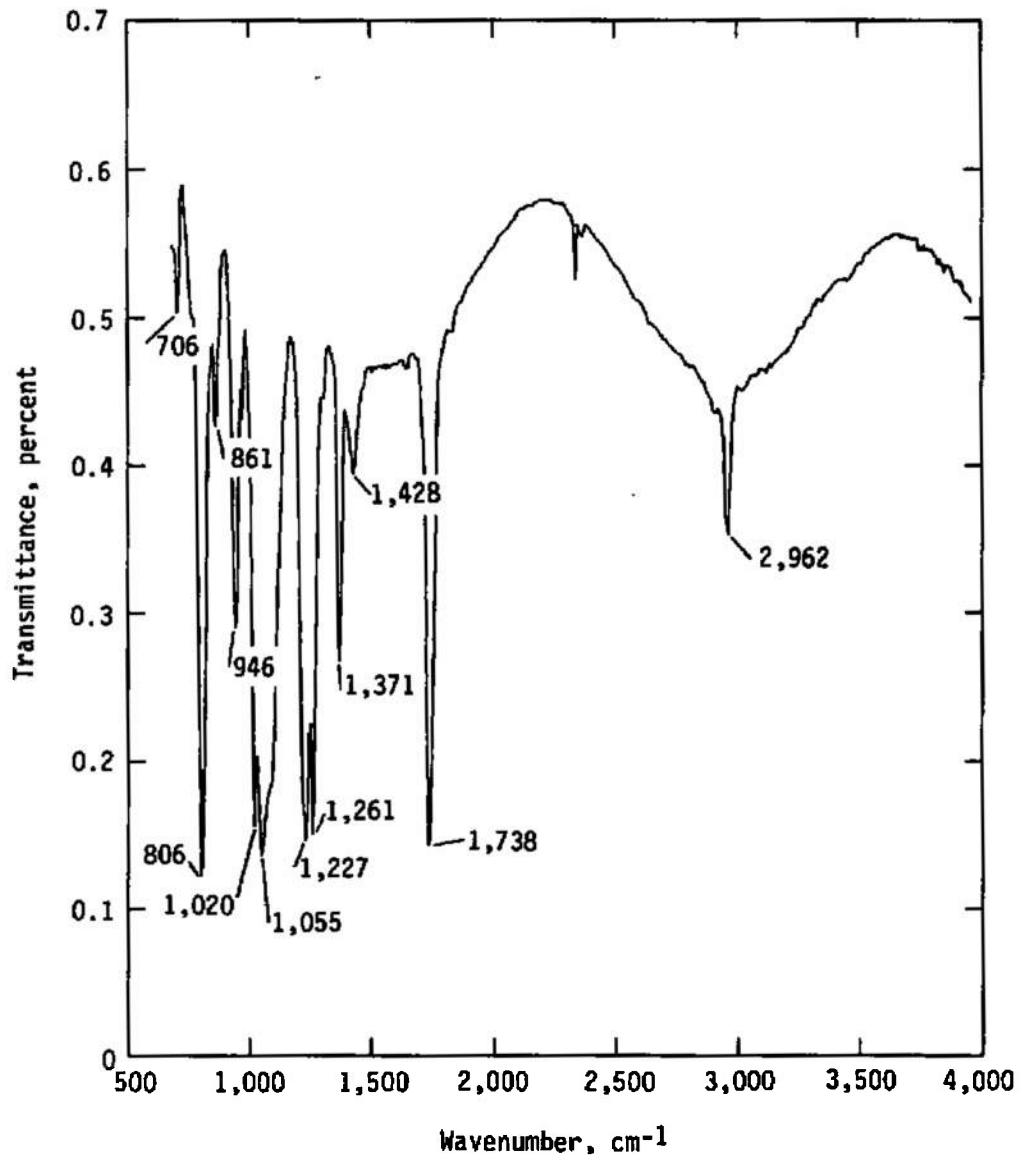
Figure 16. Transmittance of 2.29-μm-thick contaminant film condensed on 77 K germanium window, material RTV-732.
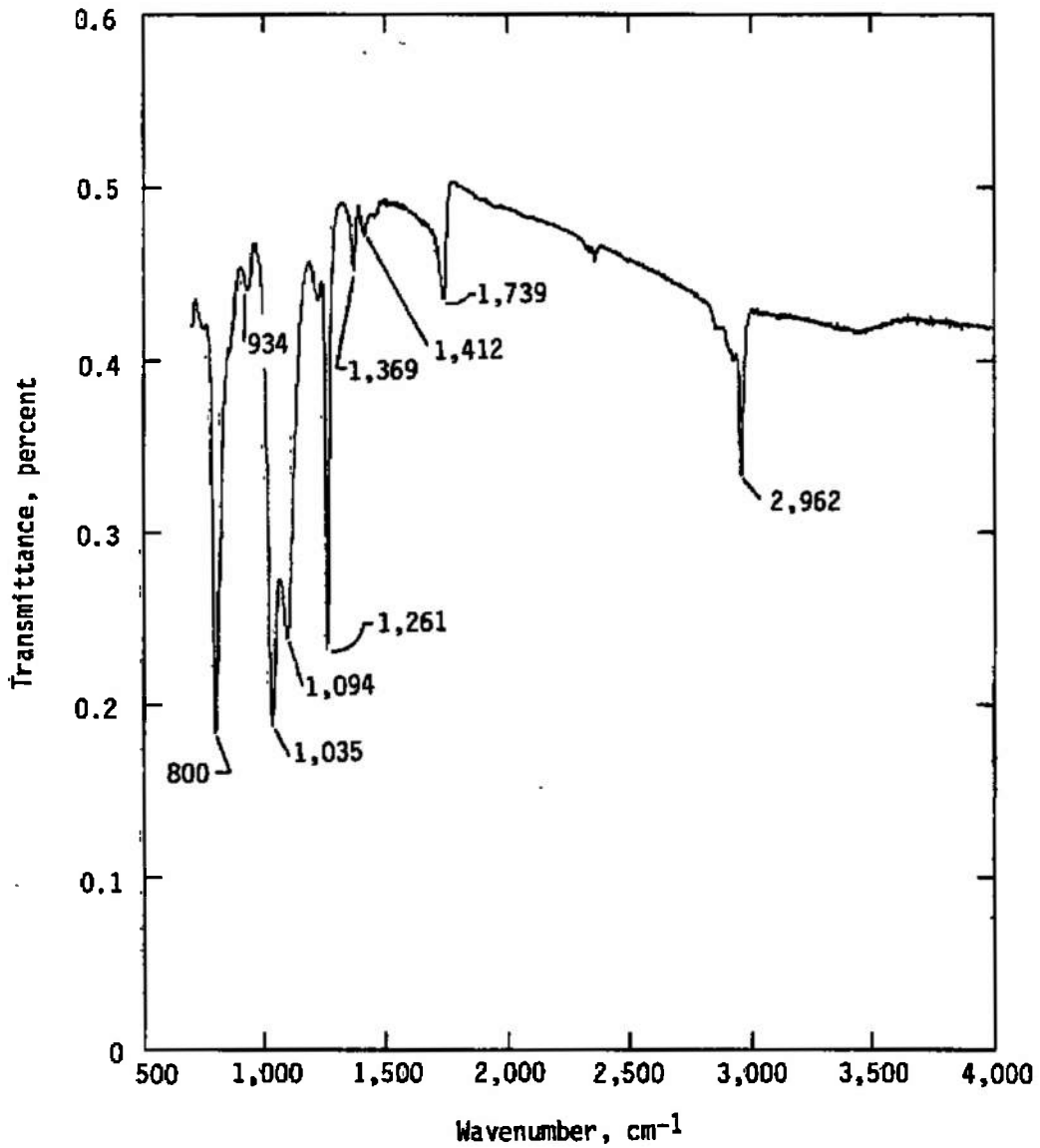
Figure 17. Transmittance of germanium window with contaminant film remaining after warmup to 10°C, material RTV-732.
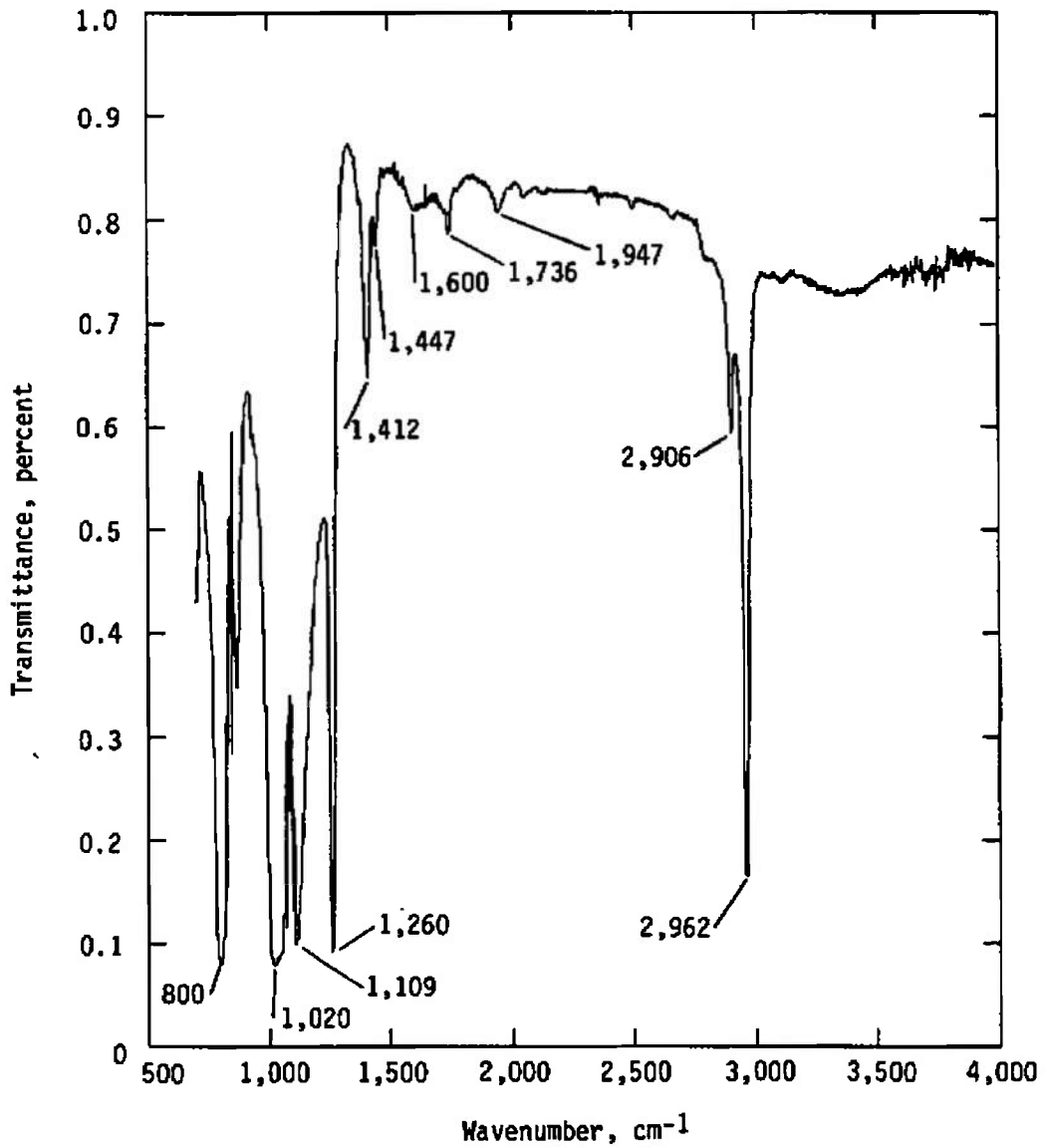
Figure 18. Transmittance of RTV-732 Silastic® smeared on an NaCl window at 25°C and at atmospheric pressure.
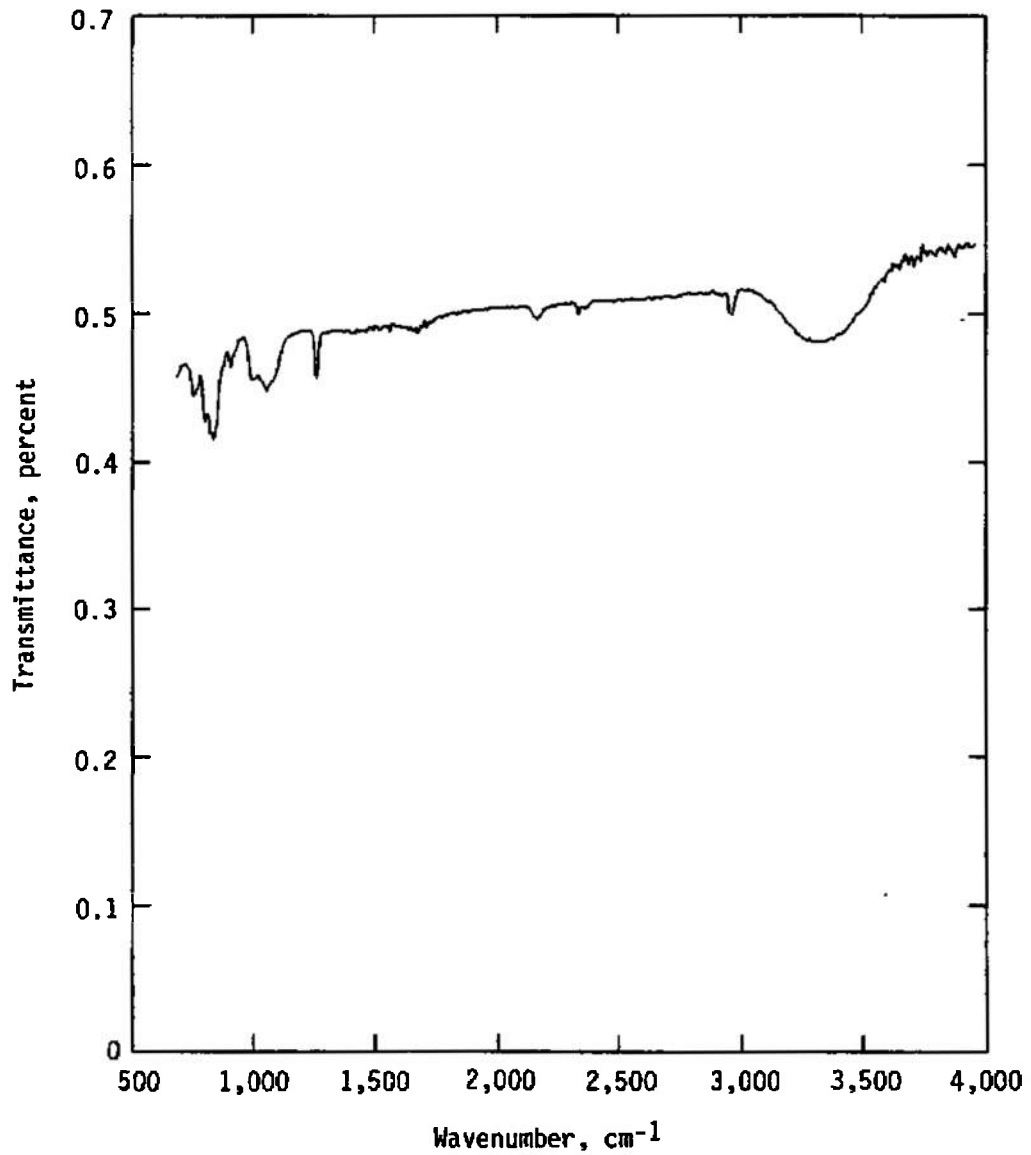
Figure 19. Transmittance of 0.23-μm-thick contaminant film condensed on 77 K germanium window, material DC93-500.
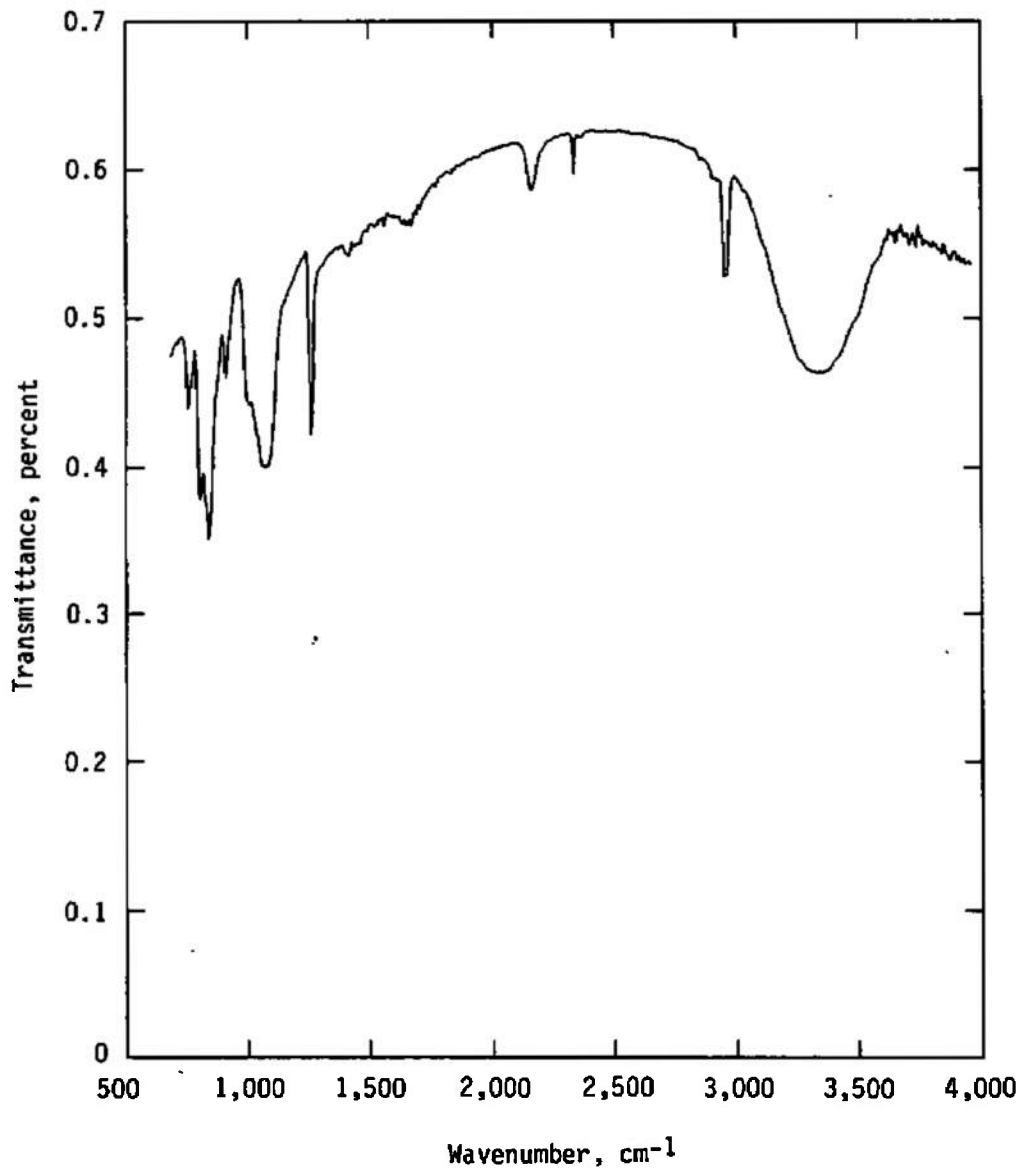
Figure 20. Transmittance of 0.69-μm-thick contaminant film condensed on 77 K germanium window, material DC93-500.
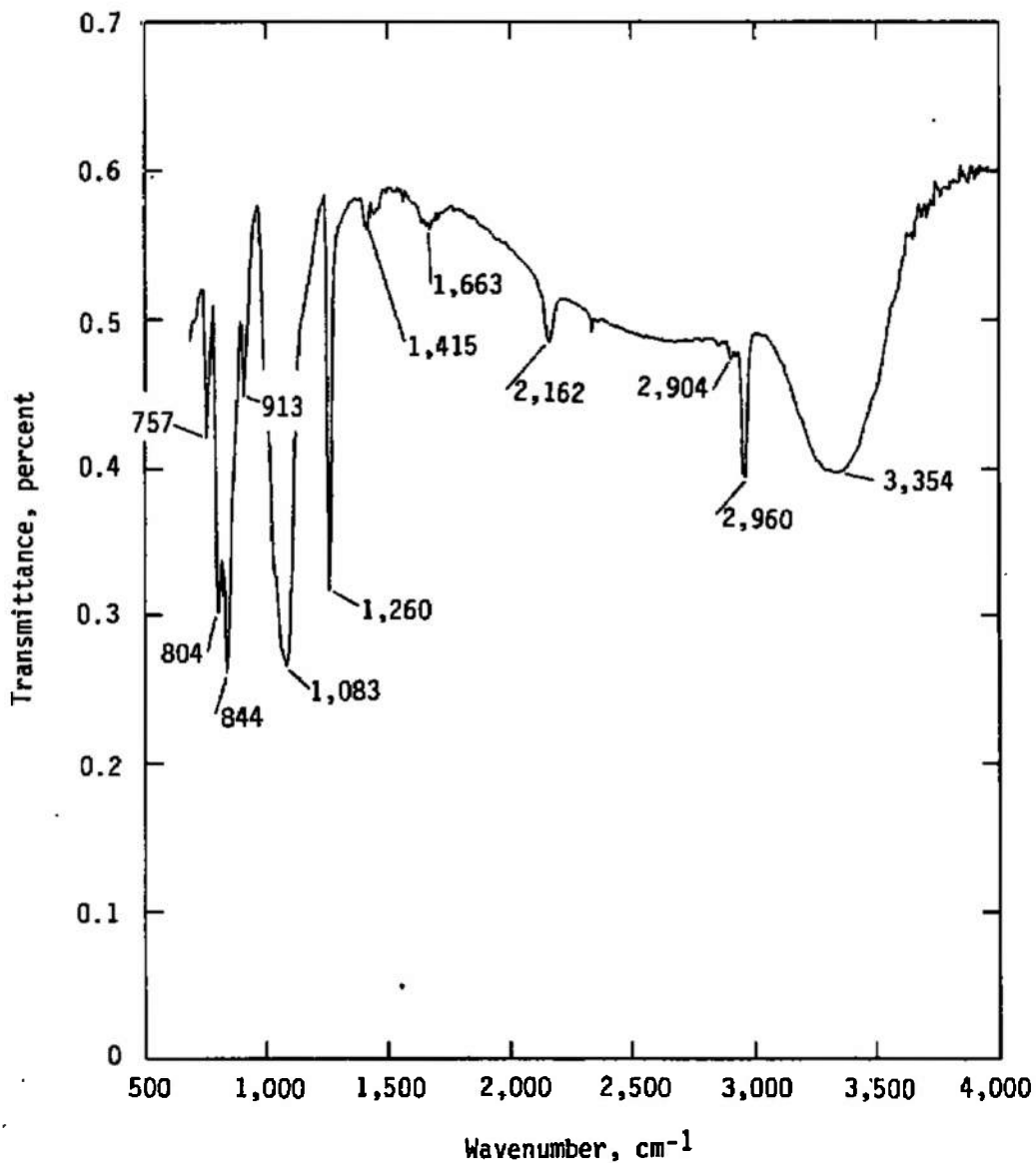
Figure 21. Transmittance of 1.26-μm-thick contaminant film condensed on 77 K germanium window, material DC93-500.
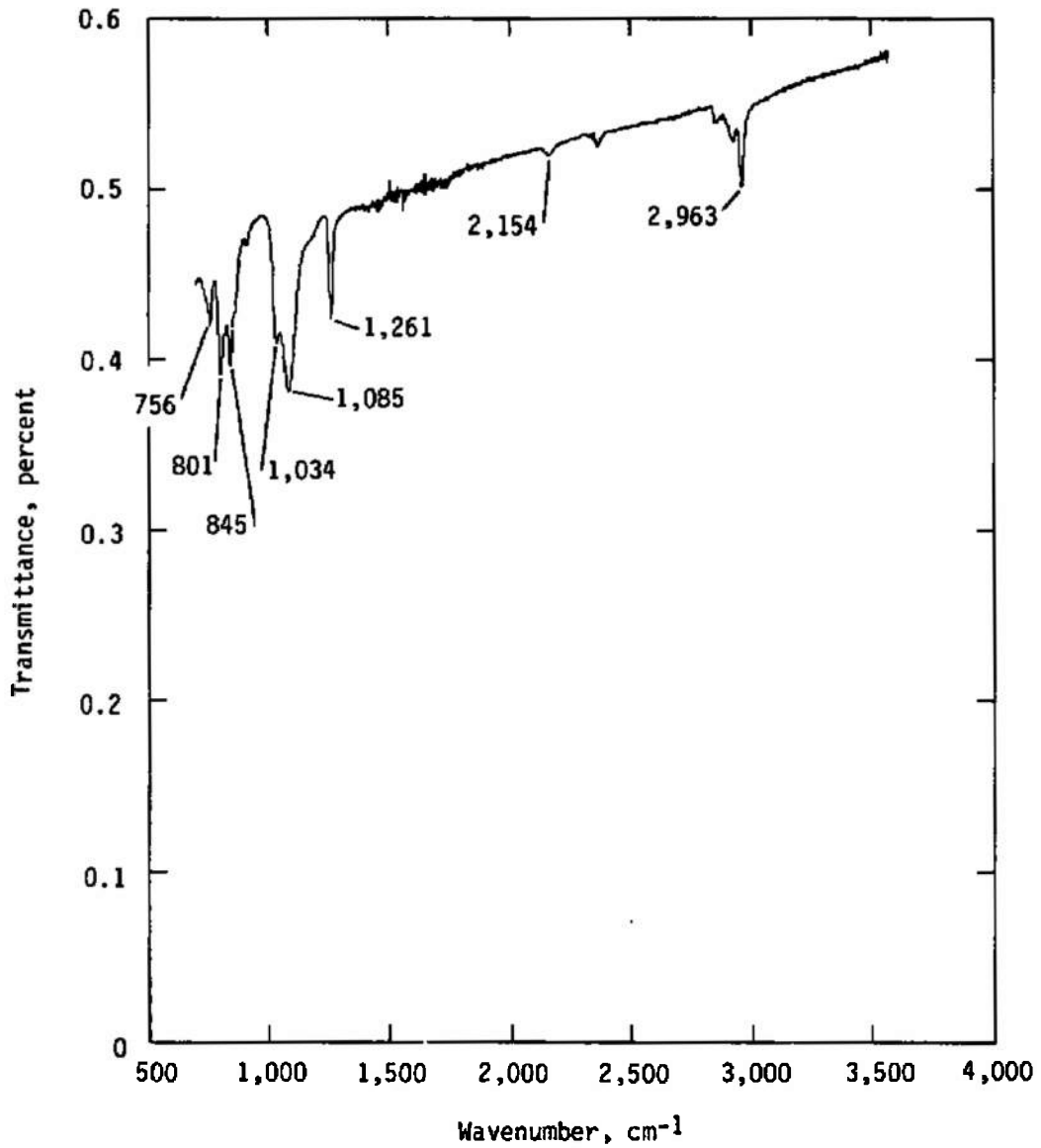
Figure 22. Transmittance of germanium window with contaminant film remaining after warmup to 2°C, material DC93-500.
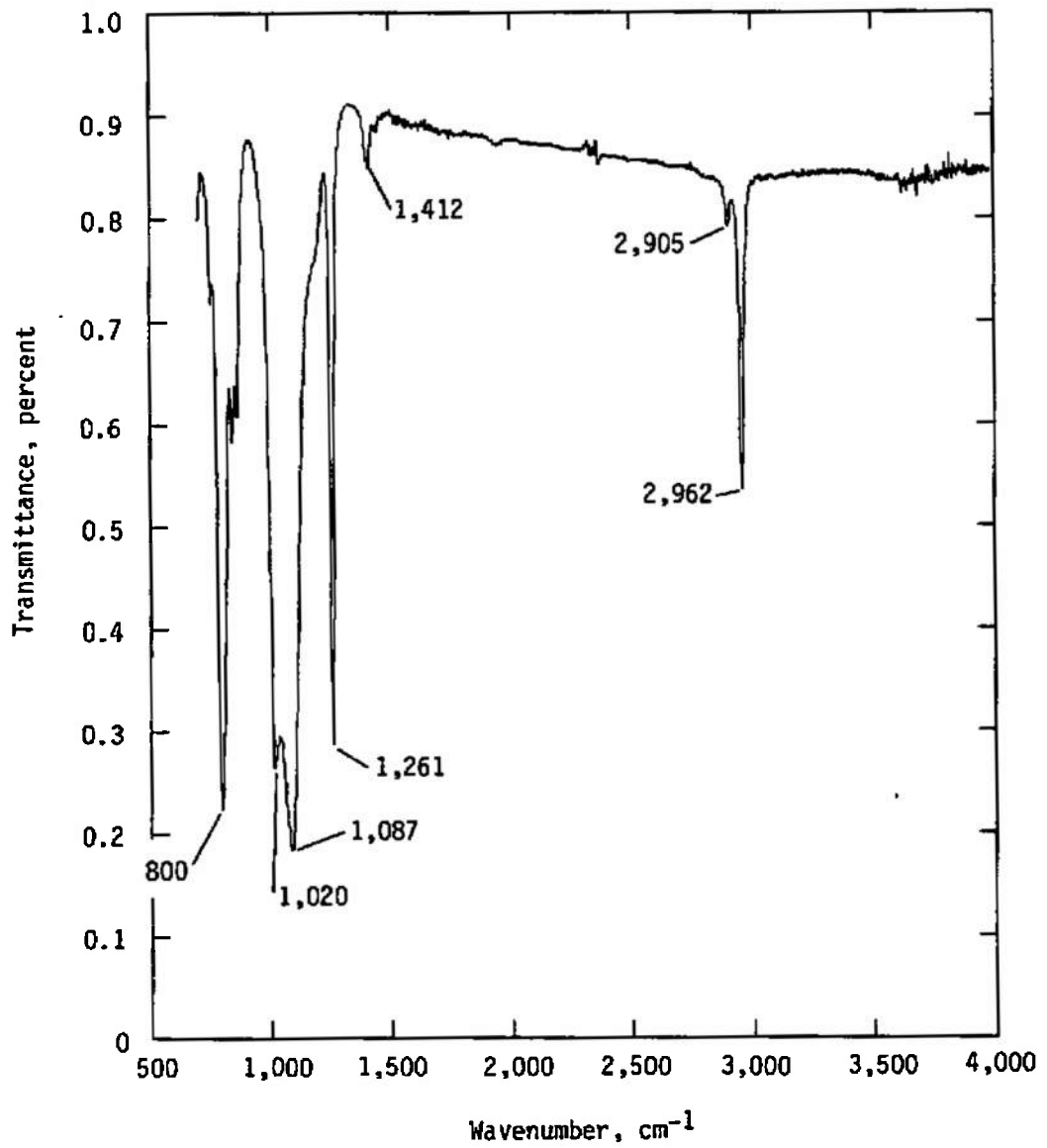
Figure 23. Transmittance of DC93-500 encapsulant at 25°C and at atmospheric pressure.
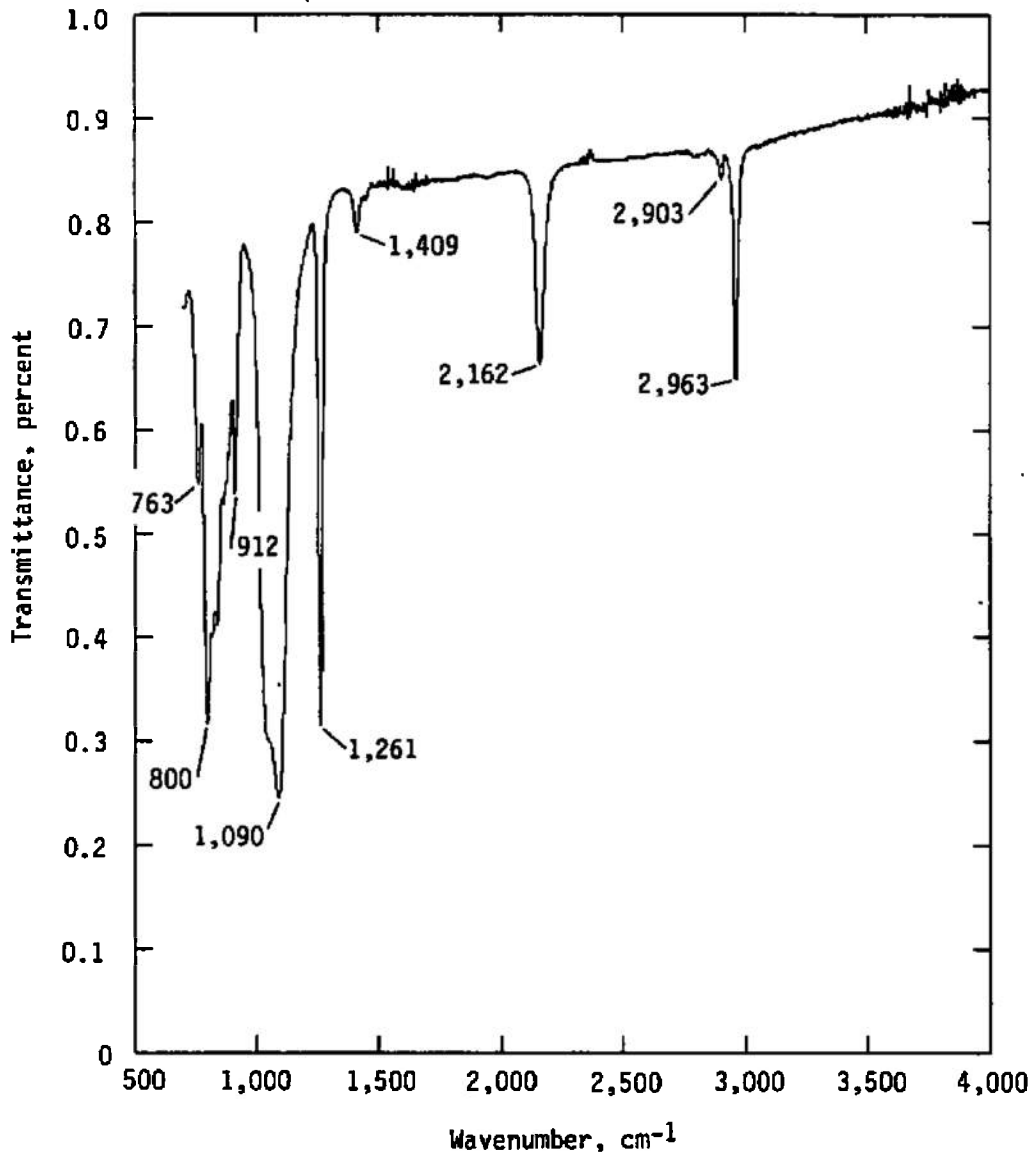
Figure 24. Transmittance of DC93-500 curing agent at 25°C and at atmospheric pressure.
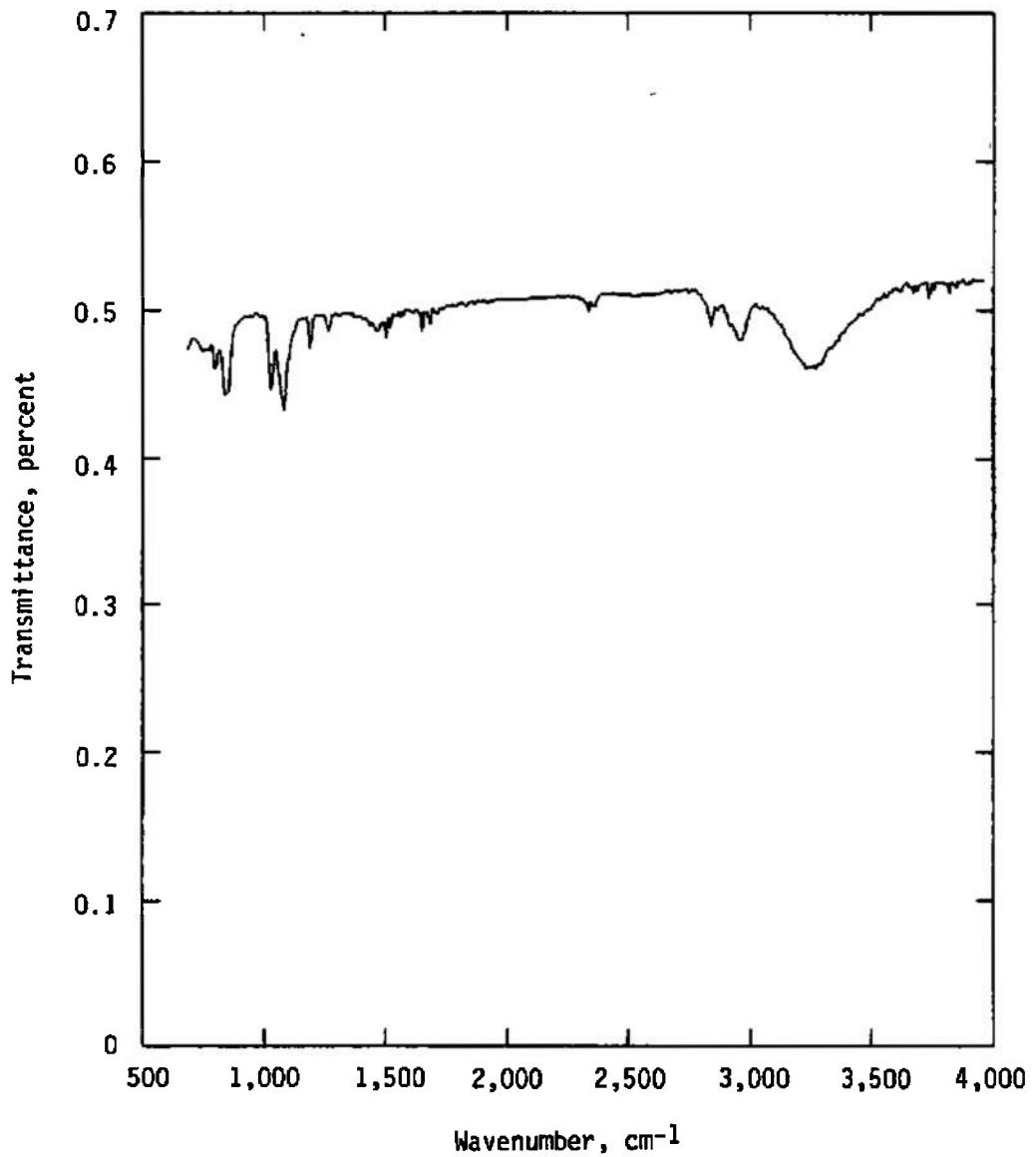
Figure 25. Transmittance of 0.23-μm-thick contaminant film condensed on 77 K germanium window, material DC6-1104.
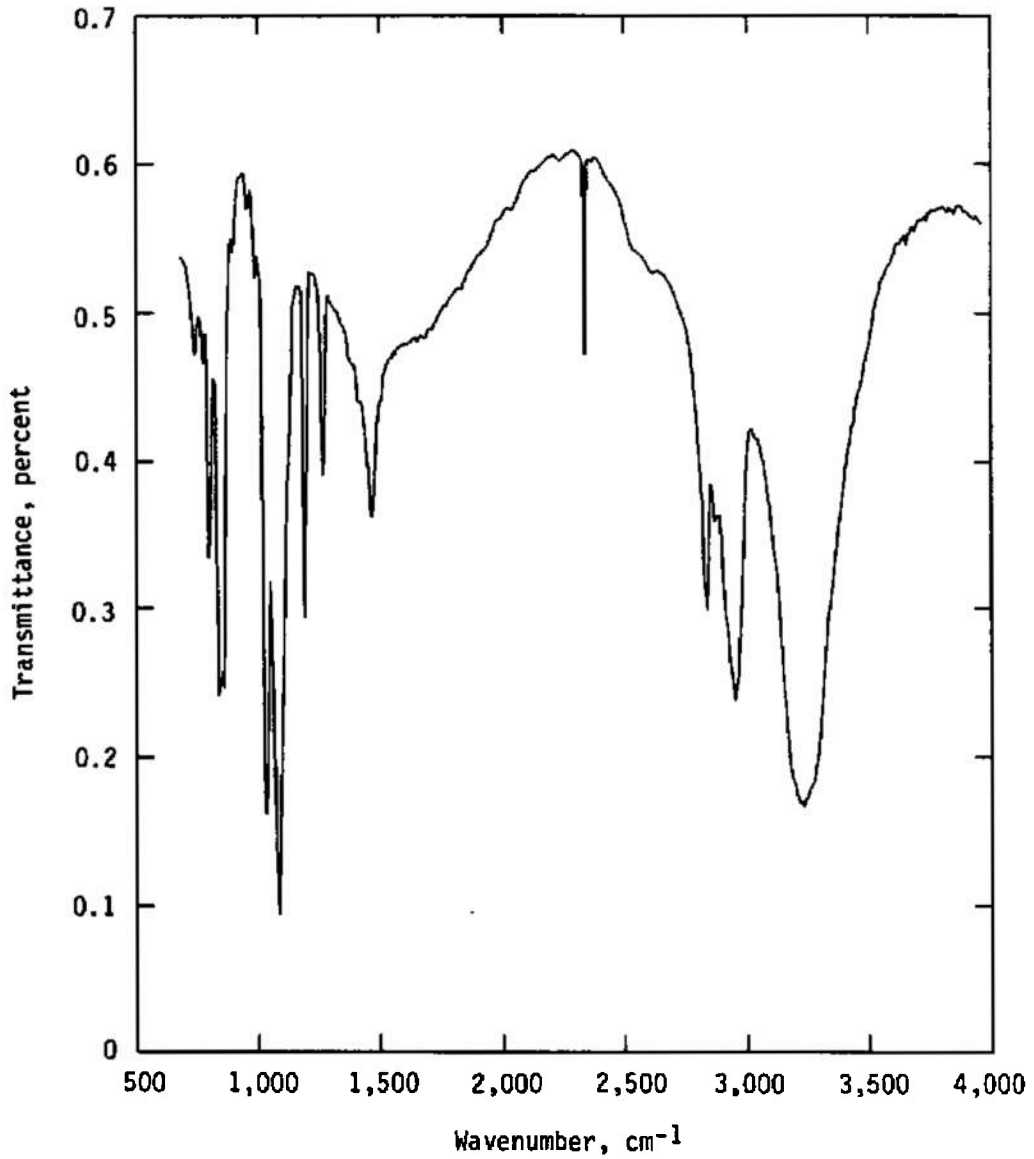
Figure 26. Transmittance of 2.26-μm-thick contaminant film condensed on 77 K germanium window, material DC6-1104.
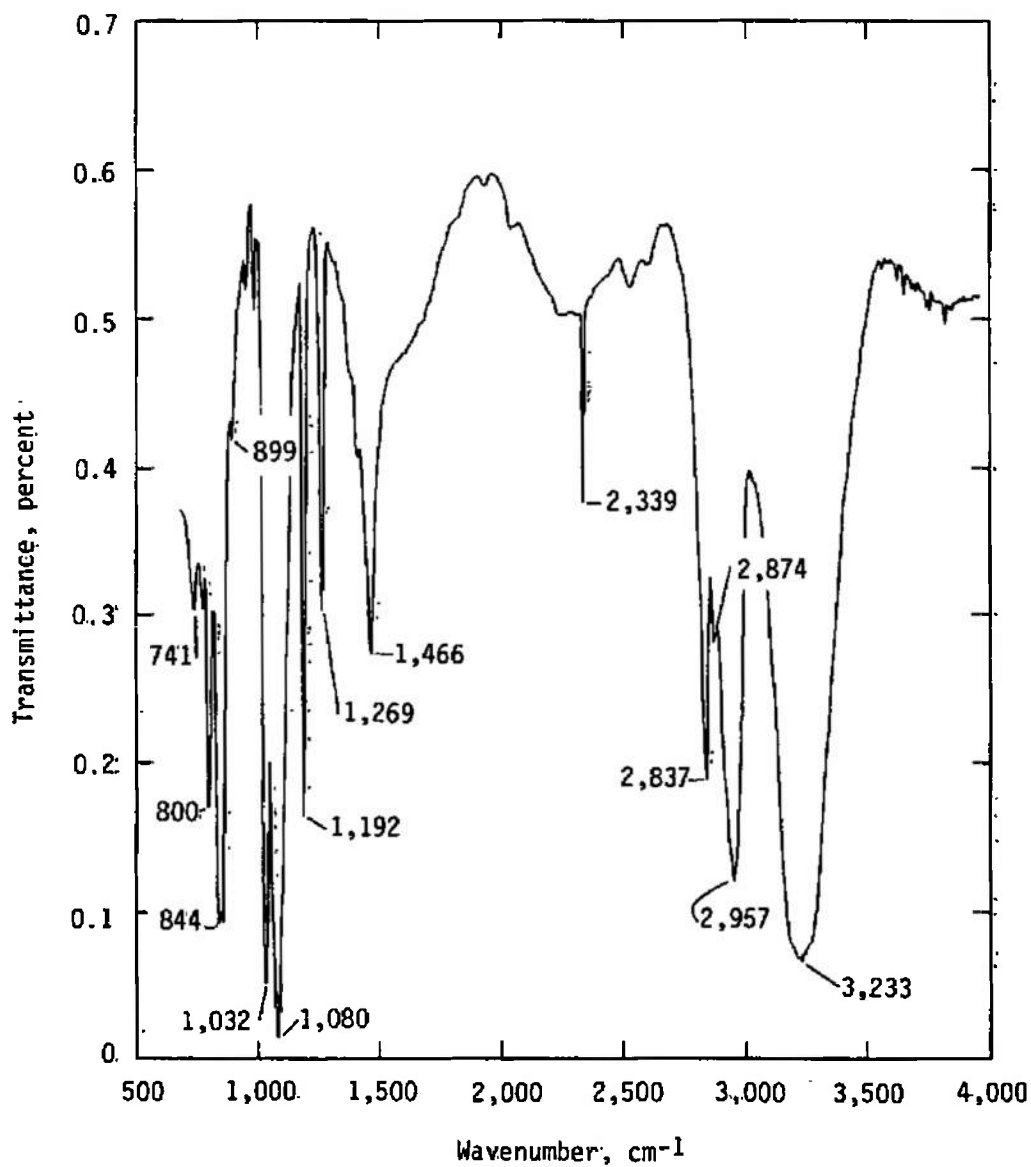
Figure 27. Transmittance of 4.53-μm-thick contaminant film condensed on 77 K germanium window, material DC6-1104.
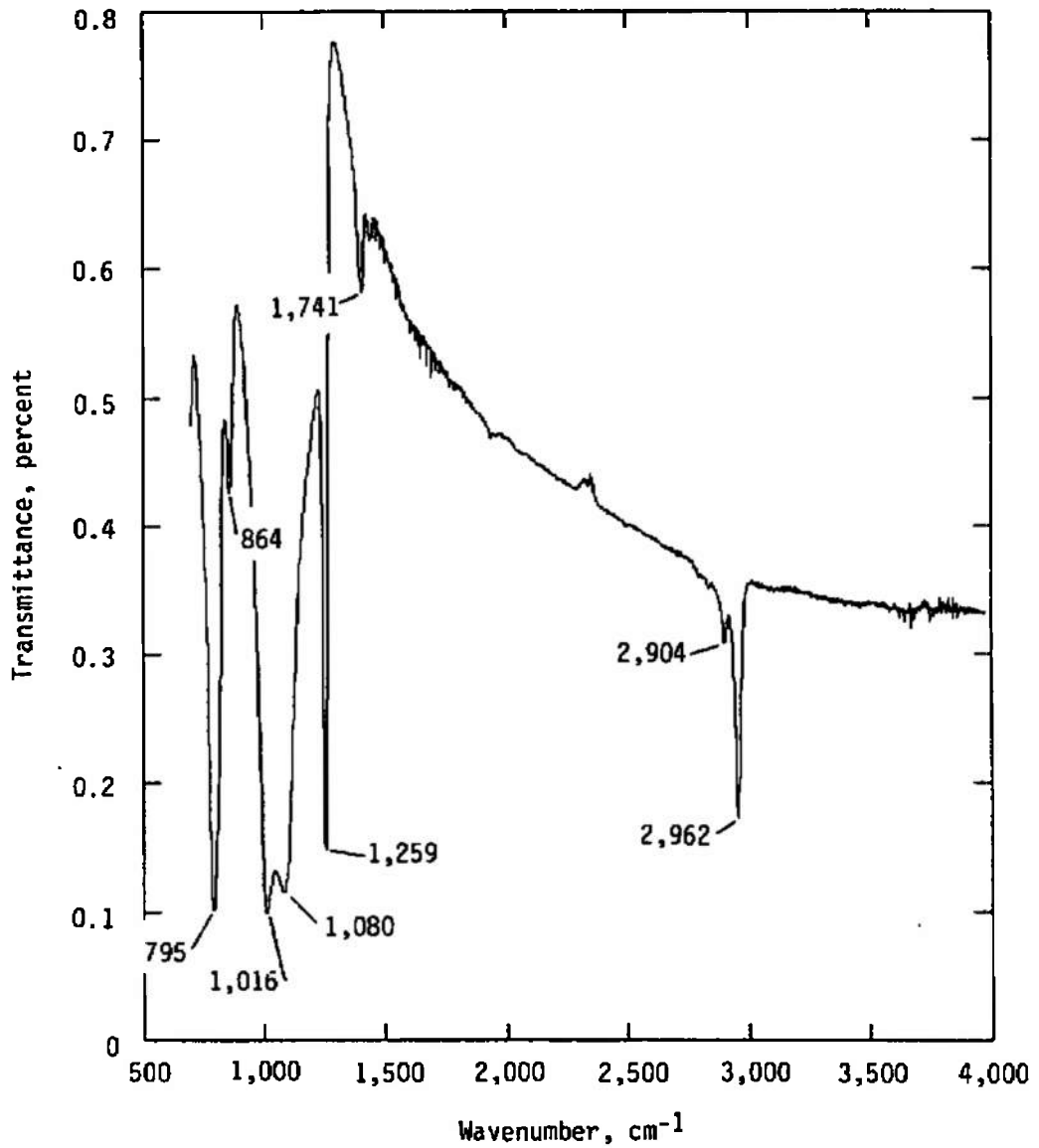
Figure 28. Transmittance of DC6-1104 smeared on a germanium window at 25°C and atmospheric pressure.
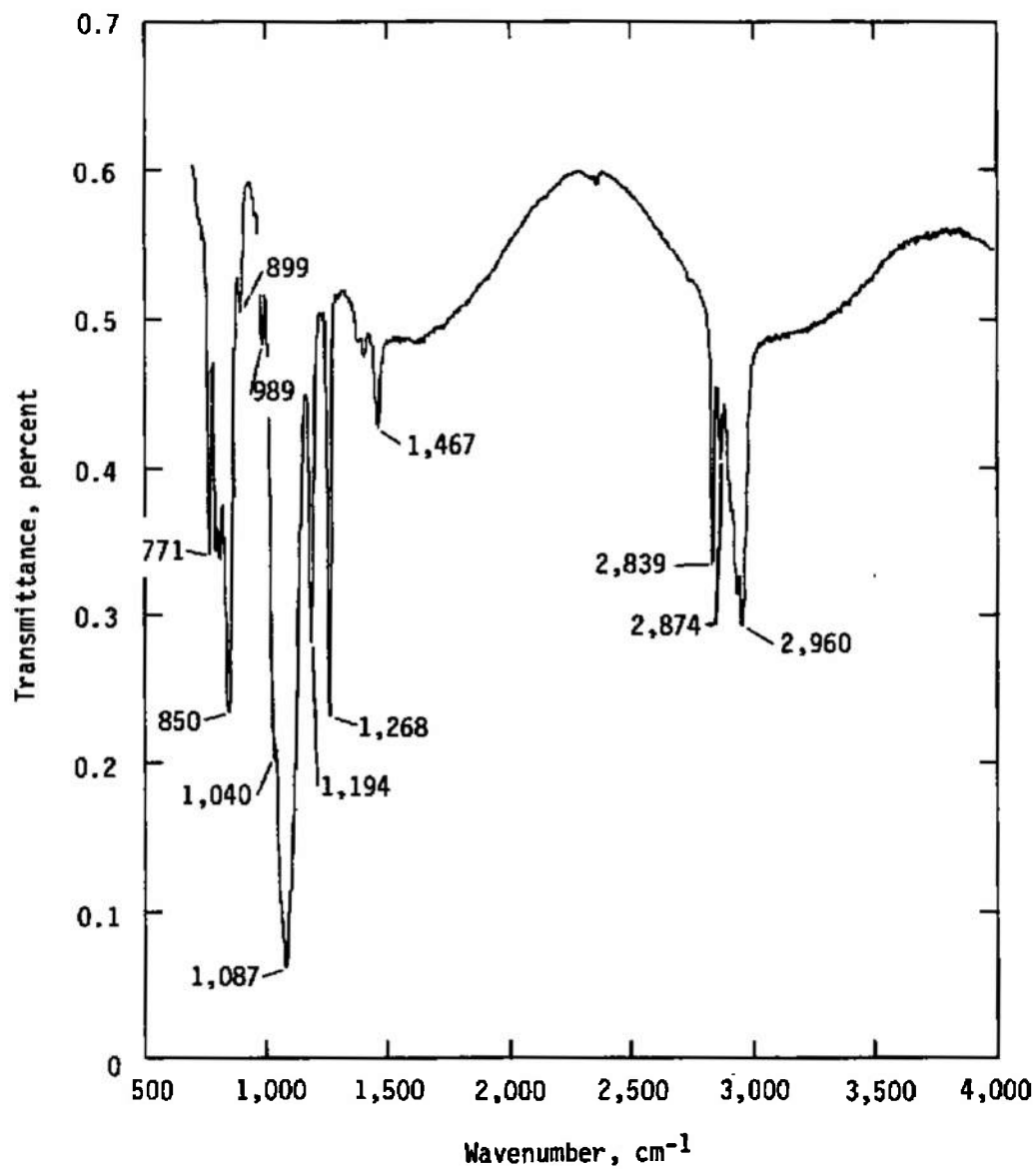
Figure 29. Transmittance of germanium window with contaminant film left after warmup to 185 K, material DC6-1104.
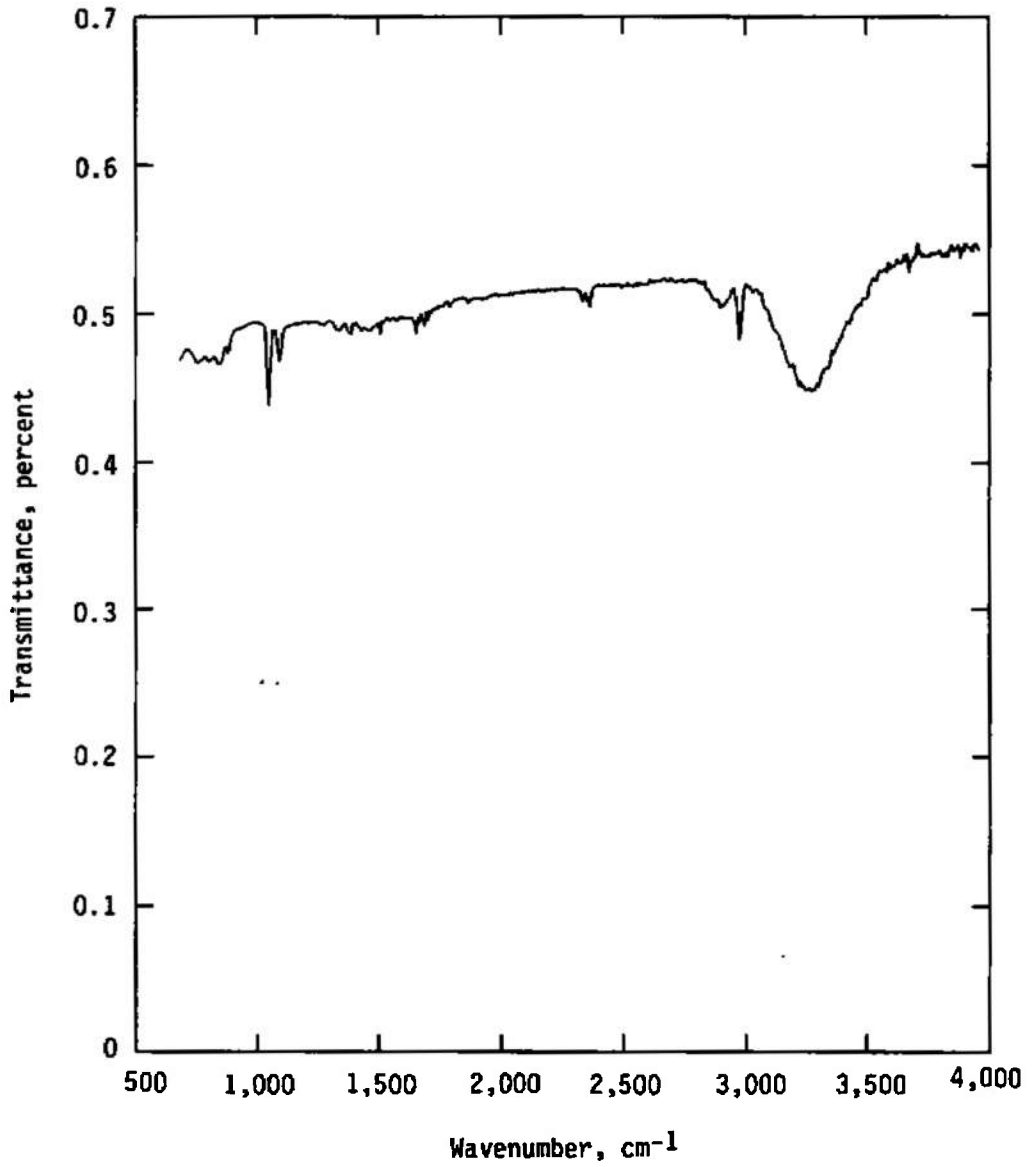
Figure 30. Transmittance of 0.23-μm-thick contaminant film condensed on 77 K germanium window, material RTV566.
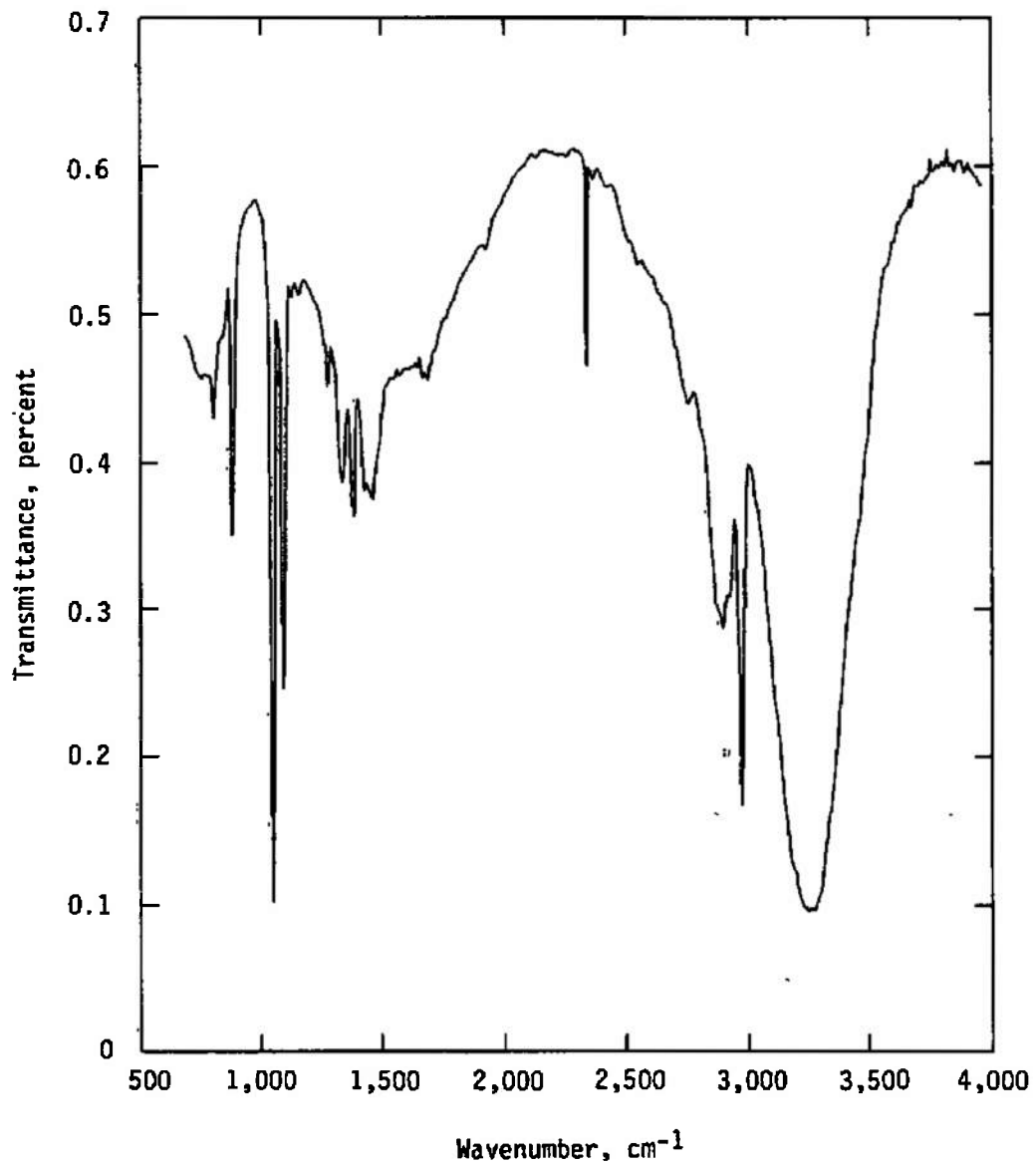
Figure 31. Transmittance of 2.29-μm-thick contaminant film condensed on 77 K germanium window, material RTV566.
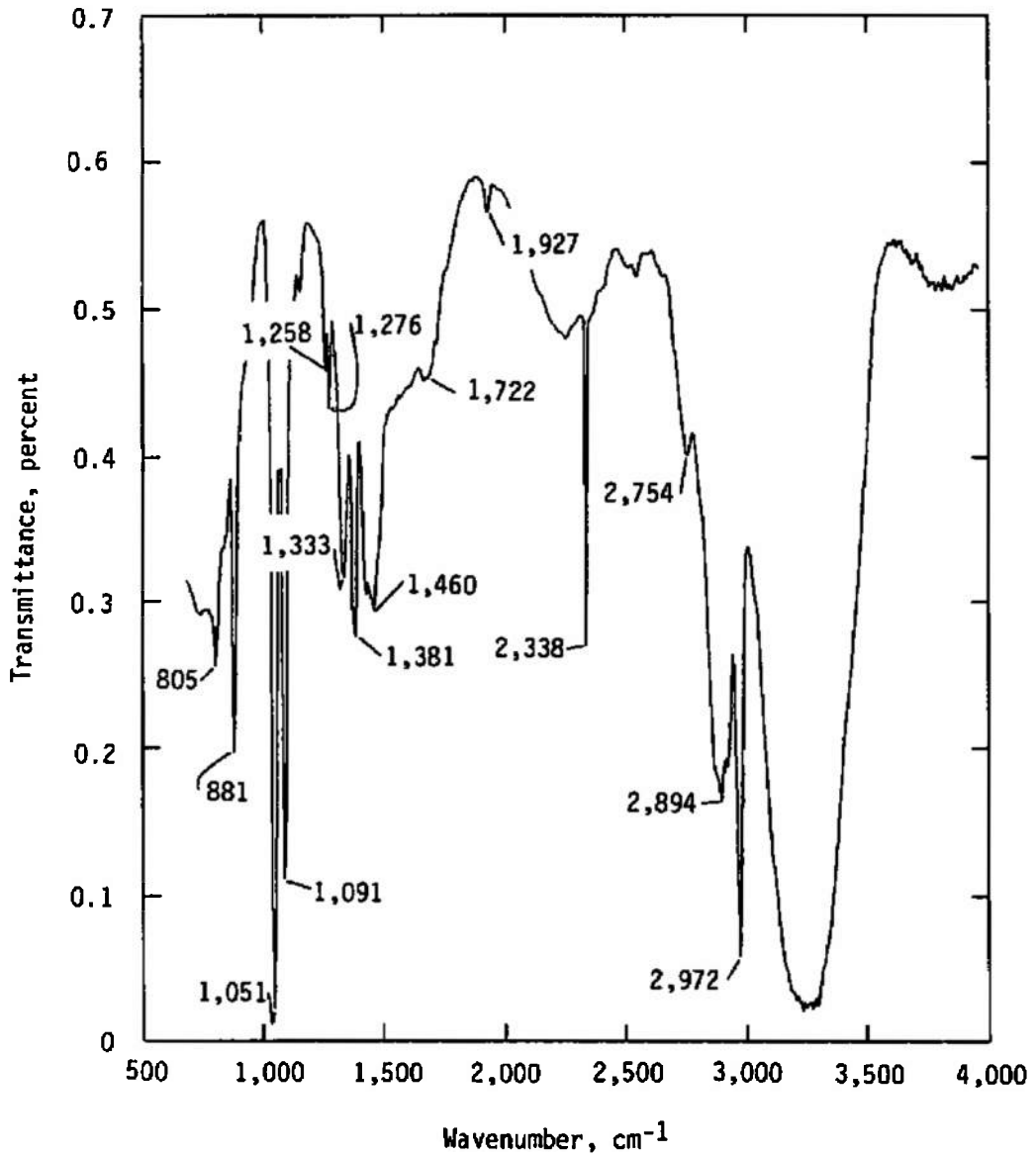
Figure 32. Transmittance of 4.59-μm-thick contaminant film condensed on 77 K germanium window, material RTV566.
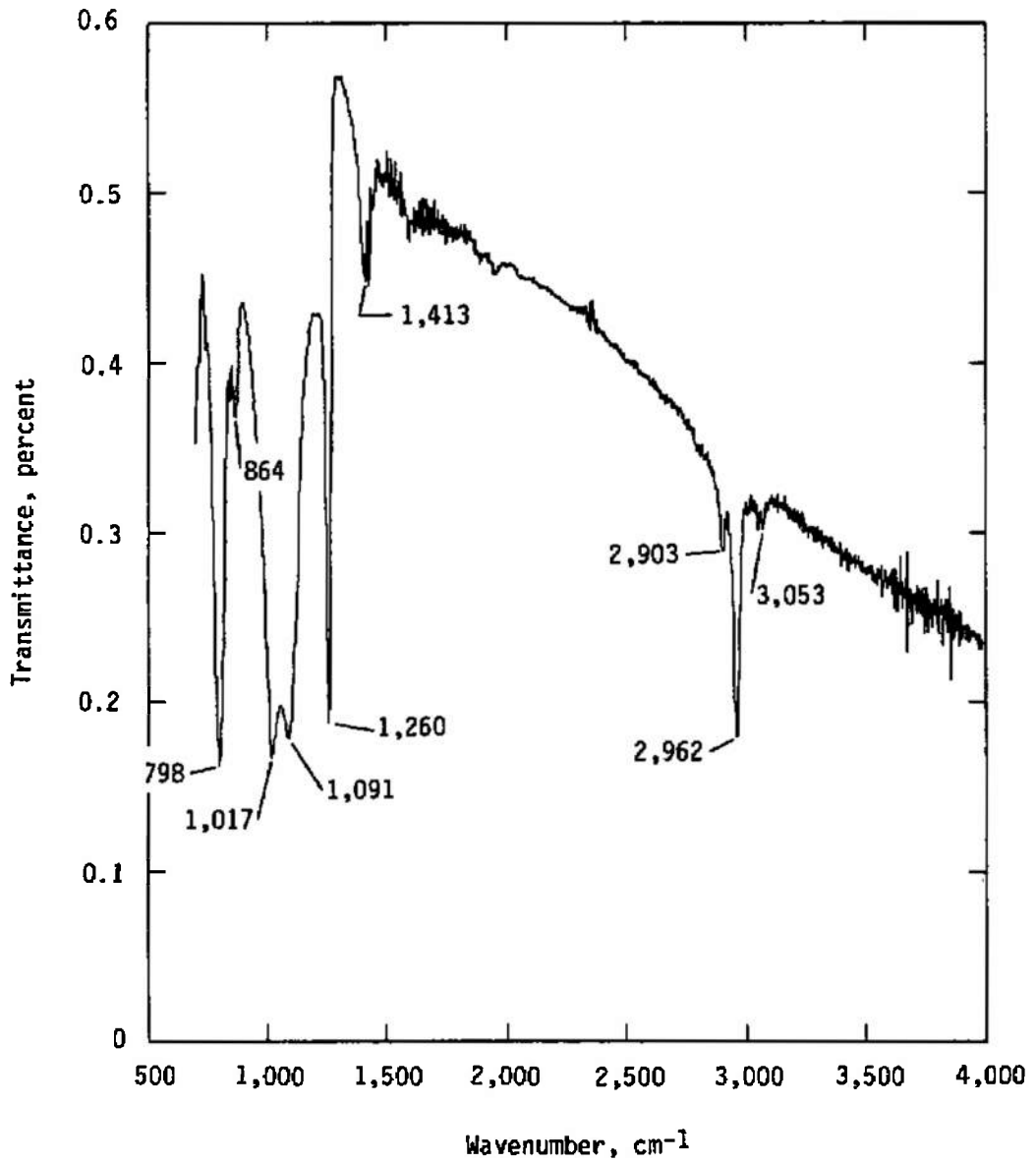
Figure 33. Transmittance of RTV566-A silicone base at 25°C and at atmospheric pressure.
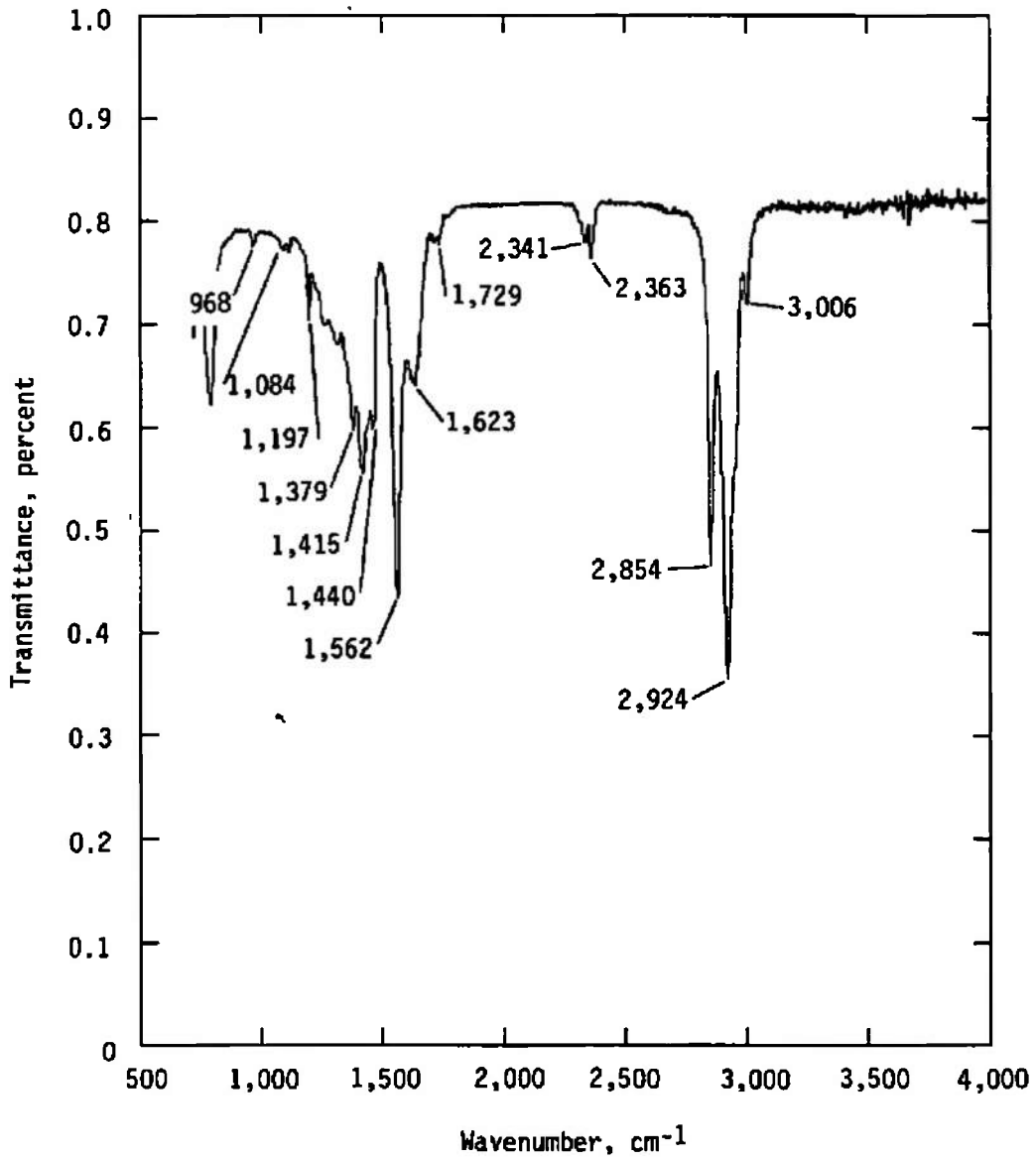
Figure 34. Transmittance of RTV566-B catalyst at 25°C and at atmospheric pressure.
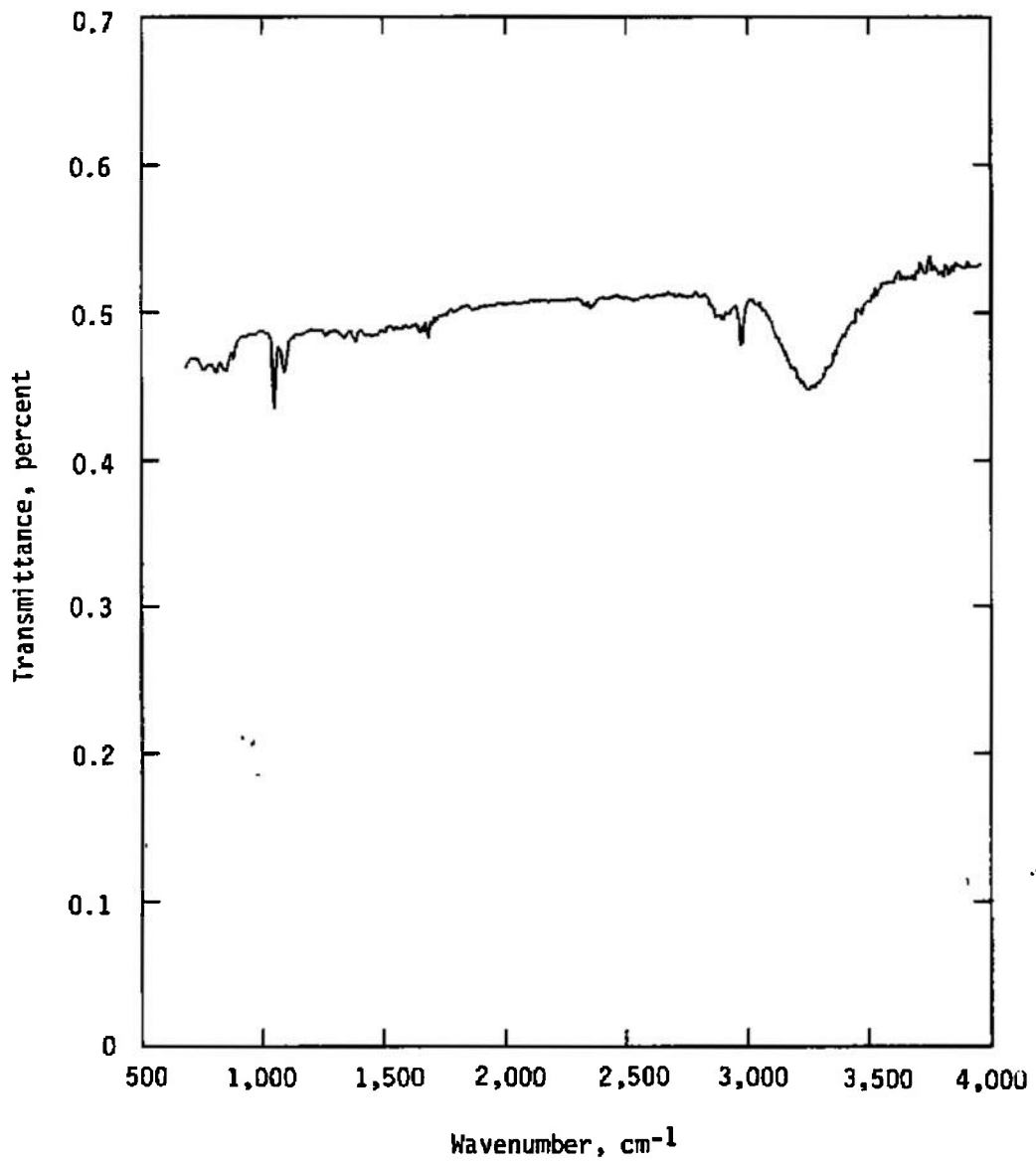
Figure 35. Transmittance of 0.23-μm-thick contaminant film condensed on 77 K germanium window, material RTV560.
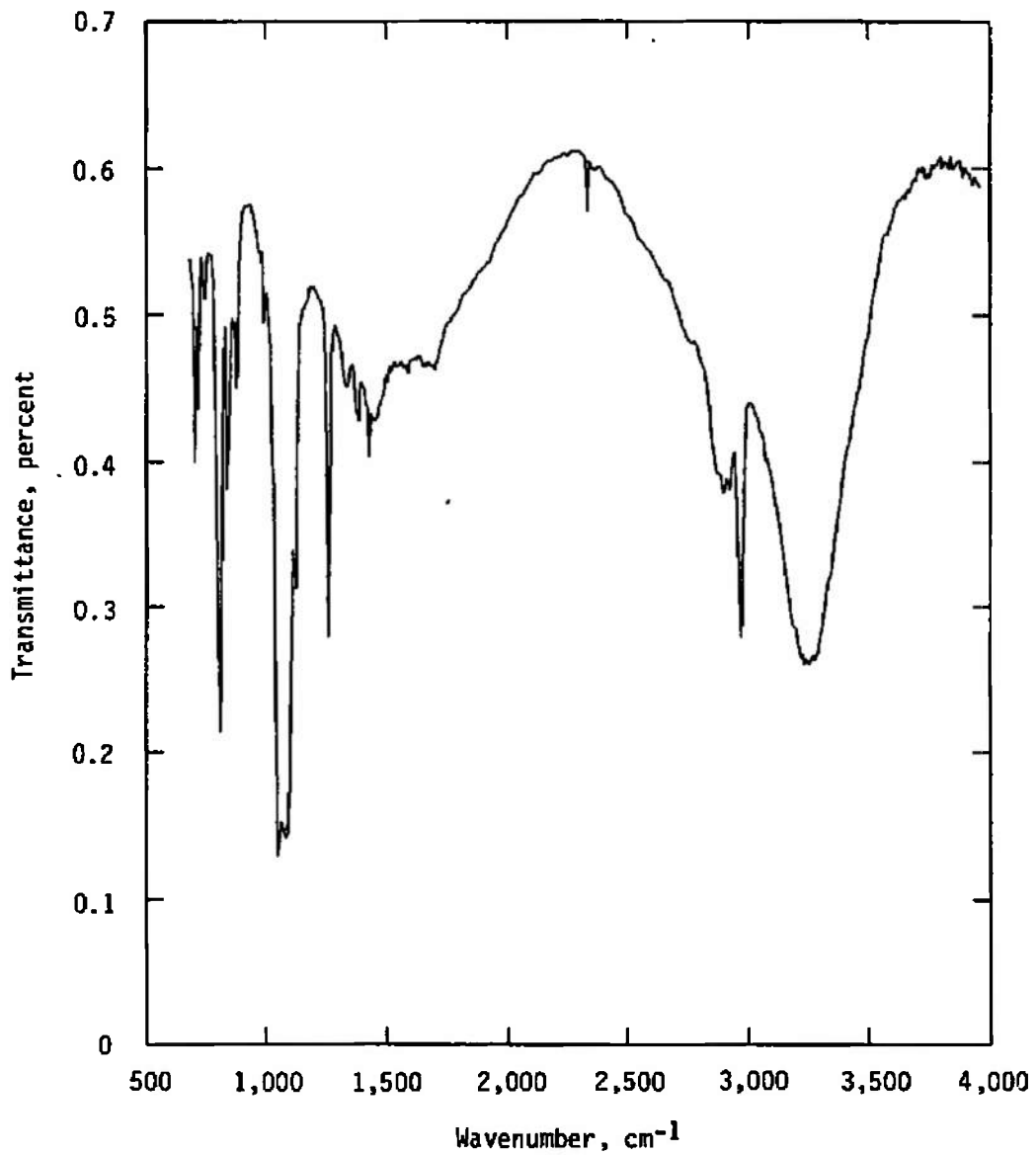
Figure 36. Transmittance of 2.32-μm-thick contaminant film condensed on 77 K germanium window, material RTV560.
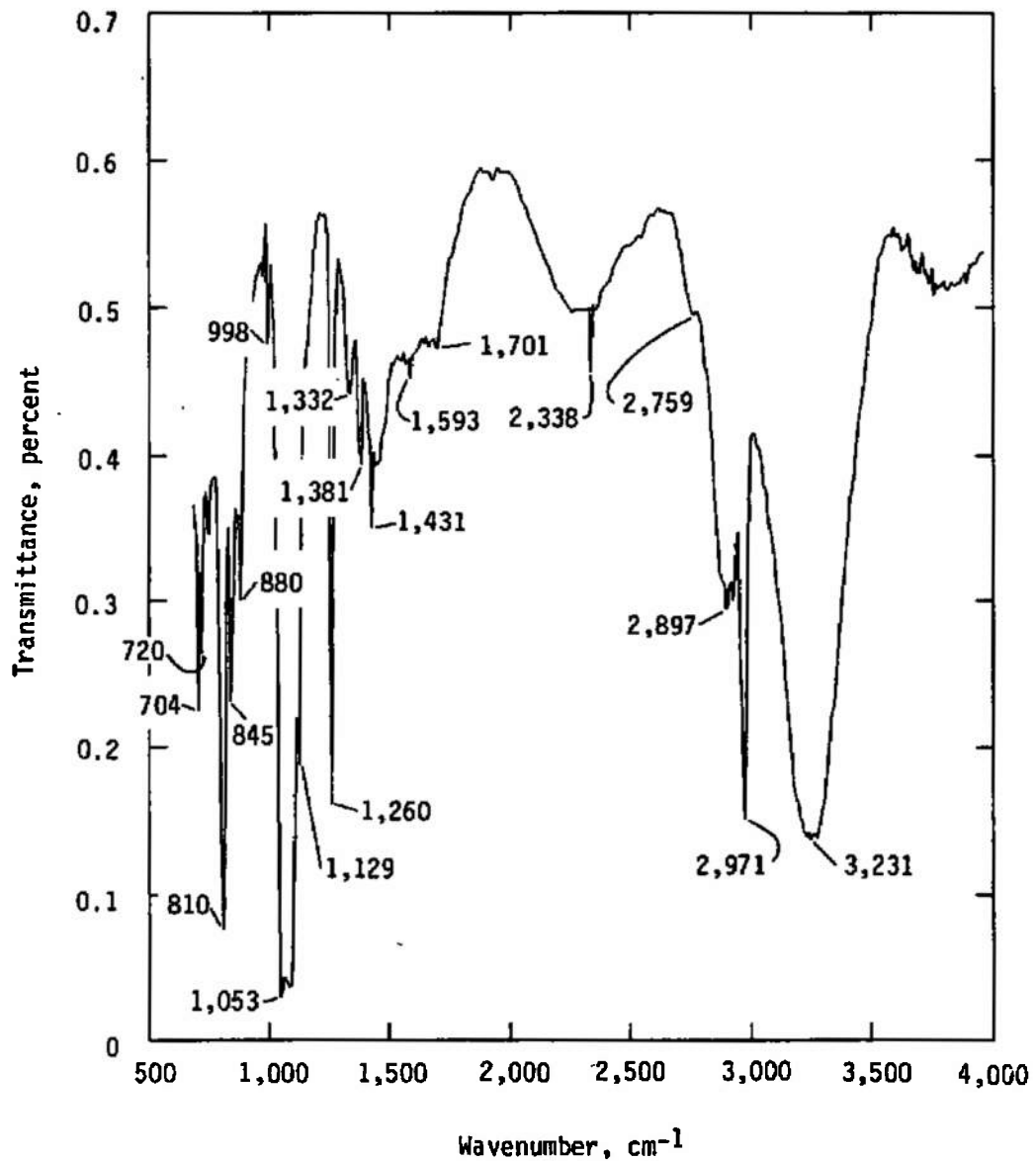
Figure 37. Transmittance of 4.69-μm-thick contaminant film condensed on 77 K germanium window, material RTV560.
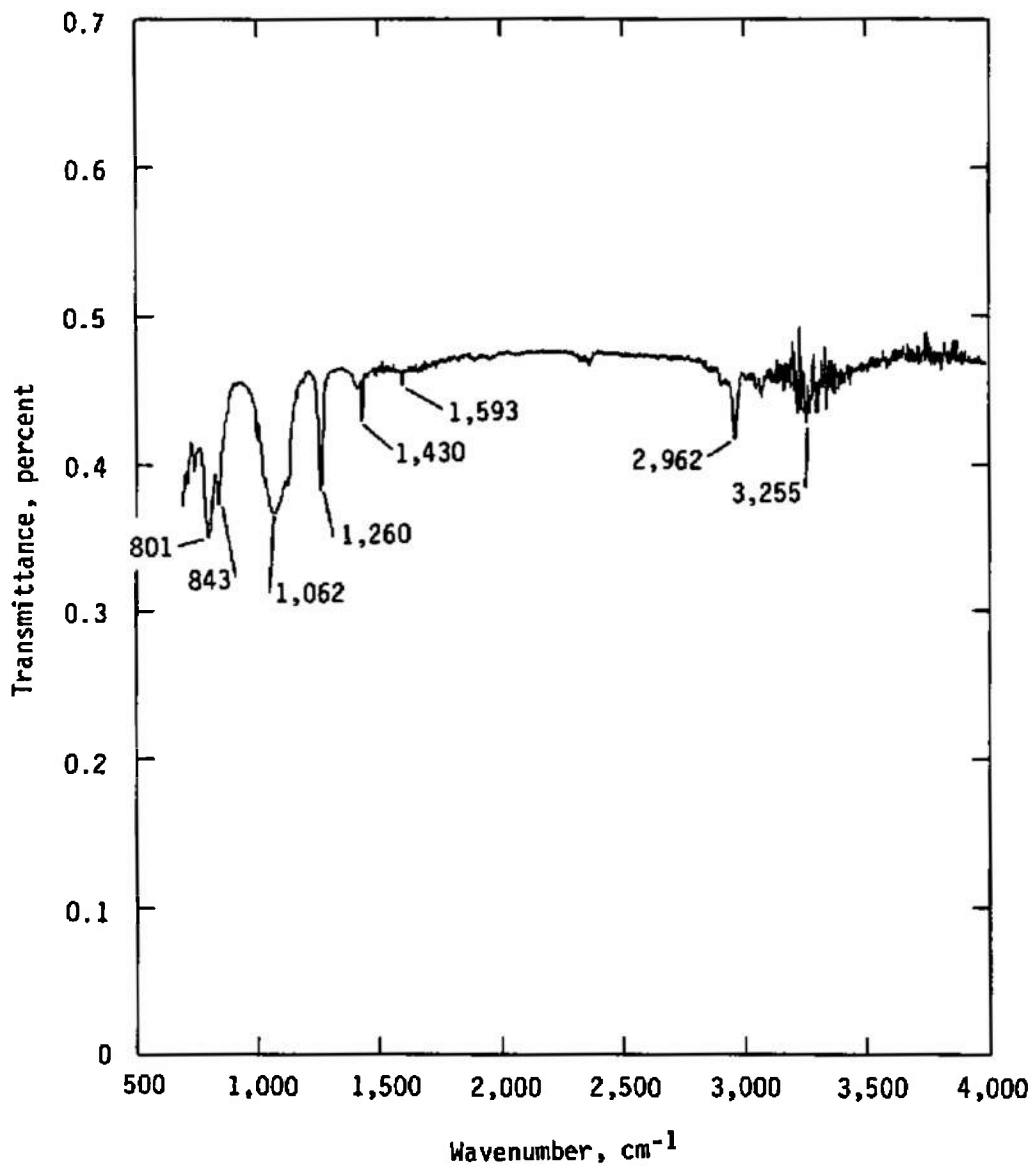
Figure 38. Transmittance of RTV560 contaminant film on germanium window after warmup to 5°C.
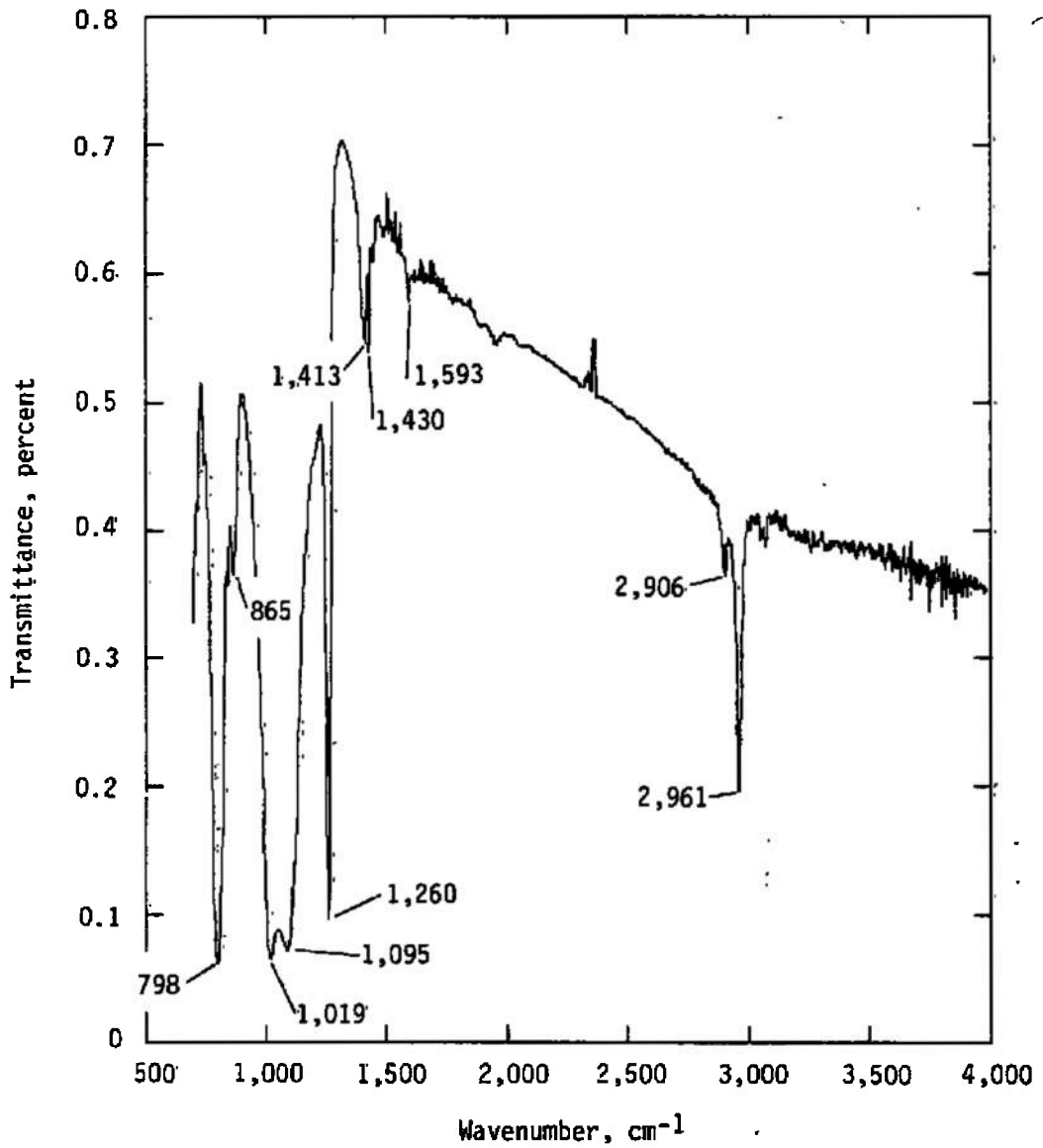
Figure 39. Transmittance of RTV560-A adhesive at 25°C and at atmospheric pressure.
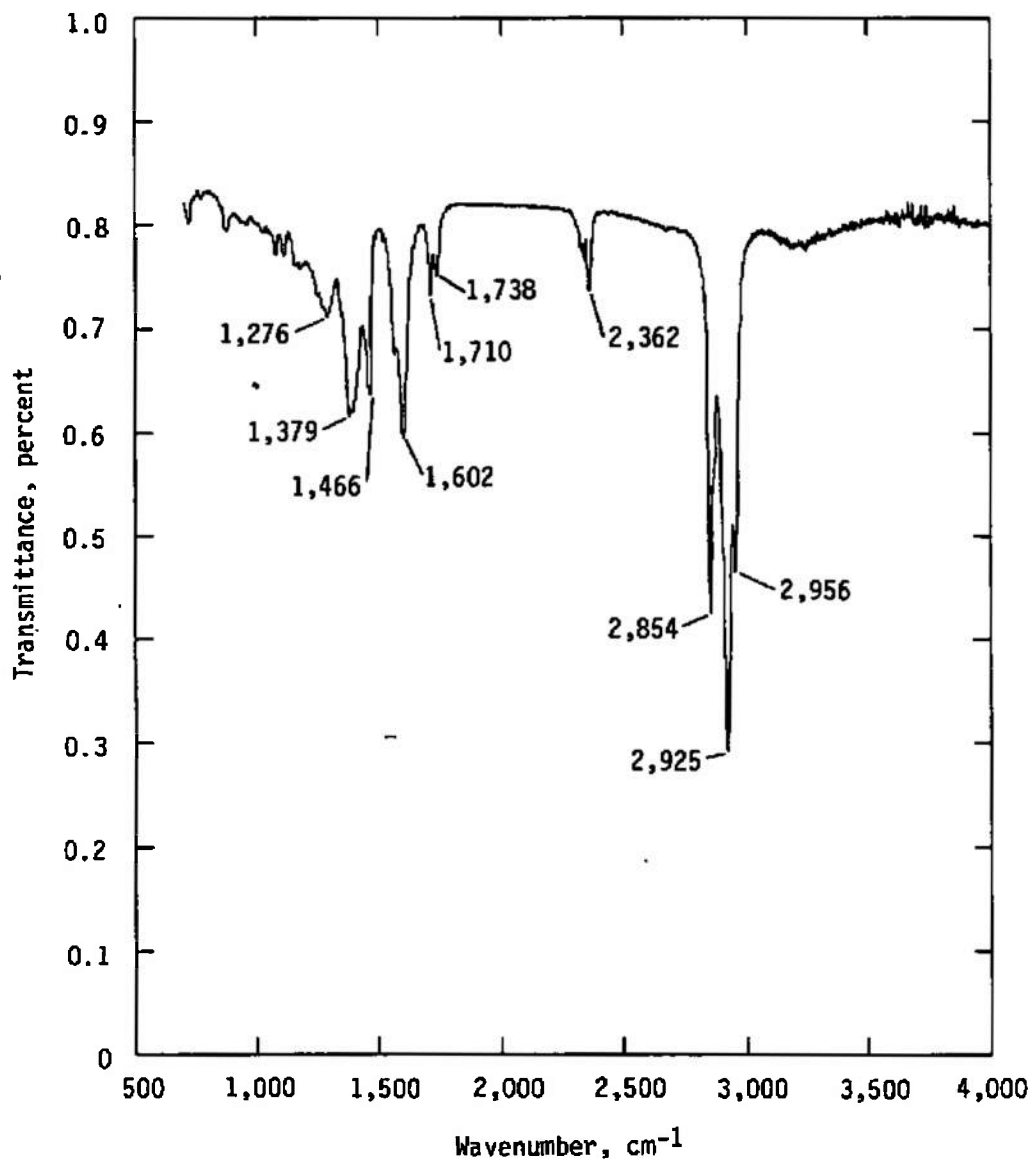
Figure 40. Transmittance of RTV560-B catalyst at 25°C and at atmospheric pressure.

78
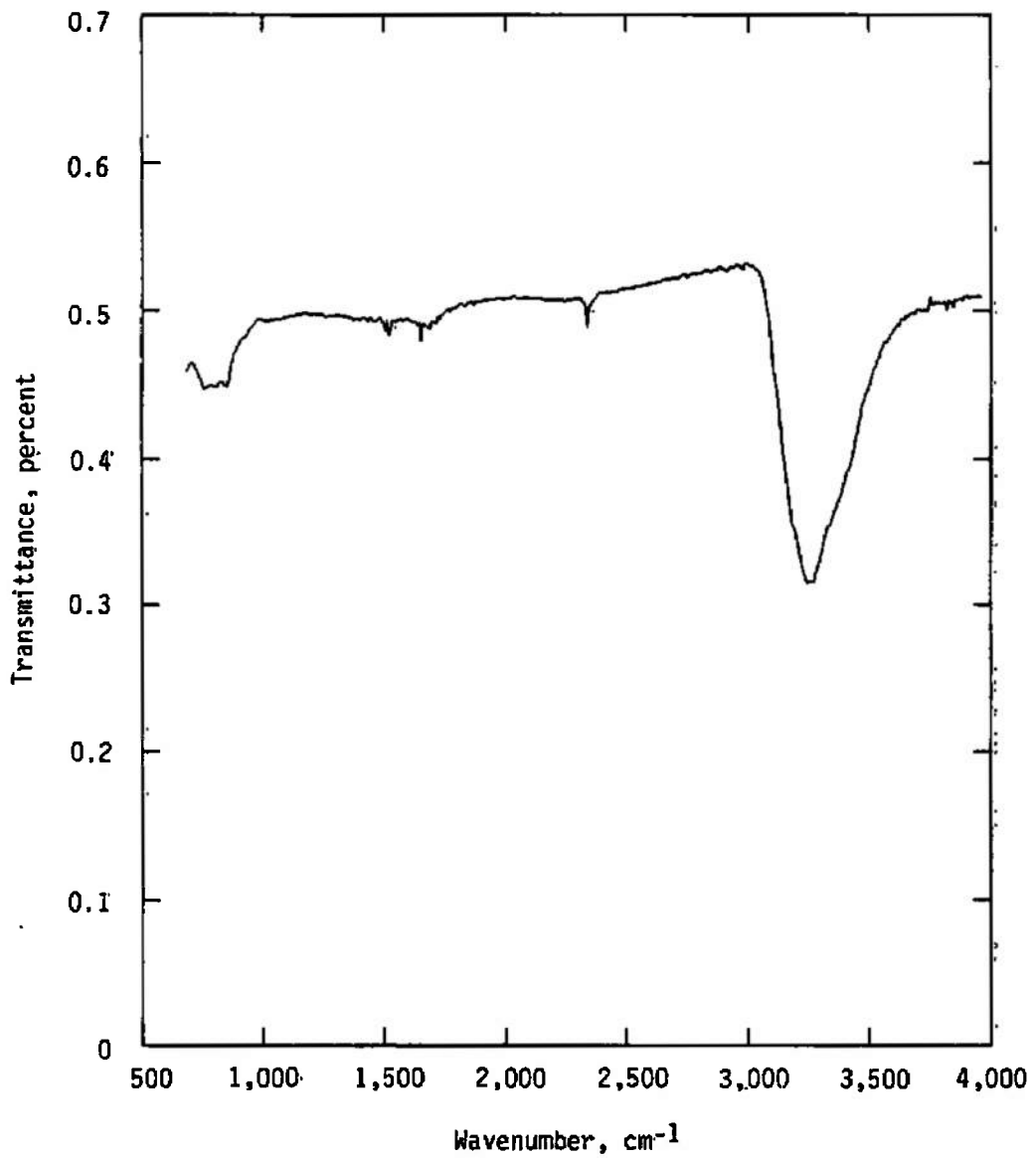
Figure 41. Transmittance of 0.25-μm-thick contaminant film condensed on 77 K germanium window, material S13G/LO paint.

79
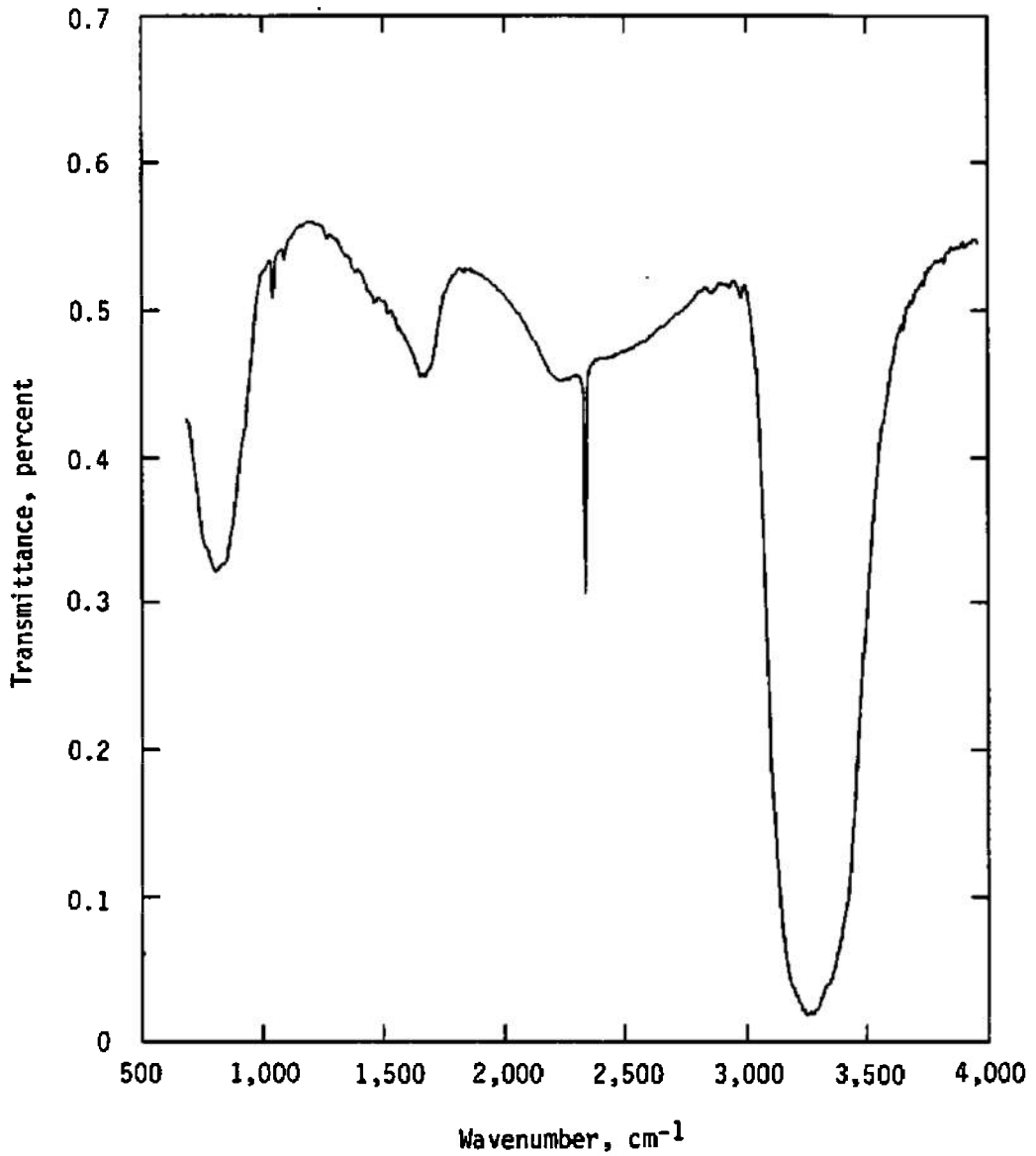
Figure 42. Transmittance of 1.78-μm-thick contaminant film condensed on 77 K germanium
window, material S13G/LO paint.
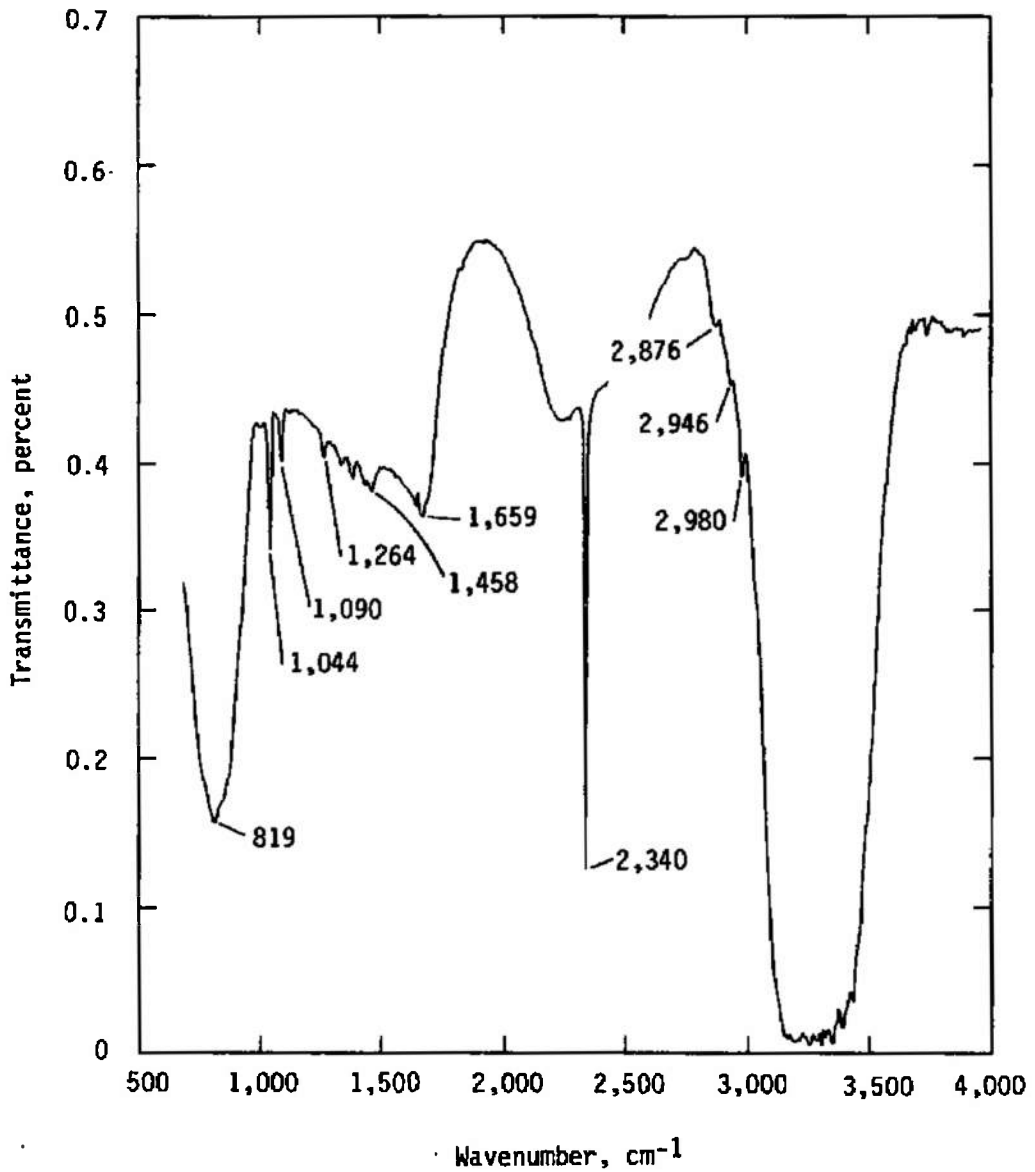
Figure 43. Transmittance of 2.96-μm-thick contaminant film condensed on 77 K germanium window, material S13G/LO paint.
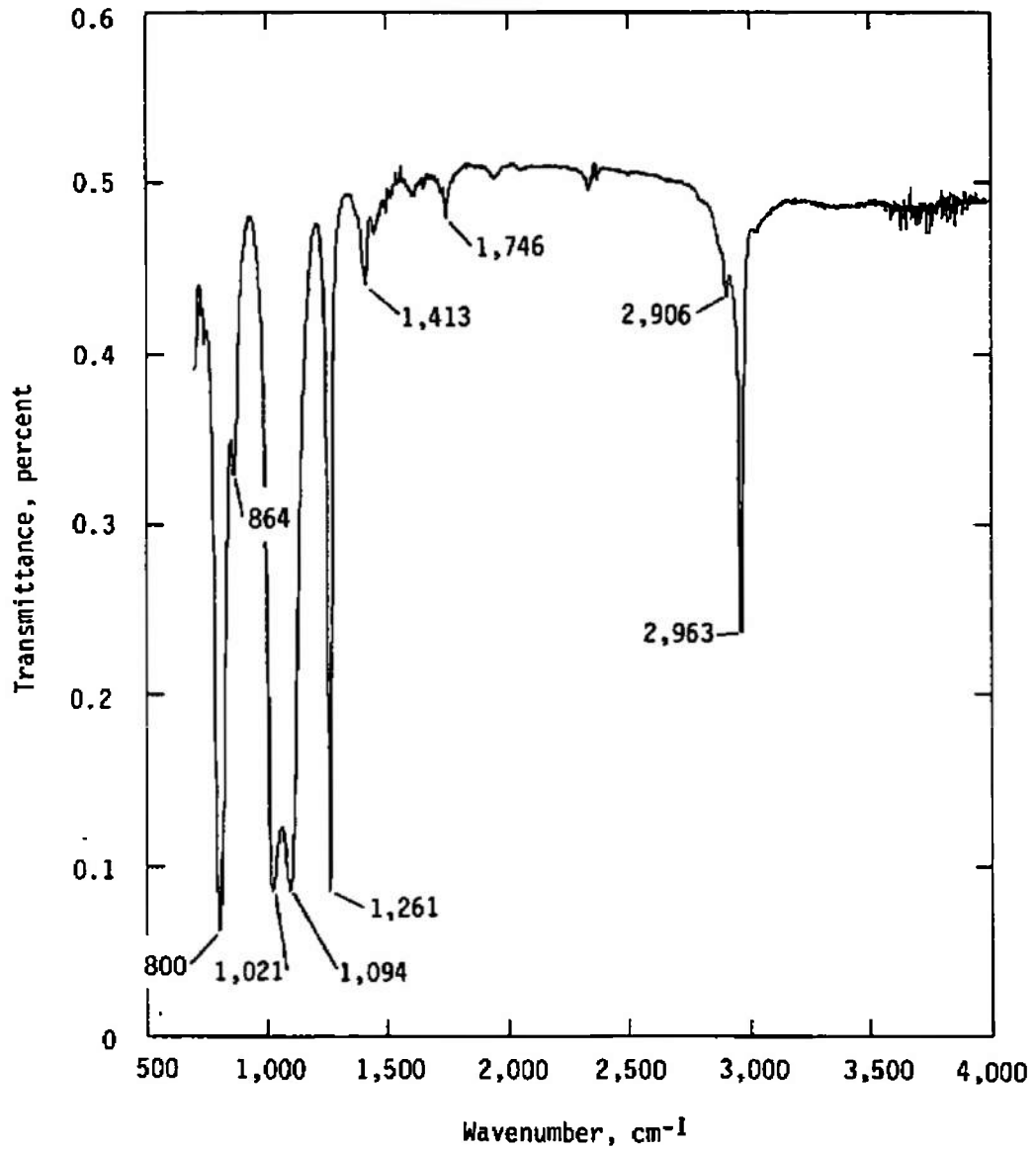
Figure 44. Transmittance of S13G/LO-1, V-10 resin on a 25°C germanium window at atmospheric pressure.
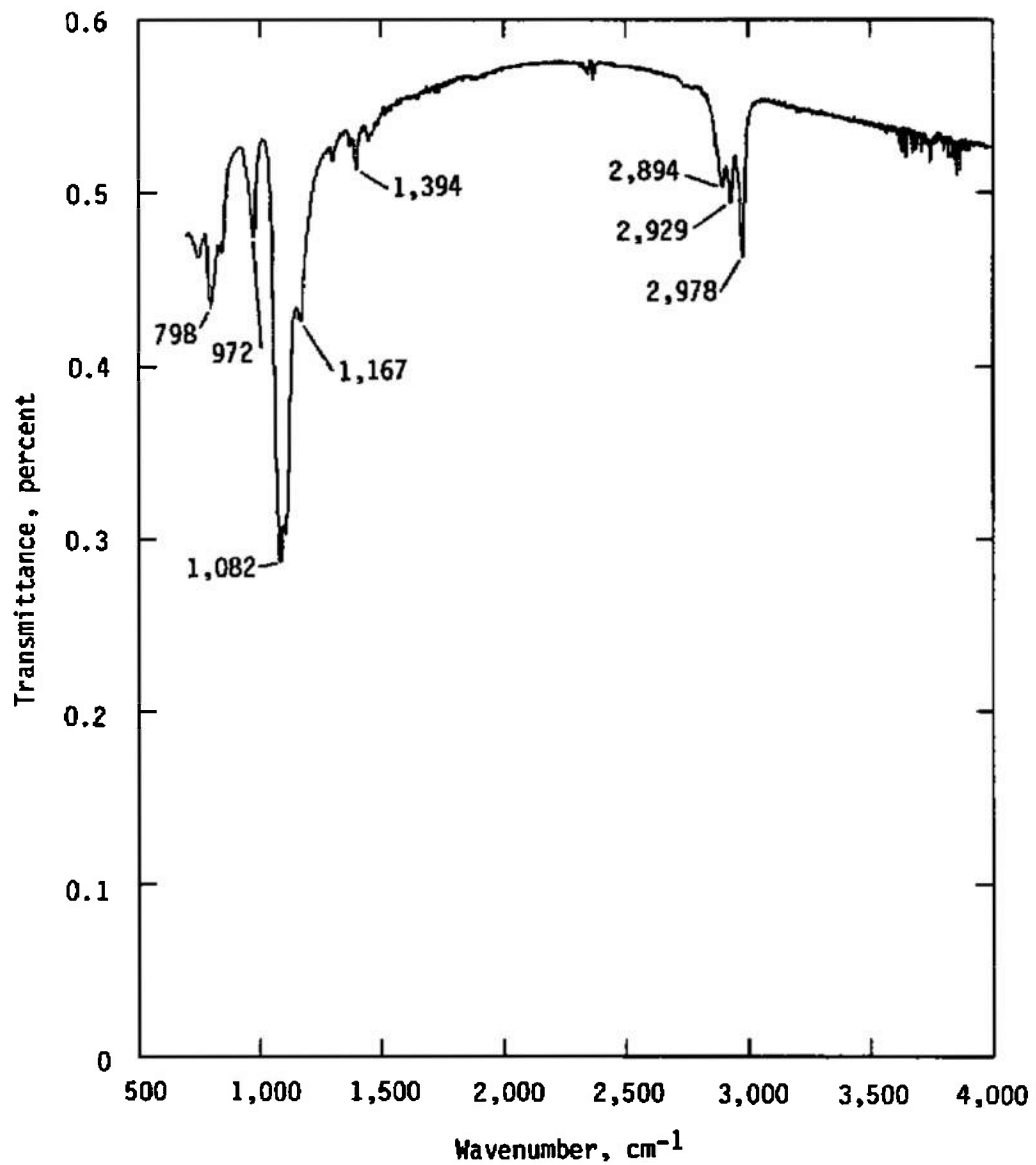
Figure 45. Transmittance of S13G/LO-1 catalyst on a 25°C germanium window at
atmospheric pressure.
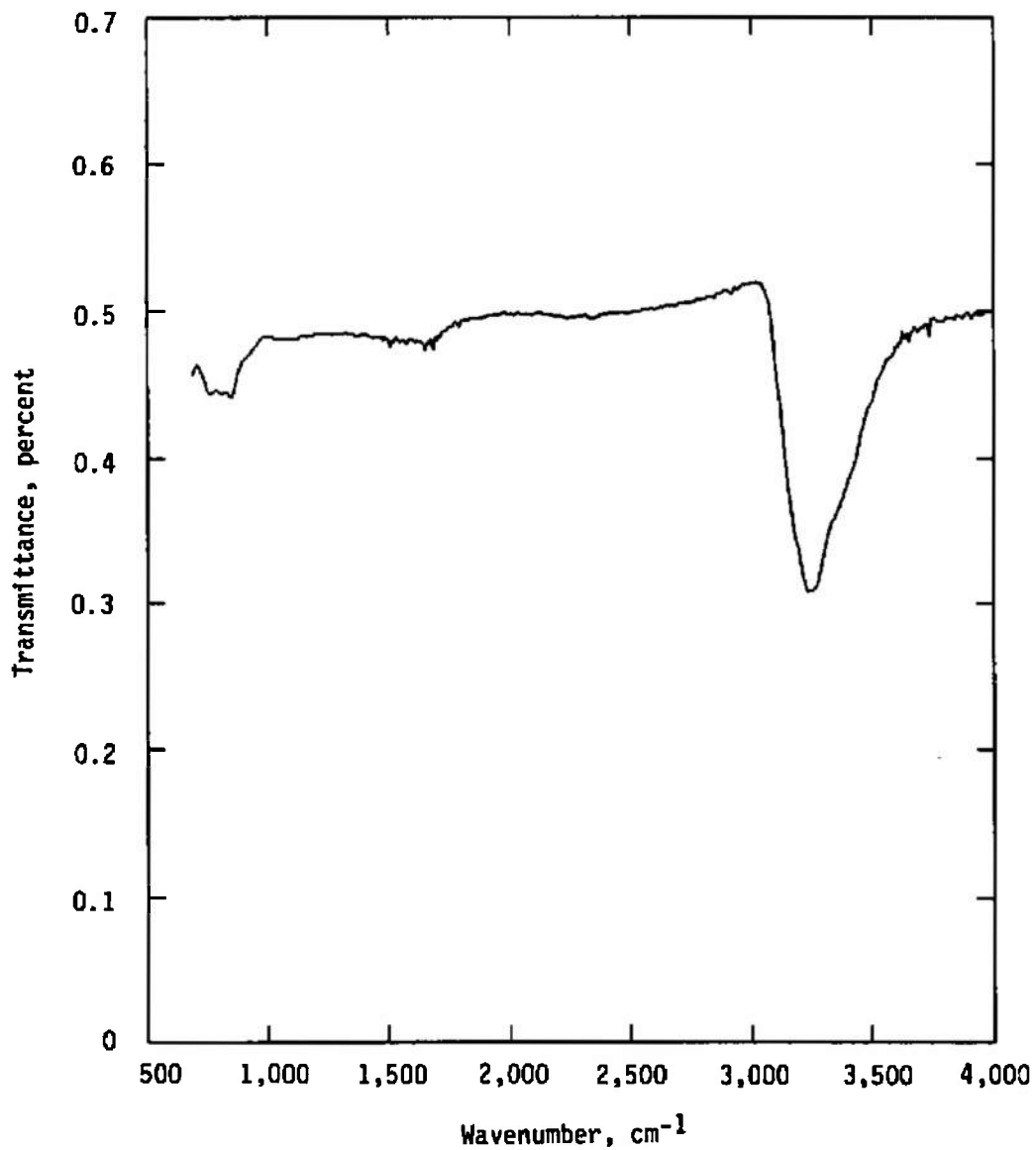
Figure 46. Transmittance of 0.28-μm-thick contaminant film condensed on 77 K germanium window, material Kapton®.
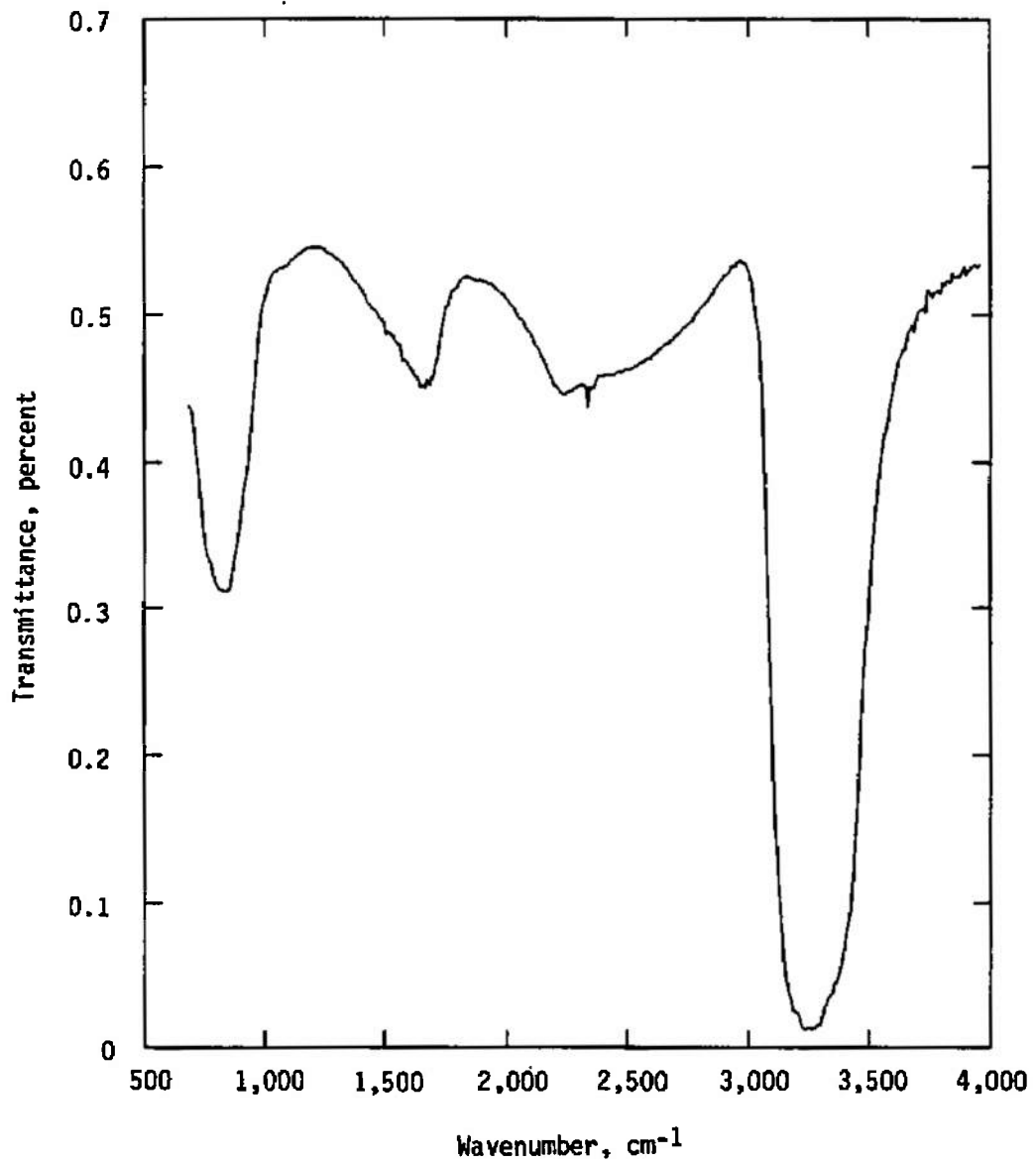
Figure 47. Transmittance of 1.66-μm-thick contaminant film condensed on 77 K germanium window, material Kapton® .
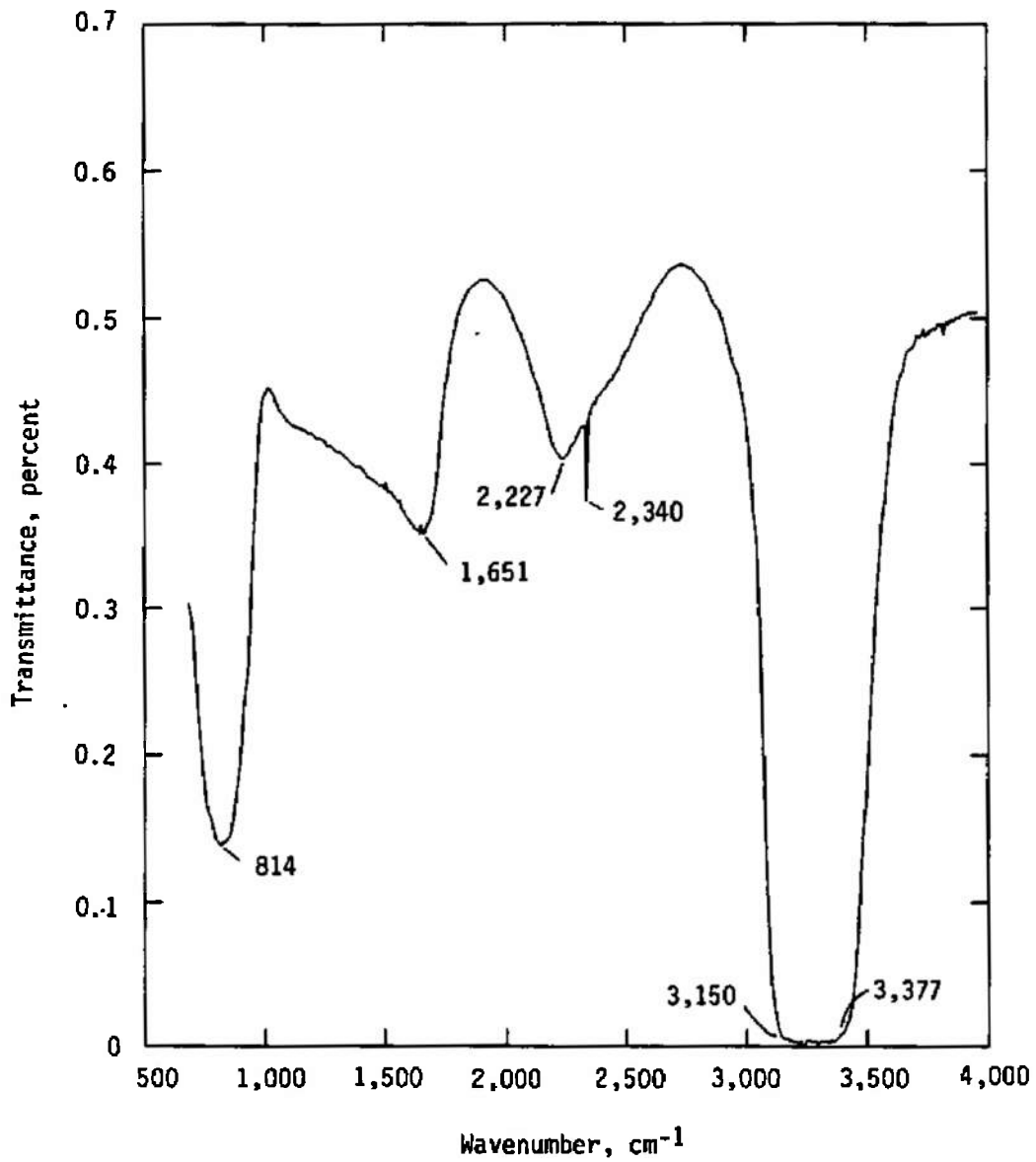
Figure 48. Transmittance of 3.59-μm-thick contaminant film condensed on 77 K germanium window, material Kapton®.
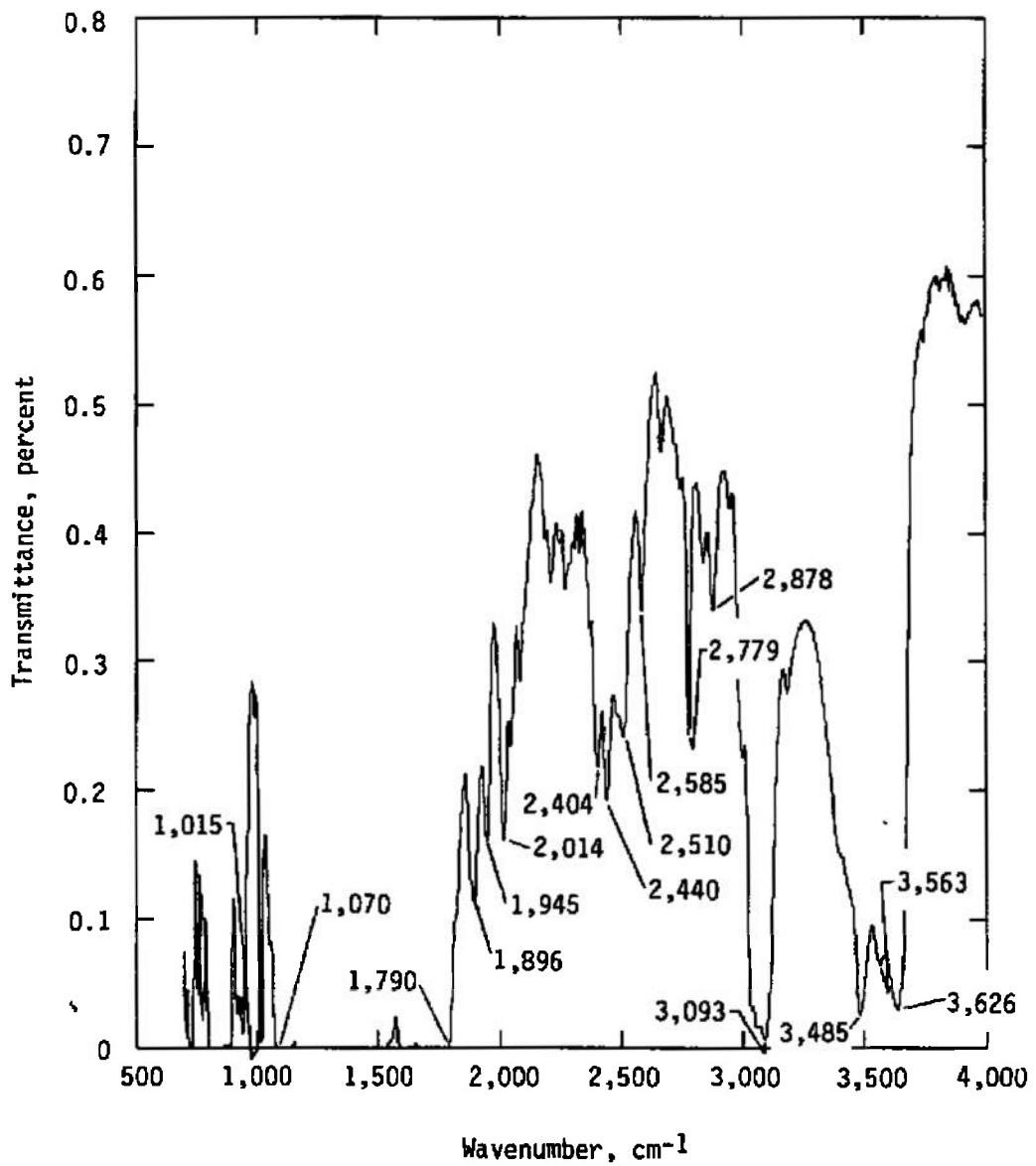
Figure 49. Transmittance of 5-mil-thick Kapton® film at 25°C and at atmospheric pressure.
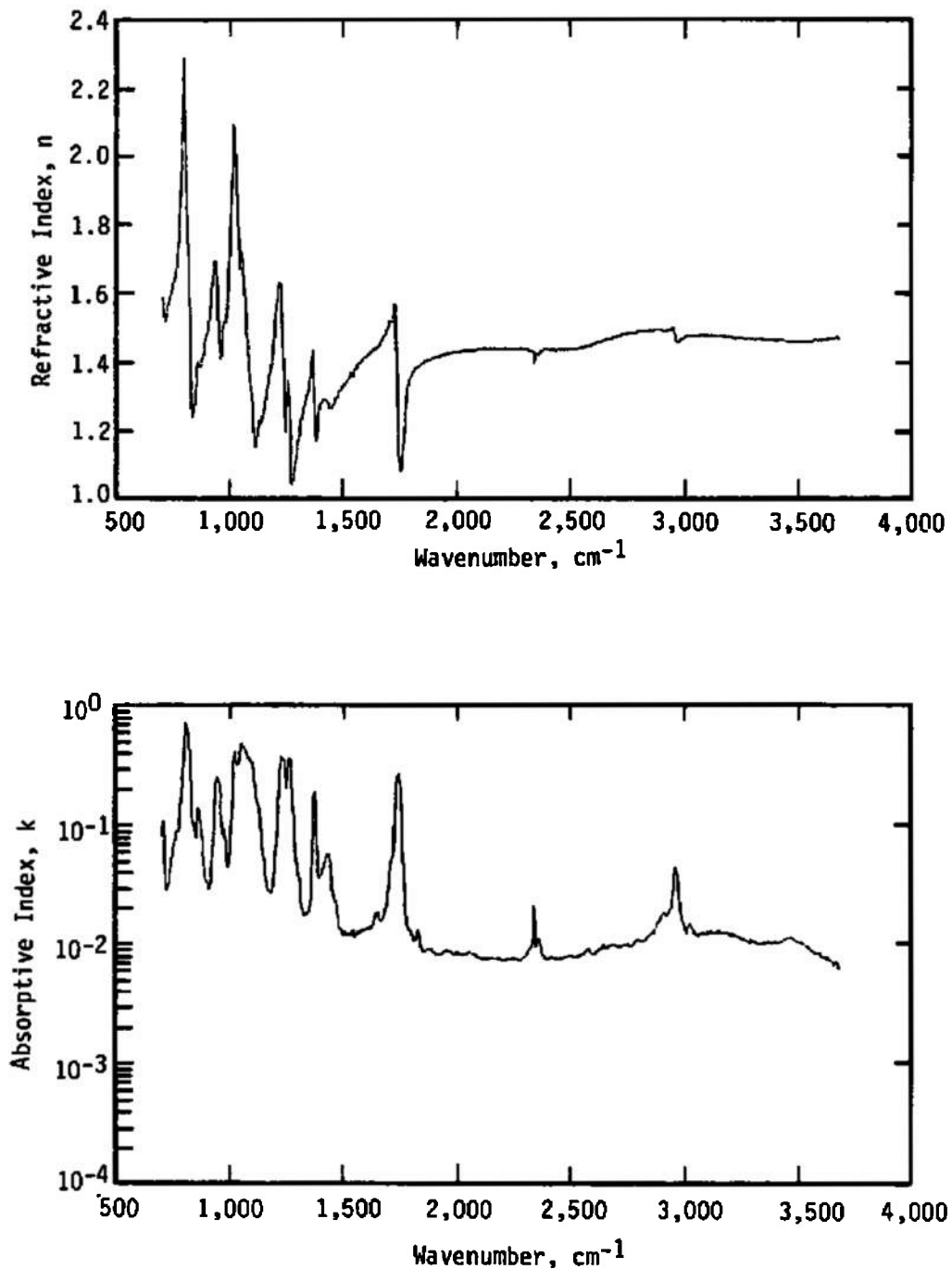
Figure 50. Refractive and absorptive indices for RTV-732 outgassing products condensed on 77 K surface.
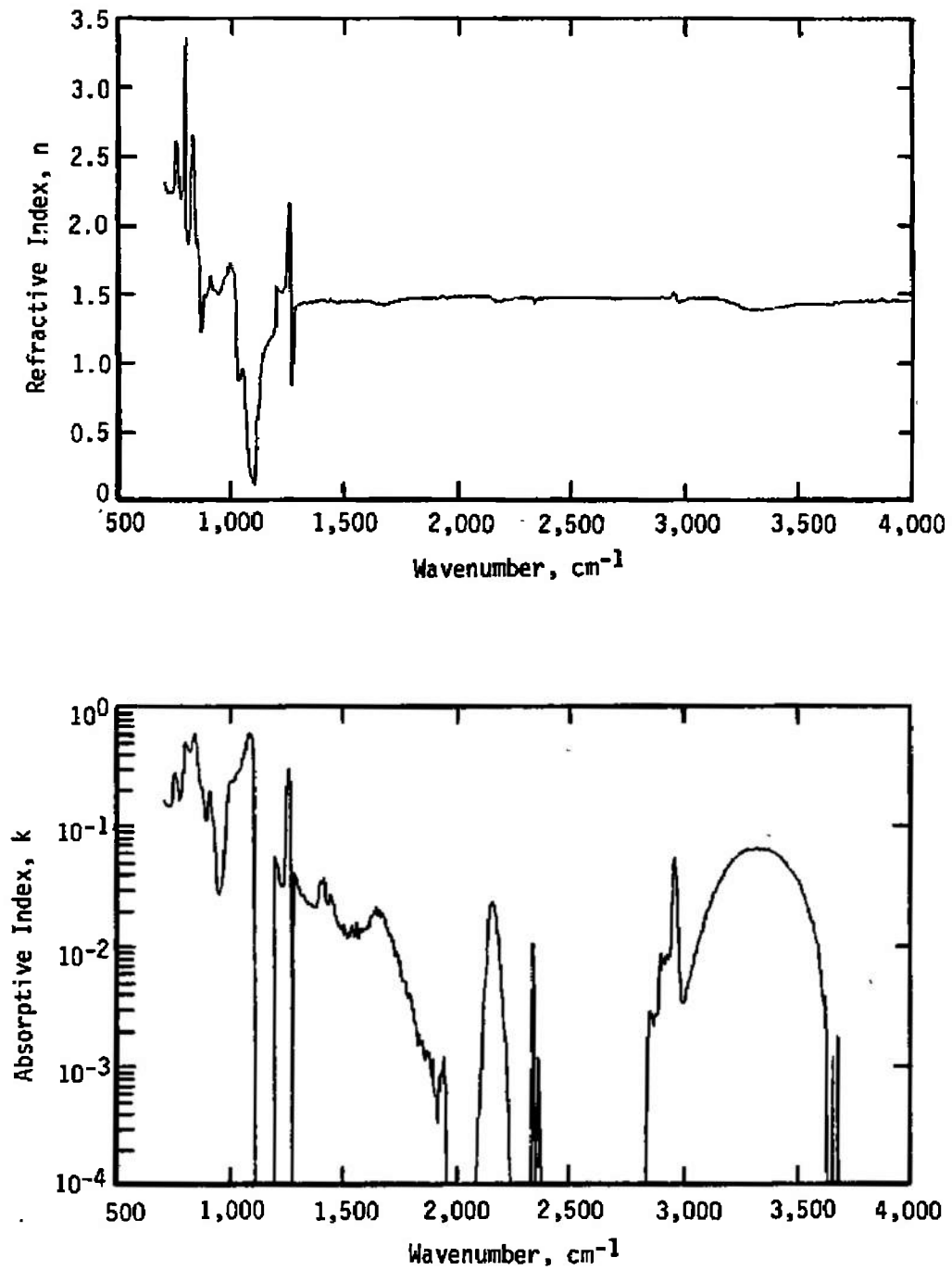
Figure 51. Refractive and absorptive indices for DC93-500 outgassing products condensed on 77 K surface.
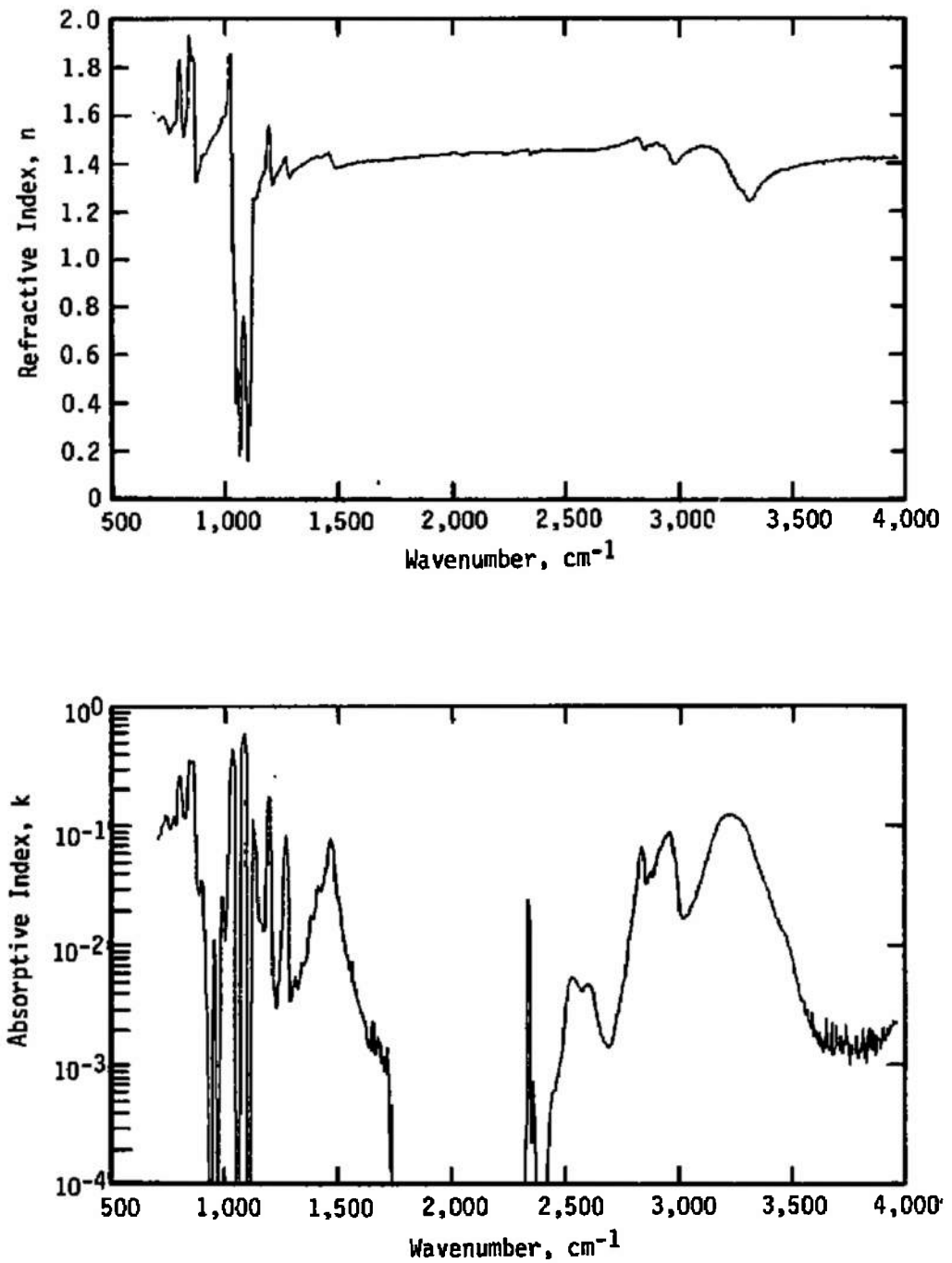
Figure 52. Refractive and absorptive indices for DC6-1104 outgassing products condensed on 77 K surface.
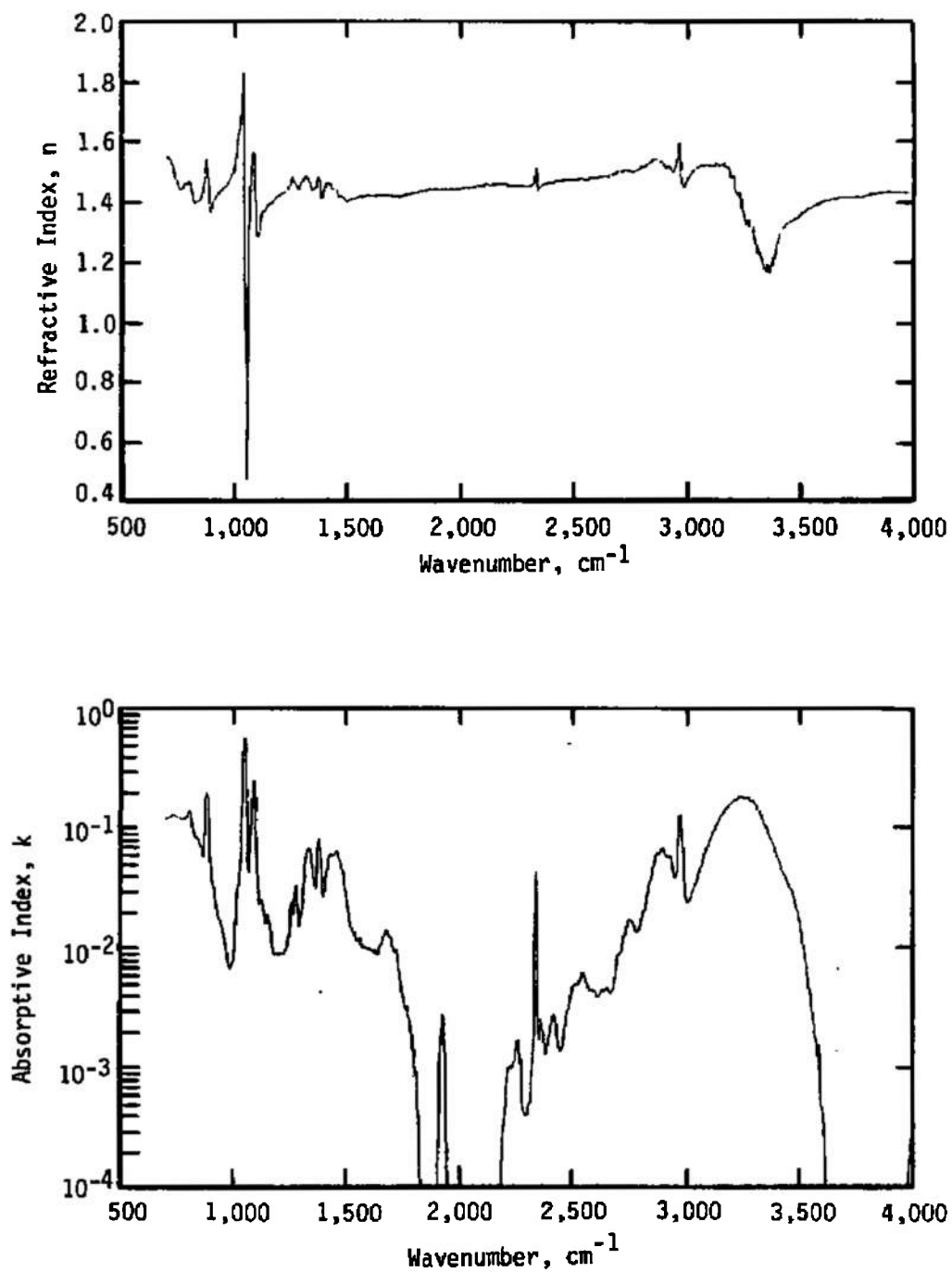
Figure 53. Refractive and absorptive indices for RTV566 outgassing products condensed on
77 K surface.

91
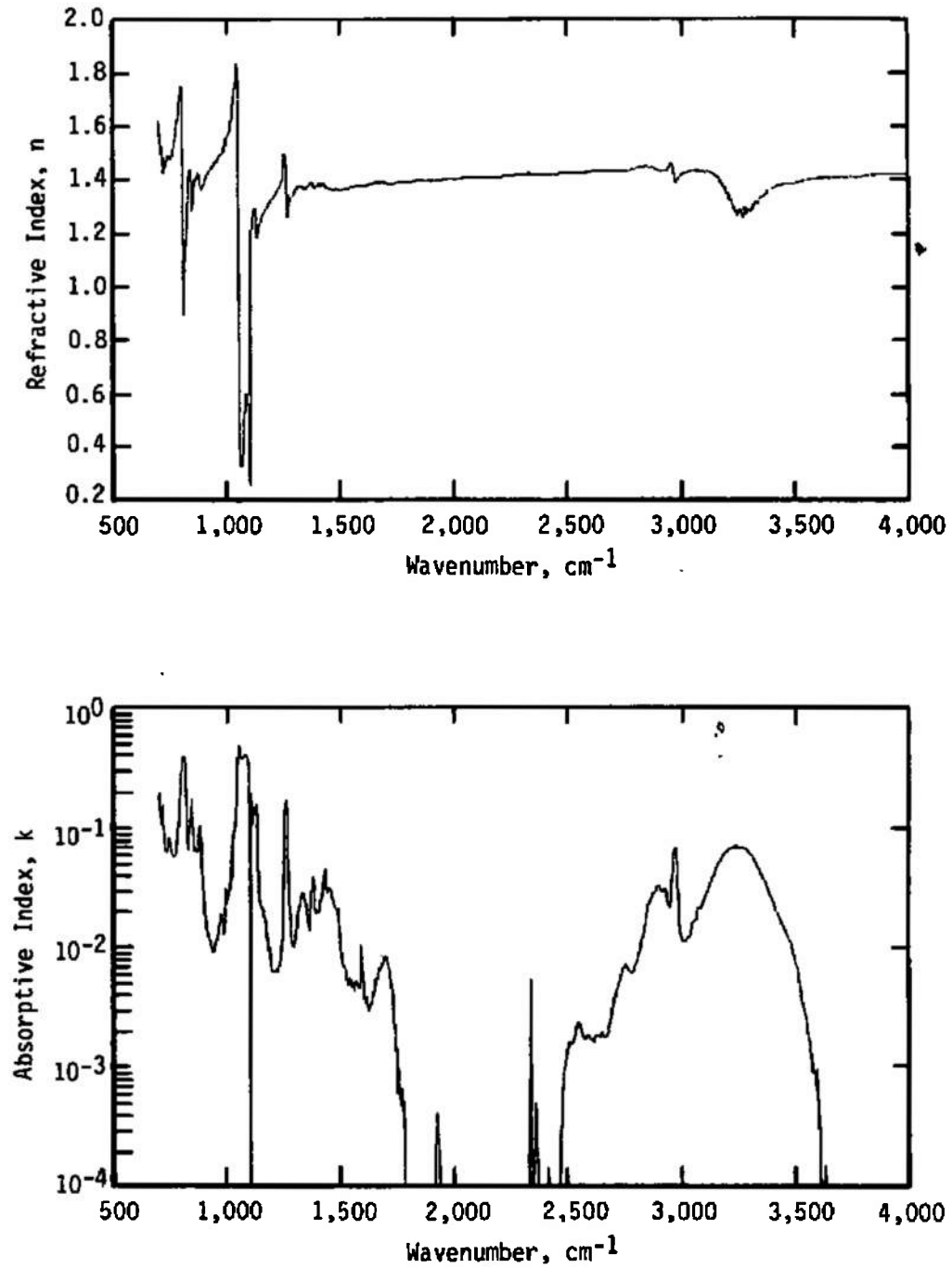
Figure 54. Refractive and absorptive indices for RTV560 outgassing products condensed on 77 K surface.
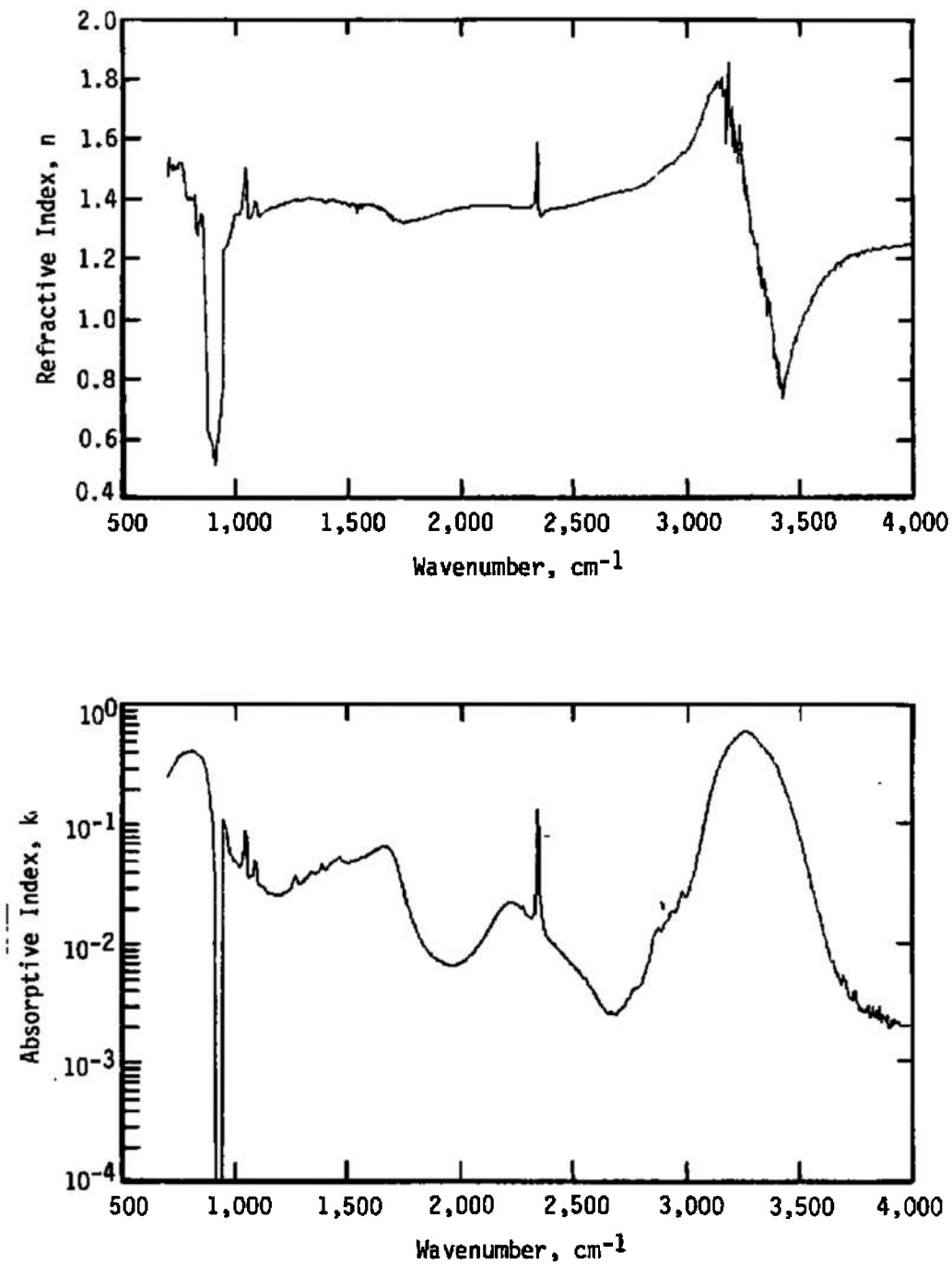
Figure 55. Refractive and absorptive indices for S13G/LO outgassing products condensed on 77 K surface.
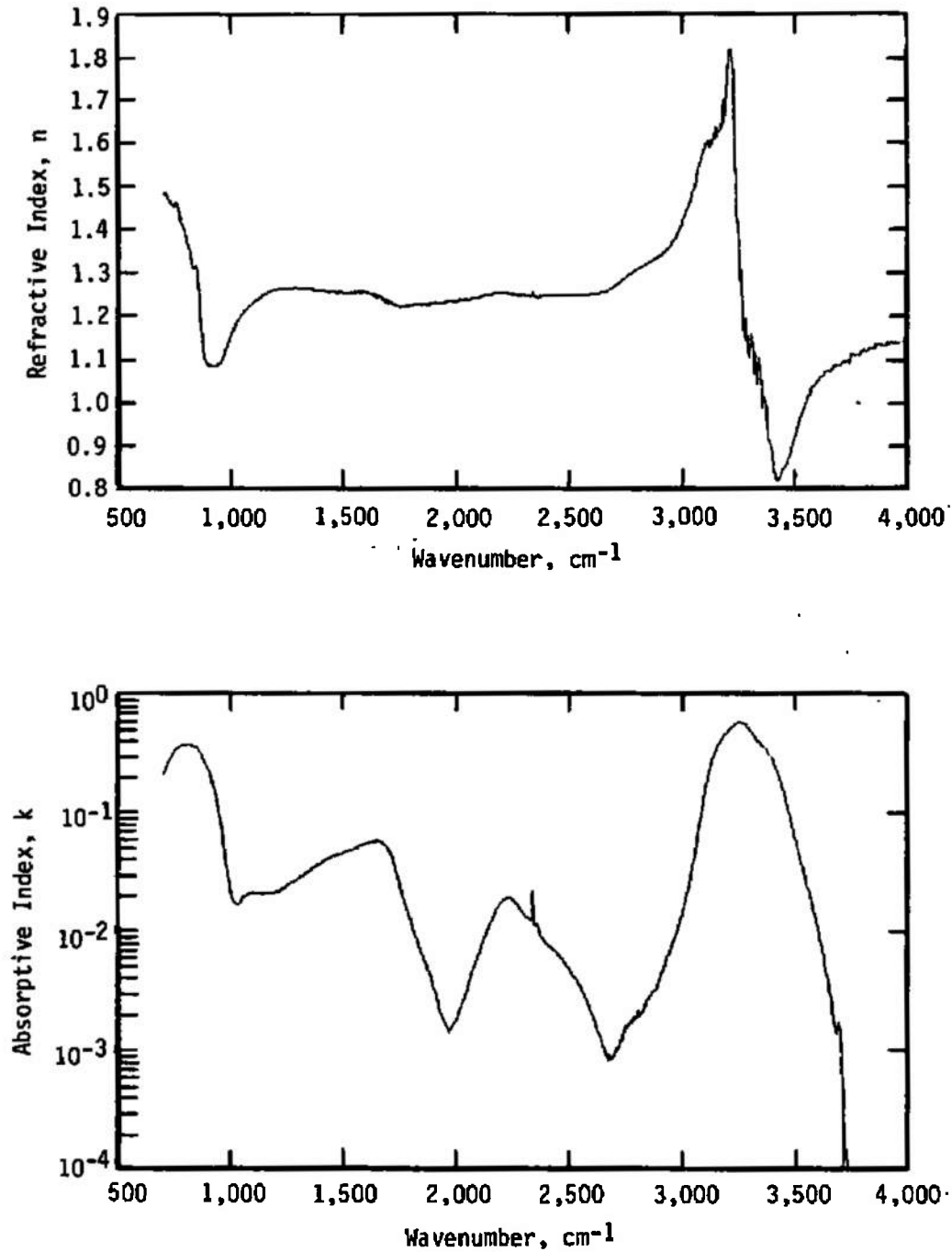
Figure 56. Refractive and absorptive indices for Kapton® outgassing products condensed on
77 K surface.
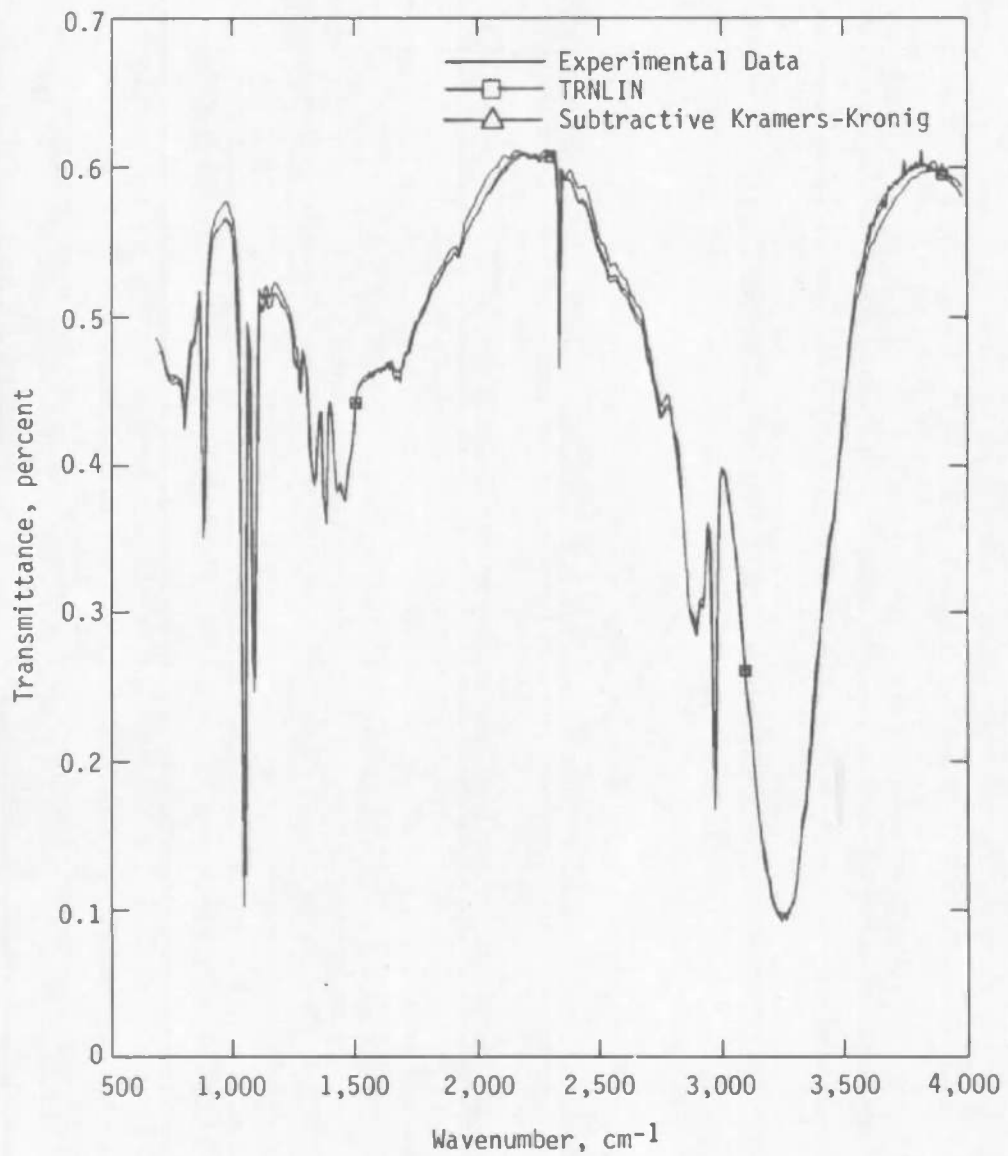
Figure 57. Transmittance versus wavenumber for experimental and CALCRT calculations for a 2.30-μm-thick RTV566 contaminant film.
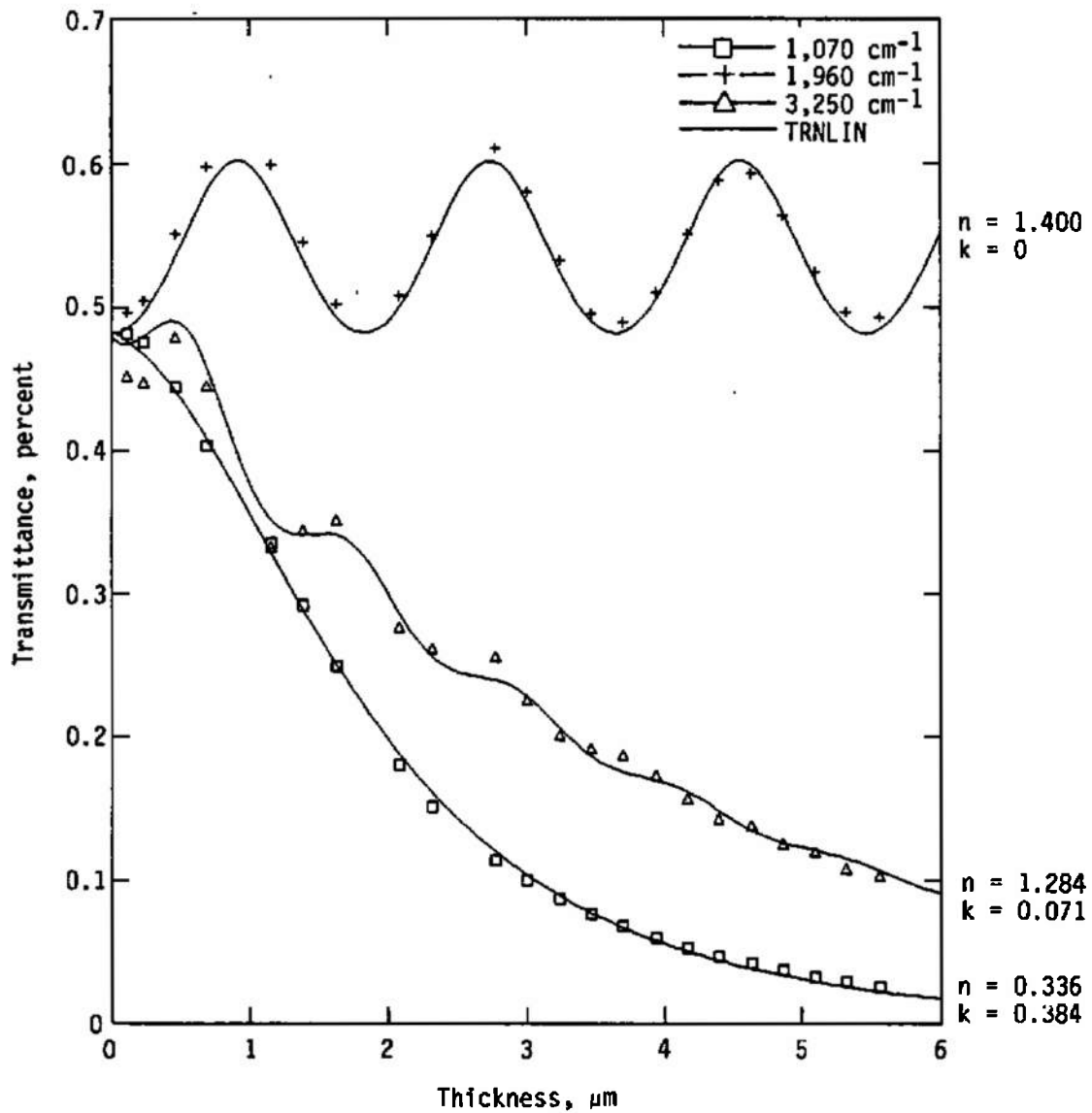
Figure 58. Comparison of calculated and experimental transmittance values versus film thickness for RTV560 contaminant films for 1,070, 1,960, and 3,250 cm⁻¹.
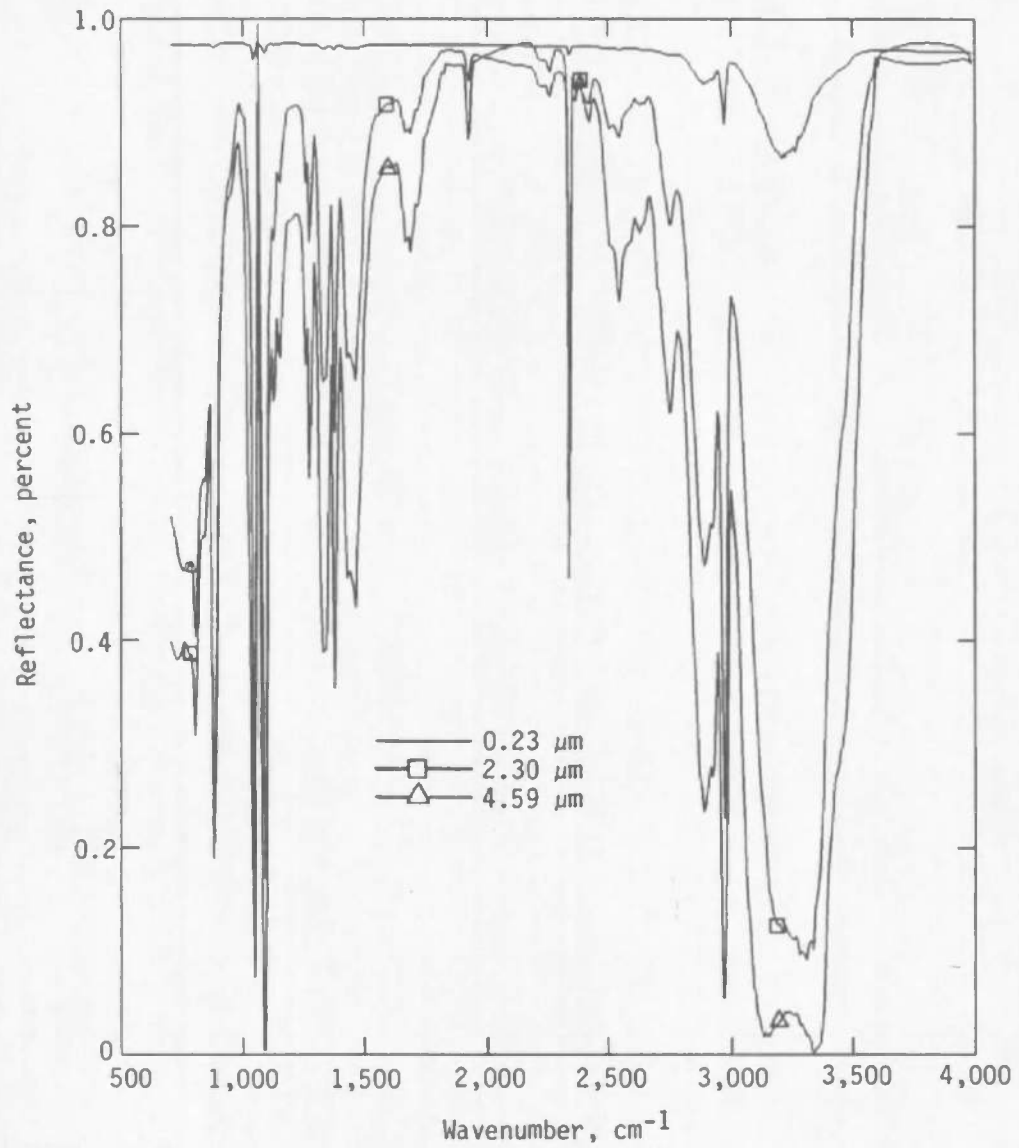
Figure 59. Calculated reflectance curves versus wavenumber for RTV566 films of 0.23-, 2.30-, and 4.59-μm thickness for a mirror having n* = 1.8 + 18 i.
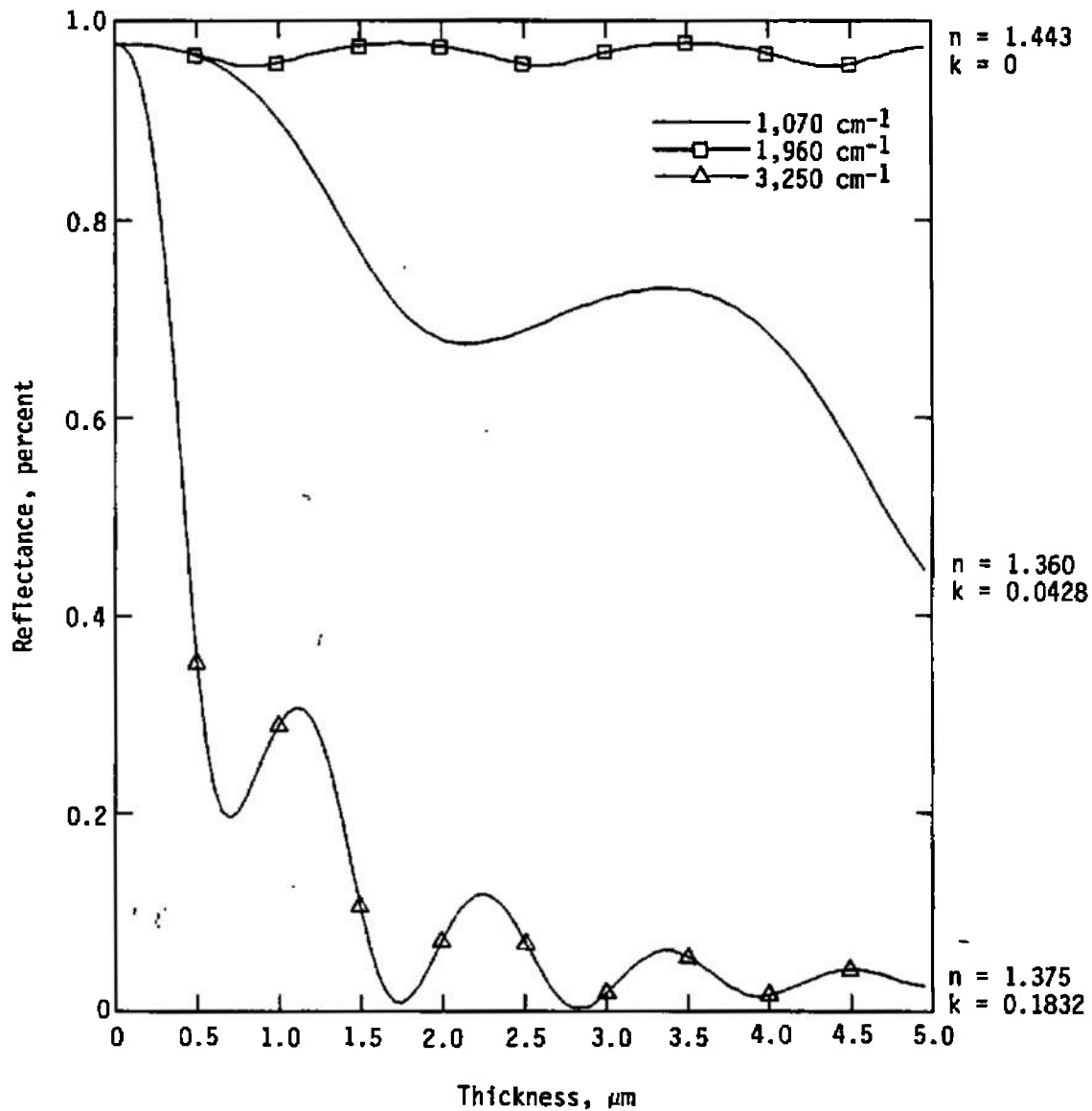
Figure 60. Calculated mirror reflectance versus RTV566 film thickness for 1,070, 1,960, and 3,250 cm^{-1}, mirror optical constants given by n* = 1.8 + 18 i.

Table 1. Materials List for Contamination Outgassing Kinetics and Surface Effects Studies.

Adhesives

1. DC93-500
2. DC6-1104
3. RTV566
4. RTV560
5. Solithane 113

Films

6. Kapton®
7. Mylar®
8. FEP Teflon®

Fluids and Lubricants

9. Braykote 8152 (Bray Oil Co.)
10. 40CS PAO-XRM-109 (Mobil)
11. Krytoc 143 AD (Dupont)
12. Braykote 600 Grease (Bray Oil Co.)

Paints

13. Chemglaze Z 306
14. Chemglaze A 237
15. Replacement for S-13GLO (Using V-10 Binder)
16. Replacement for S-13GLO (Using RTV-12 Binder)
17. Silver Flake/Silicon Silicate Thermal Control Developmental Coating

Composites

18. Polyimide Organic Matrix Composite
19. P75S Pitch 934 Graphite Epoxy
20. Graphite Epoxy Composite (HY-E1334A)

Others

21. Polyster Velcro®
22. Silicon Fluoride Rubber (Used to Make Elecrical Connectors)
23. 966 Acrylic Transfer Tape Made by 3M
24. Dimethyl Silicone Elastomer
25. Shrink Tubing
26. PC Board

Table 2. Summary of Materials Heated to 125°C under vacuum and outgassing products condensed on a 77 K germanium window.

Material	Test Weight, gm	TML, percent	Refractive index at 0.6328 μm	Cure Time, hr	Comment
RTV-732	21.1	4.53	1.44	1	Lot EQ075820
DC93-500	66.6	0.09	1.44	46	Lot GA115893
DC6-1104	107	---	1.455	92	Lot GA016912
RTV566	95.4	0.57	1.43	44	Batch FD 239 Catalyst-EA105
RTV560	78	2.0	1.42	45	Batch FD 873 Catalyst - DBT
S13G/LO	53	0.16	1.34	45	Batch L-024 V-10 Resin
Kapton®	126	1.26	1.21	—	Obtained from Lockheed

Table 3. Tabulated Refractive and Absorptive Indices for RTV566

cm^{-1}	n	k	cm^{-1}	n	k	cm^{-1}	n	k
702	1.54855	0.12188E+00	802	1.46579	0.14376E+00	902	1.38426	0.46197E-01
704	1.54913	0.12176E+00	804	1.45662	0.14608E+00	904	1.39067	0.42394E-01
706	1.54781	0.12170E+00	806	1.45003	0.14452E+00	906	1.39523	0.39471E-01
708	1.54780	0.12220E+00	808	1.44393	0.14016E+00	908	1.39945	0.36896E-01
710	1.54415	0.12262E+00	810	1.43885	0.13498E+00	910	1.40382	0.34580E-01
712	1.54214	0.12346E+00	812	1.43691	0.12978E+00	912	1.40670	0.32545E-01
714	1.54155	0.12369E+00	814	1.43259	0.12496E+00	914	1.40986	0.30583E-01
716	1.53743	0.12429E+00	816	1.42738	0.11924E+00	916	1.41217	0.28945E-01
718	1.53513	0.12519E+00	818	1.42020	0.11263E+00	918	1.41538	0.27345E-01
720	1.53176	0.12639E+00	820	1.41315	0.10672E+00	920	1.41712	0.25698E-01
722	1.52587	0.12709E+00	822	1.40631	0.10105E+00	922	1.41978	0.24286E-01
724	1.52484	0.12706E+00	824	1.39979	0.95867E-01	924	1.42181	0.23070E-01
726	1.52066	0.12727E+00	826	1.39587	0.91382E-01	926	1.42441	0.22113E-01
728	1.51468	0.12760E+00	828	1.39521	0.88034E-01	928	1.42657	0.21246E-01
730	1.50970	0.12786E+00	830	1.39815	0.86238E-01	930	1.42864	0.20405E-01
732	1.50180	0.12834E+00	832	1.39928	0.85165E-01	932	1.43087	0.19768E-01
734	1.49557	0.12850E+00	834	1.40195	0.84713E-01	934	1.43243	0.19015E-01
736	1.49263	0.12856E+00	836	1.40451	0.84585E-01	936	1.43413	0.18517E-01
738	1.48913	0.12870E+00	838	1.40678	0.84961E-01	938	1.43570	0.17882E-01
740	1.48177	0.12864E+00	840	1.40785	0.85490E-01	940	1.43702	0.17208E-01
742	1.47663	0.12842E+00	842	1.40669	0.85050E-01	942	1.43870	0.16894E-01
744	1.47010	0.12805E+00	844	1.40409	0.84094E-01	944	1.43980	0.16383E-01
746	1.46865	0.12757E+00	846	1.40379	0.82318E-01	946	1.44115	0.16091E-01
748	1.46316	0.12706E+00	848	1.40318	0.79979E-01	948	1.44247	0.15678E-01
750	1.45934	0.12650E+00	850	1.40415	0.77302E-01	950	1.44292	0.15059E-01
752	1.45426	0.12618E+00	852	1.40946	0.74630E-01	952	1.44444	0.14556E-01
754	1.44861	0.12551E+00	854	1.41635	0.71909E-01	954	1.44615	0.13914E-01
756	1.44530	0.12493E+00	856	1.42341	0.69169E-01	956	1.44745	0.13546E-01
758	1.44014	0.12453E+00	858	1.43079	0.66702E-01	958	1.44824	0.13293E-01
760	1.44256	0.12391E+00	860	1.43991	0.64318E-01	960	1.44925	0.12789E-01
762	1.44143	0.12355E+00	862	1.44825	0.62190E-01	962	1.45006	0.12194E-01
764	1.44017	0.12286E+00	864	1.45603	0.59990E-01	964	1.45238	0.11189E-01
766	1.44288	0.12222E+00	866	1.46577	0.58629E-01	966	1.45491	0.10405E-01
768	1.44243	0.12180E+00	868	1.47728	0.58856E-01	968	1.45730	0.95295E-02
770	1.44397	0.12132E+00	870	1.49378	0.63011E-01	970	1.45936	0.89612E-02
772	1.44749	0.12122E+00	872	1.51278	0.74422E-01	972	1.46216	0.86158E-02
774	1.45116	0.12132E+00	874	1.53124	0.98169E-01	974	1.46408	0.81211E-02
776	1.45697	0.12150E+00	876	1.54856	0.13664E+00	976	1.46639	0.77041E-02
778	1.45965	0.12193E+00	878	1.54418	0.17583E+00	978	1.46939	0.74789E-02
780	1.46104	0.12218E+00	880	1.51782	0.19693E+00	980	1.47170	0.71115E-02
782	1.46227	0.12239E+00	882	1.48513	0.19899E+00	982	1.47524	0.70174E-02
784	1.45966	0.12251E+00	884	1.45948	0.19258E+00	984	1.47857	0.69226E-02
786	1.45914	0.12211E+00	886	1.43945	0.18474E+00	986	1.48146	0.67610E-02
788	1.45636	0.12167E+00	888	1.41826	0.17186E+00	988	1.48430	0.66778E-02
790	1.45634	0.12107E+00	890	1.39229	0.14922E+00	990	1.48813	0.66445E-02
792	1.45957	0.12121E+00	892	1.36979	0.12075E+00	992	1.49112	0.69916E-02
794	1.45936	0.12304E+00	894	1.36026	0.93528E-01	994	1.49479	0.75211E-02
796	1.46612	0.12638E+00	896	1.36210	0.73080E-01	996	1.49847	0.80744E-02
798	1.46960	0.13176E+00	898	1.36978	0.59717E-01	998	1.50230	0.78875E-02
800	1.46990	0.13829E+00	900	1.37760	0.51438E-01	1000	1.50936	0.79408E-02

Table 3. Continued

cm⁻¹	n	k	cm⁻¹	n	k	cm⁻¹	n	k
1002	1.51412	0.86320E-02	1102	1.29066	0.96260E-01	1202	1.42296	0.88137E-02
1004	1.52049	0.97177E-02	1104	1.28018	0.65875E-01	1204	1.42394	0.88826E-02
1006	1.52812	0.11251E-01	1106	1.28238	0.46569E-01	1206	1.42464	0.89044E-02
1008	1.53643	0.12964E-01	1108	1.29041	0.35473E-01	1208	1.42565	0.89777E-02
1010	1.54623	0.14956E-01	1110	1.30287	0.28983E-01	1210	1.42629	0.89661E-02
1012	1.55728	0.17261E-01	1112	1.31518	0.25231E-01	1212	1.42683	0.89333E-02
1014	1.57127	0.19958E-01	1114	1.32557	0.23410E-01	1214	1.42831	0.88461E-02
1016	1.58657	0.22895E-01	1116	1.33600	0.23171E-01	1216	1.42915	0.88294E-02
1018	1.60282	0.26204E-01	1118	1.34438	0.23823E-01	1218	1.43032	0.88770E-02
1020	1.62016	0.29391E-01	1120	1.35080	0.24934E-01	1220	1.43086	0.89757E-02
1022	1.63551	0.32187E-01	1122	1.35484	0.25484E-01	1222	1.43202	0.90835E-02
1024	1.64919	0.34601E-01	1124	1.35922	0.25679E-01	1224	1.43315	0.91584E-02
1026	1.66111	0.36400E-01	1126	1.36285	0.25636E-01	1226	1.43403	0.91913E-02
1028	1.66939	0.38639E-01	1128	1.36556	0.25521E-01	1228	1.43470	0.93310E-02
1030	1.67968	0.42141E-01	1130	1.36710	0.24936E-01	1230	1.43576	0.94960E-02
1032	1.69190	0.48914E-01	1132	1.36834	0.23425E-01	1232	1.43771	0.96350E-02
1034	1.70748	0.61198E-01	1134	1.36882	0.21443E-01	1234	1.43821	0.98597E-02
1036	1.72520	0.81802E-01	1136	1.37220	0.19517E-01	1236	1.44004	0.10112E-01
1038	1.74489	0.11502E+00	1138	1.37503	0.17835E-01	1238	1.44097	0.10343E-01
1040	1.77485	0.16447E+00	1140	1.37799	0.16637E-01	1240	1.44290	0.10591E-01
1042	1.82992	0.23483E+00	1142	1.38113	0.16059E-01	1242	1.44576	0.10991E-01
1044	1.91356	0.32761E+00	1144	1.38393	0.16191E-01	1244	1.44855	0.11657E-01
1046	1.77485	0.43335E+00	1146	1.38746	0.16910E-01	1246	1.45218	0.12569E-01
1048	1.07011	0.53236E+00	1148	1.38997	0.18098E-01	1248	1.45645	0.13818E-01
1050	1.00685	0.57737E+00	1150	1.39196	0.19418E-01	1250	1.46259	0.15449E-01
1052	0.91782	0.57029E+00	1152	1.39212	0.20042E-01	1252	1.47103	0.17939E-01
1054	0.81821	0.51540E+00	1154	1.39209	0.19622E-01	1254	1.48015	0.21090E-01
1056	0.68837	0.41497E+00	1156	1.39217	0.18631E-01	1256	1.48625	0.23692E-01
1058	0.47989	0.24679E+00	1158	1.39369	0.17665E-01	1258	1.48758	0.24940E-01
1060	0.40870	0.00000E+00	1160	1.39363	0.16994E-01	1260	1.48302	0.24545E-01
1062	1.24850	0.11194E+00	1162	1.39452	0.16165E-01	1262	1.47547	0.22705E-01
1064	1.26813	0.64847E-01	1164	1.39481	0.14882E-01	1264	1.46732	0.20585E-01
1066	1.29855	0.48137E-01	1166	1.39579	0.13296E-01	1266	1.46245	0.19411E-01
1068	1.32824	0.42781E-01	1168	1.39799	0.11947E-01	1268	1.46090	0.20147E-01
1070	1.36004	0.42831E-01	1170	1.39981	0.11070E-01	1270	1.46149	0.23423E-01
1072	1.39780	0.47554E-01	1172	1.40200	0.10409E-01	1272	1.46200	0.28459E-01
1074	1.44149	0.57524E-01	1174	1.40420	0.99093E-02	1274	1.45872	0.32784E-01
1076	1.48165	0.74173E-01	1176	1.40554	0.94180E-02	1276	1.45341	0.34466E-01
1078	1.51365	0.98674E-01	1178	1.40706	0.91174E-02	1278	1.44802	0.33429E-01
1080	1.53892	0.12995E+00	1180	1.40826	0.89257E-02	1280	1.44328	0.30279E-01
1082	1.55832	0.16413E+00	1182	1.41026	0.89041E-02	1282	1.44149	0.25990E-01
1084	1.56463	0.19705E+00	1184	1.41223	0.87712E-02	1284	1.44126	0.21847E-01
1086	1.56636	0.22485E+00	1186	1.41392	0.88132E-02	1286	1.44320	0.18658E-01
1088	1.54716	0.24586E+00	1188	1.41488	0.88280E-02	1288	1.44621	0.16676E-01
1090	1.52298	0.25680E+00	1190	1.41609	0.88633E-02	1290	1.44961	0.15668E-01
1092	1.49079	0.25583E+00	1192	1.41739	0.89429E-02	1292	1.45272	0.15384E-01
1094	1.44779	0.24199E+00	1194	1.41907	0.89051E-02	1294	1.45634	0.15611E-01
1096	1.40799	0.21580E+00	1196	1.42014	0.89338E-02	1296	1.45908	0.16292E-01
1098	1.36004	0.17883E+00	1198	1.42083	0.88995E-02	1298	1.46209	0.17133E-01
1100	1.32060	0.13635E+00	1200	1.42175	0.88574E-02	1300	1.46481	0.18354E-01

Table 3. Continued

cm^{-1}	n	k	cm^{-1}	n	k	cm^{-1}	n	k
1302	1.46790	0.19900E-01	1402	1.44912	0.28702E-01	1502	1.40341	0.23064E-01
1304	1.47158	0.21940E-01	1404	1.45172	0.30653E-01	1504	1.40410	0.22172E-01
1306	1.47477	0.24537E-01	1406	1.45600	0.32564E-01	1506	1.40477	0.22338E-01
1308	1.47774	0.27815E-01	1408	1.45920	0.34897E-01	1508	1.40709	0.19533E-01
1310	1.48080	0.31587E-01	1410	1.46153	0.37765E-01	1510	1.40512	0.17984E-01
1312	1.48356	0.35951E-01	1412	1.46271	0.40918E-01	1512	1.40568	0.17697E-01
1314	1.48660	0.40591E-01	1414	1.46389	0.44068E-01	1514	1.40721	0.17065E-01
1316	1.48718	0.45239E-01	1416	1.46412	0.47435E-01	1516	1.40689	0.17004E-01
1318	1.48767	0.49771E-01	1418	1.46211	0.50855E-01	1518	1.40851	0.15279E-01
1320	1.48609	0.54039E-01	1420	1.46046	0.54179E-01	1520	1.40768	0.15979E-01
1322	1.48486	0.57709E-01	1422	1.46032	0.57140E-01	1522	1.40914	0.14947E-01
1324	1.48261	0.60831E-01	1424	1.45724	0.59355E-01	1524	1.40909	0.14894E-01
1326	1.47918	0.63558E-01	1426	1.45673	0.61445E-01	1526	1.40961	0.14175E-01
1328	1.47579	0.65714E-01	1428	1.45385	0.62692E-01	1528	1.41078	0.13857E-01
1330	1.47024	0.67292E-01	1430	1.44991	0.62988E-01	1530	1.41161	0.13579E-01
1332	1.46628	0.68207E-01	1432	1.44800	0.62800E-01	1532	1.41121	0.13648E-01
1334	1.46231	0.68470E-01	1434	1.44463	0.61562E-01	1534	1.41130	0.12683E-01
1336	1.45752	0.68155E-01	1436	1.44092	0.60408E-01	1536	1.41313	0.12832E-01
1338	1.45368	0.67136E-01	1438	1.44396	0.58397E-01	1538	1.41628	0.13617E-01
1340	1.44832	0.64791E-01	1440	1.44581	0.58854E-01	1540	1.40833	0.12790E-01
1342	1.44598	0.62342E-01	1442	1.44631	0.60081E-01	1542	1.41345	0.12451E-01
1344	1.44367	0.59133E-01	1444	1.44533	0.61193E-01	1544	1.41325	0.12452E-01
1346	1.44256	0.55285E-01	1446	1.44269	0.62088E-01	1546	1.41434	0.11623E-01
1348	1.44112	0.51174E-01	1448	1.43962	0.62353E-01	1548	1.41584	0.11973E-01
1350	1.44177	0.46755E-01	1450	1.44011	0.63020E-01	1550	1.41541	0.11829E-01
1352	1.44221	0.42994E-01	1452	1.43792	0.63945E-01	1552	1.41595	0.11804E-01
1354	1.44311	0.40136E-01	1454	1.43623	0.65315E-01	1554	1.41546	0.11882E-01
1356	1.44496	0.37933E-01	1456	1.42813	0.66195E-01	1556	1.41606	0.11852E-01
1358	1.44633	0.36209E-01	1458	1.42409	0.65604E-01	1558	1.41955	0.12046E-01
1360	1.44717	0.34186E-01	1460	1.42520	0.65749E-01	1560	1.41689	0.10355E-01
1362	1.44868	0.31809E-01	1462	1.42343	0.64521E-01	1562	1.41633	0.10856E-01
1364	1.45717	0.28969E-01	1464	1.41849	0.62124E-01	1564	1.41745	0.11163E-01
1366	1.46911	0.32077E-01	1466	1.41746	0.58151E-01	1566	1.41742	0.10661E-01
1368	1.48093	0.42202E-01	1468	1.41874	0.55953E-01	1568	1.41883	0.11169E-01
1370	1.48766	0.55390E-01	1470	1.41951	0.54296E-01	1570	1.41670	0.10156E-01
1372	1.48533	0.64372E-01	1472	1.41505	0.52515E-01	1572	1.41817	0.10575E-01
1374	1.47740	0.69078E-01	1474	1.41665	0.49831E-01	1574	1.41872	0.10798E-01
1376	1.47739	0.73350E-01	1476	1.41658	0.48996E-01	1576	1.41959	0.10622E-01
1378	1.47513	0.78614E-01	1478	1.41615	0.47812E-01	1578	1.41845	0.10218E-01
1380	1.46833	0.83308E-01	1480	1.41502	0.46606E-01	1580	1.41890	0.10249E-01
1382	1.45198	0.83102E-01	1482	1.41393	0.44762E-01	1582	1.41920	0.10281E-01
1384	1.42909	0.75115E-01	1484	1.41417	0.44349E-01	1584	1.41899	0.10199E-01
1386	1.41148	0.61840E-01	1486	1.41353	0.44632E-01	1586	1.41906	0.10076E-01
1388	1.40950	0.44606E-01	1488	1.41084	0.43573E-01	1588	1.41922	0.99675E-02
1390	1.41535	0.35242E-01	1490	1.40521	0.40672E-01	1590	1.41939	0.99219E-02
1392	1.42416	0.30162E-01	1492	1.40599	0.37388E-01	1592	1.41986	0.98994E-02
1394	1.43030	0.28639E-01	1494	1.40384	0.34664E-01	1594	1.42036	0.10017E-01
1396	1.43730	0.27093E-01	1496	1.40183	0.31612E-01	1596	1.41975	0.97976E-02
1398	1.44006	0.27439E-01	1498	1.40211	0.28467E-01	1598	1.42000	0.97999E-02
1400	1.44571	0.27566E-01	1500	1.40318	0.24996E-01	1600	1.42051	0.98149E-02

Table 3. Continued

cm⁻¹	n	k	cm⁻¹	n	k	cm⁻¹	n	k
1602	1.42066	0.99318E-02	1702	1.41727	0.10594E-01	1802	1.43272	0.10627E-02
1604	1.42032	0.98913E-02	1704	1.41935	0.10584E-01	1804	1.43260	0.93798E-03
1606	1.42080	0.10047E-01	1706	1.41994	0.10255E-01	1806	1.43306	0.86526E-03
1608	1.42082	0.97956E-02	1708	1.41868	0.95882E-02	1808	1.43342	0.73357E-03
1610	1.42078	0.95423E-02	1710	1.41846	0.95017E-02	1810	1.43412	0.91670E-03
1612	1.42072	0.95210E-02	1712	1.41900	0.93656E-02	1812	1.43415	0.53234E-03
1614	1.42096	0.95859E-02	1714	1.42009	0.95828E-02	1814	1.43455	0.47133E-03
1616	1.42110	0.10185E-01	1716	1.41940	0.95018E-02	1816	1.43487	0.50042E-03
1618	1.41988	0.91694E-02	1718	1.42064	0.91994E-02	1818	1.43506	0.36311E-03
1620	1.42123	0.92990E-02	1720	1.41893	0.94240E-02	1820	1.43533	0.32899E-03
1622	1.42181	0.97109E-02	1722	1.41869	0.97155E-02	1822	1.43526	0.31234E-03
1624	1.42033	0.88108E-02	1724	1.41681	0.89845E-02	1824	1.43574	0.43677E-03
1626	1.42150	0.92245E-02	1726	1.41705	0.83076E-02	1826	1.43547	0.00000E+00
1628	1.42101	0.89698E-02	1728	1.41754	0.75208E-02	1828	1.43638	0.35357E-03
1630	1.42182	0.89739E-02	1730	1.41742	0.68339E-02	1830	1.43656	0.00000E+00
1632	1.42186	0.89569E-02	1732	1.41883	0.67408E-02	1832	1.43700	0.00000E+00
1634	1.42351	0.96727E-02	1734	1.41809	0.61867E-02	1834	1.43697	0.00000E+00
1636	1.42207	0.91465E-02	1736	1.41893	0.54241E-02	1836	1.43771	0.00000E+00
1638	1.42146	0.88236E-02	1738	1.42027	0.54542E-02	1838	1.43776	0.00000E+00
1640	1.42282	0.90205E-02	1740	1.41962	0.46850E-02	1840	1.43793	0.00000E+00
1642	1.42265	0.92068E-02	1742	1.42191	0.48260E-02	1842	1.43816	0.00000E+00
1644	1.42356	0.95819E-02	1744	1.42046	0.41465E-02	1844	1.43802	0.00000E+00
1646	1.42365	0.10365E-01	1746	1.42158	0.43202E-02	1846	1.43808	0.00000E+00
1648	1.42092	0.96468E-02	1748	1.42141	0.42701E-02	1848	1.43884	0.00000E+00
1650	1.42415	0.10359E-01	1750	1.42275	0.41045E-02	1850	1.43929	0.00000E+00
1652	1.42721	0.11488E-01	1752	1.42229	0.34189E-02	1852	1.43989	0.00000E+00
1654	1.42131	0.10573E-01	1754	1.42338	0.36135E-02	1854	1.43994	0.00000E+00
1656	1.42307	0.10982E-01	1756	1.42443	0.38455E-02	1856	1.44018	0.00000E+00
1658	1.42363	0.11391E-01	1758	1.42436	0.34030E-02	1858	1.44029	0.00000E+00
1660	1.42397	0.11790E-01	1760	1.42526	0.36024E-02	1860	1.44067	0.00000E+00
1662	1.42354	0.12267E-01	1762	1.42404	0.30993E-02	1862	1.44068	0.00000E+00
1664	1.42311	0.12163E-01	1764	1.42560	0.32129E-02	1864	1.44043	0.00000E+00
1666	1.42400	0.12675E-01	1766	1.42597	0.32263E-02	1866	1.44027	0.00000E+00
1668	1.42579	0.13647E-01	1768	1.42589	0.30521E-02	1868	1.44105	0.41096E-04
1670	1.42380	0.13274E-01	1770	1.42754	0.32762E-02	1870	1.44132	0.00000E+00
1672	1.42306	0.13250E-01	1772	1.42847	0.29089E-02	1872	1.44165	0.00000E+00
1674	1.42454	0.14049E-01	1774	1.42742	0.26828E-02	1874	1.44168	0.00000E+00
1676	1.42150	0.13131E-01	1776	1.42688	0.23792E-02	1876	1.44149	0.00000E+00
1678	1.42269	0.13731E-01	1778	1.42785	0.25201E-02	1878	1.44152	0.00000E+00
1680	1.42219	0.13812E-01	1780	1.42826	0.24645E-02	1880	1.44176	0.00000E+00
1682	1.42281	0.14079E-01	1782	1.42828	0.20736E-02	1882	1.44196	0.00000E+00
1684	1.42457	0.13823E-01	1784	1.42909	0.21466E-02	1884	1.44192	0.00000E+00
1686	1.42069	0.12976E-01	1786	1.42869	0.17485E-02	1886	1.44175	0.00000E+00
1688	1.42139	0.13138E-01	1788	1.42938	0.17674E-02	1888	1.44211	0.00000E+00
1690	1.42080	0.12705E-01	1790	1.43064	0.18889E-02	1890	1.44206	0.00000E+00
1692	1.42037	0.12422E-01	1792	1.43080	0.18690E-02	1892	1.44211	0.00000E+00
1694	1.42089	0.12661E-01	1794	1.43088	0.14164E-02	1894	1.44253	0.00000E+00
1696	1.42060	0.11806E-01	1796	1.43141	0.14252E-02	1896	1.44246	0.00000E+00
1698	1.42025	0.11719E-01	1798	1.43192	0.14664E-02	1898	1.44245	0.00000E+00
1700	1.42096	0.11374E-01	1800	1.43172	0.11835E-02	1900	1.44249	0.00000E+00

Table 3. Continued

cm^{-1}	n	k	cm^{-1}	n	k	cm^{-1}	n	k
1902	1.44283	0.00000E+00	2002	1.44456	0.00000E+00	2102	1.45469	0.00000E+00
1904	1.44286	0.78353E-04	2004	1.44494	0.00000E+00	2104	1.45511	0.00000E+00
1906	1.44301	0.21425E-03	2006	1.44540	0.00000E+00	2106	1.45545	0.00000E+00
1908	1.44360	0.33544E-03	2008	1.44558	0.00000E+00	2108	1.45569	0.00000E+00
1910	1.44373	0.46724E-03	2010	1.44580	0.00000E+00	2110	1.45610	0.00000E+00
1912	1.44382	0.68984E-03	2012	1.44602	0.00000E+00	2112	1.45628	0.00000E+00
1914	1.44365	0.10573E-02	2014	1.44604	0.00000E+00	2114	1.45625	0.00000E+00
1916	1.44429	0.13697E-02	2016	1.44603	0.00000E+00	2116	1.45671	0.00000E+00
1918	1.44395	0.17359E-02	2018	1.44617	0.00000E+00	2118	1.45672	0.00000E+00
1920	1.44427	0.21026E-02	2020	1.44675	0.00000E+00	2120	1.45695	0.00000E+00
1922	1.44378	0.26331E-02	2022	1.44658	0.00000E+00	2122	1.45684	0.00000E+00
1924	1.44324	0.25570E-02	2024	1.44649	0.00000E+00	2124	1.45676	0.00000E+00
1926	1.44324	0.27633E-02	2026	1.44711	0.00000E+00	2126	1.45660	0.00000E+00
1928	1.44276	0.27434E-02	2028	1.44731	0.00000E+00	2128	1.45611	0.00000E+00
1930	1.44293	0.25627E-02	2030	1.44740	0.00000E+00	2130	1.45648	0.00000E+00
1932	1.44253	0.22666E-02	2032	1.44752	0.00000E+00	2132	1.45571	0.00000E+00
1934	1.44173	0.18696E-02	2034	1.44754	0.00000E+00	2134	1.45571	0.00000E+00
1936	1.44139	0.14319E-02	2036	1.44788	0.00000E+00	2136	1.45572	0.00000E+00
1938	1.44135	0.99643E-03	2038	1.44794	0.00000E+00	2138	1.45595	0.00000E+00
1940	1.44126	0.60982E-03	2040	1.44807	0.00000E+00	2140	1.45600	0.00000E+00
1942	1.44137	0.57686E-03	2042	1.44827	0.00000E+00	2142	1.45618	0.00000E+00
1944	1.44134	0.00000E+00	2044	1.44852	0.00000E+00	2144	1.45638	0.00000E+00
1946	1.44148	0.00000E+00	2046	1.44881	0.00000E+00	2146	1.45642	0.00000E+00
1948	1.44160	0.00000E+00	2048	1.44889	0.00000E+00	2148	1.45689	0.00000E+00
1950	1.44204	0.00000E+00	2050	1.44897	0.00000E+00	2150	1.45706	0.00000E+00
1952	1.44254	0.00000E+00	2052	1.44934	0.00000E+00	2152	1.45717	0.00000E+00
1954	1.44279	0.00000E+00	2054	1.44954	0.00000E+00	2154	1.45721	0.00000E+00
1956	1.44274	0.00000E+00	2056	1.44954	0.00000E+00	2156	1.45718	0.00000E+00
1958	1.44294	0.00000E+00	2058	1.44970	0.00000E+00	2158	1.45734	0.00000E+00
1960	1.44333	0.00000E+00	2060	1.45003	0.00000E+00	2160	1.45750	0.00000E+00
1962	1.44324	0.00000E+00	2062	1.45028	0.00000E+00	2162	1.45784	0.00000E+00
1964	1.44315	0.00000E+00	2064	1.45050	0.00000E+00	2164	1.45762	0.00000E+00
1966	1.44301	0.00000E+00	2066	1.45065	0.00000E+00	2166	1.45742	0.00000E+00
1968	1.44300	0.00000E+00	2068	1.45079	0.00000E+00	2168	1.45713	0.00000E+00
1970	1.44366	0.00000E+00	2070	1.45105	0.00000E+00	2170	1.45723	0.00000E+00
1972	1.44325	0.00000E+00	2072	1.45111	0.00000E+00	2172	1.45712	0.00000E+00
1974	1.44365	0.00000E+00	2074	1.45111	0.00000E+00	2174	1.45718	0.00000E+00
1976	1.44350	0.00000E+00	2076	1.45148	0.00000E+00	2176	1.45709	0.00000E+00
1978	1.44367	0.00000E+00	2078	1.45253	0.00000E+00	2178	1.45679	0.00000E+00
1980	1.44380	0.00000E+00	2080	1.45259	0.00000E+00	2180	1.45674	0.00000E+00
1982	1.44409	0.00000E+00	2082	1.45272	0.00000E+00	2182	1.45660	0.24129E-04
1984	1.44394	0.00000E+00	2084	1.45263	0.00000E+00	2184	1.45611	0.75138E-04
1986	1.44430	0.00000E+00	2086	1.45274	0.00000E+00	2186	1.45635	0.12591E-03
1988	1.44429	0.00000E+00	2088	1.45325	0.00000E+00	2188	1.45640	0.18364E-03
1990	1.44444	0.00000E+00	2090	1.45361	0.00000E+00	2190	1.45641	0.22683E-03
1992	1.44484	0.00000E+00	2092	1.45402	0.00000E+00	2192	1.45620	0.21997E-03
1994	1.44452	0.00000E+00	2094	1.45395	0.00000E+00	2194	1.45616	0.29233E-03
1996	1.44465	0.00000E+00	2096	1.45380	0.00000E+00	2196	1.45667	0.32397E-03
1998	1.44493	0.00000E+00	2098	1.45353	0.00000E+00	2198	1.45619	0.36638E-03
2000	1.44490	0.00000E+00	2100	1.45419	0.00000E+00	2200	1.45665	0.46572E-03

Table 3. Continued

cm⁻¹	n	k	cm⁻¹	n	k	cm⁻¹	n	k
2202	1.45627	0.50639E-03	2302	1.45455	0.41327E-03	2402	1.46464	0.22354E-02
2204	1.45596	0.61810E-03	2304	1.45474	0.46646E-03	2404	1.46468	0.23230E-02
2206	1.45628	0.66815E-03	2306	1.45488	0.47849E-03	2406	1.46538	0.23533E-02
2208	1.45662	0.77472E-03	2308	1.45540	0.55001E-03	2408	1.46531	0.24080E-02
2210	1.45642	0.86938E-03	2310	1.45561	0.52371E-03	2410	1.46564	0.24917E-02
2212	1.45600	0.92334E-03	2312	1.45555	0.56082E-03	2412	1.46583	0.25626E-02
2214	1.45563	0.99361E-03	2314	1.45585	0.51967E-03	2414	1.46599	0.27044E-02
2216	1.45564	0.95717E-03	2316	1.45570	0.59367E-03	2416	1.46588	0.27426E-02
2218	1.45569	0.99863E-03	2318	1.45784	0.80116E-03	2418	1.46610	0.27554E-02
2220	1.45563	0.10138E-02	2320	1.45725	0.10557E-02	2420	1.46653	0.26585E-02
2222	1.45555	0.10107E-02	2322	1.45847	0.11452E-02	2422	1.46715	0.25402E-02
2224	1.45534	0.10392E-02	2324	1.45891	0.11062E-02	2424	1.46705	0.24323E-02
2226	1.45517	0.10197E-02	2326	1.46130	0.12788E-02	2426	1.46735	0.22658E-02
2228	1.45544	0.10150E-02	2328	1.46226	0.15396E-02	2428	1.46771	0.20766E-02
2230	1.45517	0.99150E-03	2330	1.46523	0.20171E-02	2430	1.46809	0.18620E-02
2232	1.45533	0.10724E-02	2332	1.47071	0.33513E-02	2432	1.46839	0.18119E-02
2234	1.45555	0.10628E-02	2334	1.48064	0.87290E-02	2434	1.46827	0.16995E-02
2236	1.45546	0.10552E-02	2336	1.49738	0.26109E-01	2436	1.46809	0.16053E-02
2238	1.45485	0.10686E-02	2338	1.51006	0.44467E-01	2438	1.46874	0.15359E-02
2240	1.45484	0.10589E-02	2340	1.46598	0.36651E-01	2440	1.46923	0.14644E-02
2242	1.45501	0.11032E-02	2342	1.43649	0.17085E-01	2442	1.46965	0.14474E-02
2244	1.45463	0.10917E-02	2344	1.43569	0.65742E-02	2444	1.47032	0.13951E-02
2246	1.45496	0.11829E-02	2346	1.43987	0.29677E-02	2446	1.47079	0.13786E-02
2248	1.45490	0.12551E-02	2348	1.44301	0.16580E-02	2448	1.47065	0.13797E-02
2250	1.45472	0.13730E-02	2350	1.44625	0.16874E-02	2450	1.47076	0.14305E-02
2252	1.45473	0.15125E-02	2352	1.44797	0.16761E-02	2452	1.47186	0.14512E-02
2254	1.45455	0.16489E-02	2354	1.44871	0.18592E-02	2454	1.47196	0.15774E-02
2256	1.45430	0.17405E-02	2356	1.45100	0.20212E-02	2456	1.47213	0.15947E-02
2258	1.45408	0.17001E-02	2358	1.45265	0.21351E-02	2458	1.47246	0.16481E-02
2260	1.45366	0.16299E-02	2360	1.45470	0.23959E-02	2460	1.47262	0.17913E-02
2262	1.45325	0.14707E-02	2362	1.45555	0.25572E-02	2462	1.47328	0.18825E-02
2264	1.45346	0.13174E-02	2364	1.45311	0.21802E-02	2464	1.47331	0.20068E-02
2266	1.45331	0.11458E-02	2366	1.45638	0.20676E-02	2466	1.47400	0.21238E-02
2268	1.45360	0.10586E-02	2368	1.45551	0.19089E-02	2468	1.47378	0.22285E-02
2270	1.45350	0.10658E-02	2370	1.45707	0.19758E-02	2470	1.47392	0.23151E-02
2272	1.45337	0.12604E-02	2372	1.45594	0.16557E-02	2472	1.47447	0.24461E-02
2274	1.45340	0.11877E-02	2374	1.45684	0.16461E-02	2474	1.47457	0.26110E-02
2276	1.45351	0.77199E-03	2376	1.45850	0.16062E-02	2476	1.47448	0.27712E-02
2278	1.45334	0.53575E-03	2378	1.45844	0.13795E-02	2478	1.47466	0.29533E-02
2280	1.45350	0.48979E-03	2380	1.45846	0.12833E-02	2480	1.47466	0.30887E-02
2282	1.45367	0.44616E-03	2382	1.45921	0.13106E-02	2482	1.47487	0.31981E-02
2284	1.45352	0.42170E-03	2384	1.46013	0.13009E-02	2484	1.47511	0.33784E-02
2286	1.45358	0.40863E-03	2386	1.46066	0.13621E-02	2486	1.47511	0.34682E-02
2288	1.45371	0.40328E-03	2388	1.46079	0.13534E-02	2488	1.47539	0.36428E-02
2290	1.45389	0.42430E-03	2390	1.46167	0.14512E-02	2490	1.47633	0.37596E-02
2292	1.45340	0.34765E-03	2392	1.46230	0.16314E-02	2492	1.47640	0.39296E-02
2294	1.45455	0.40913E-03	2394	1.46277	0.17572E-02	2494	1.47665	0.41402E-02
2296	1.45422	0.40852E-03	2396	1.46270	0.18735E-02	2496	1.47578	0.43422E-02
2298	1.45439	0.40355E-03	2398	1.46264	0.20033E-02	2498	1.47581	0.44398E-02
2300	1.45430	0.38905E-03	2400	1.46397	0.21466E-02	2500	1.47617	0.45561E-02

Table 3. Continued

cm⁻¹	n	k	cm⁻¹	n	k	cm⁻¹	n	k
2502	1.47600	0.47544E-02	2602	1.48032	0.42296E-02	2702	1.49883	0.90443E-02
2504	1.47619	0.48396E-02	2604	1.48057	0.41166E-02	2704	1.49957	0.91392E-02
2506	1.47606	0.49135E-02	2606	1.48012	0.40034E-02	2706	1.49984	0.90877E-02
2508	1.47624	0.50732E-02	2608	1.48020	0.39653E-02	2708	1.49966	0.90433E-02
2510	1.47648	0.50044E-02	2610	1.48135	0.39418E-02	2710	1.50028	0.89537E-02
2512	1.47631	0.50691E-02	2612	1.48192	0.38931E-02	2712	1.50092	0.90705E-02
2514	1.47611	0.50186E-02	2614	1.48161	0.39517E-02	2714	1.50198	0.95140E-02
2516	1.47613	0.50085E-02	2616	1.48223	0.39159E-02	2716	1.50229	0.99742E-02
2518	1.47637	0.50269E-02	2618	1.48275	0.39930E-02	2718	1.50316	0.10624E-01
2520	1.47646	0.49612E-02	2620	1.48293	0.41218E-02	2720	1.50383	0.11245E-01
2522	1.47690	0.49865E-02	2622	1.48345	0.42288E-02	2722	1.50381	0.11741E-01
2524	1.47636	0.49850E-02	2624	1.48406	0.43131E-02	2724	1.50475	0.12076E-01
2526	1.47727	0.50199E-02	2626	1.48408	0.44131E-02	2726	1.50490	0.12412E-01
2528	1.47745	0.51154E-02	2628	1.48393	0.45447E-02	2728	1.50501	0.12627E-01
2530	1.47748	0.52082E-02	2630	1.48396	0.45640E-02	2730	1.50442	0.13048E-01
2532	1.47745	0.53326E-02	2632	1.48442	0.45731E-02	2732	1.50524	0.13411E-01
2534	1.47729	0.54852E-02	2634	1.48451	0.45261E-02	2734	1.50550	0.13839E-01
2536	1.47747	0.56384E-02	2636	1.48426	0.44471E-02	2736	1.50547	0.14454E-01
2538	1.47769	0.58430E-02	2638	1.48474	0.43301E-02	2738	1.50623	0.15056E-01
2540	1.47778	0.59985E-02	2640	1.48531	0.43535E-02	2740	1.50604	0.15680E-01
2542	1.47777	0.61632E-02	2642	1.48605	0.44220E-02	2742	1.50567	0.16059E-01
2544	1.47727	0.61922E-02	2644	1.48596	0.45541E-02	2744	1.50493	0.16530E-01
2546	1.47664	0.62449E-02	2646	1.48597	0.45463E-02	2746	1.50455	0.17006E-01
2548	1.47704	0.61976E-02	2648	1.48651	0.46282E-02	2748	1.50435	0.17345E-01
2550	1.47659	0.60971E-02	2650	1.48706	0.47013E-02	2750	1.50373	0.17497E-01
2552	1.47681	0.59777E-02	2652	1.48712	0.46202E-02	2752	1.50438	0.17640E-01
2554	1.47711	0.58087E-02	2654	1.48756	0.46361E-02	2754	1.50436	0.17497E-01
2556	1.47656	0.55635E-02	2656	1.48732	0.46591E-02	2756	1.50247	0.17372E-01
2558	1.47628	0.54150E-02	2658	1.48789	0.44936E-02	2758	1.50363	0.17093E-01
2560	1.47661	0.52684E-02	2660	1.48783	0.44221E-02	2760	1.50349	0.16782E-01
2562	1.47608	0.50434E-02	2662	1.48817	0.43769E-02	2762	1.50339	0.16509E-01
2564	1.47636	0.48627E-02	2664	1.48881	0.42793E-02	2764	1.50394	0.16184E-01
2566	1.47666	0.47221E-02	2666	1.48967	0.42312E-02	2766	1.50356	0.15939E-01
2568	1.47741	0.46087E-02	2668	1.49063	0.42266E-02	2768	1.50313	0.15723E-01
2570	1.47742	0.45198E-02	2670	1.49151	0.42665E-02	2770	1.50358	0.15442E-01
2572	1.47788	0.44571E-02	2672	1.49158	0.42945E-02	2772	1.50445	0.15010E-01
2574	1.47805	0.43914E-02	2674	1.49151	0.43485E-02	2774	1.50361	0.14763E-01
2576	1.47810	0.43786E-02	2676	1.49228	0.44286E-02	2776	1.50330	0.14479E-01
2578	1.47933	0.44218E-02	2678	1.49298	0.46481E-02	2778	1.50564	0.14289E-01
2580	1.47883	0.44796E-02	2680	1.49337	0.48797E-02	2780	1.50541	0.14210E-01
2582	1.47881	0.44345E-02	2682	1.49524	0.51000E-02	2782	1.50765	0.14014E-01
2584	1.47874	0.45024E-02	2684	1.49600	0.54338E-02	2784	1.50831	0.13990E-01
2586	1.47879	0.44509E-02	2686	1.49531	0.57782E-02	2786	1.50883	0.13937E-01
2588	1.47892	0.44066E-02	2688	1.49689	0.62375E-02	2788	1.50848	0.14117E-01
2590	1.47895	0.43859E-02	2690	1.49732	0.66248E-02	2790	1.50929	0.14312E-01
2592	1.47984	0.43970E-02	2692	1.49740	0.70598E-02	2792	1.51098	0.14565E-01
2594	1.48003	0.44327E-02	2694	1.49846	0.74613E-02	2794	1.51111	0.14917E-01
2596	1.48011	0.44154E-02	2696	1.49950	0.79240E-02	2796	1.51265	0.15338E-01
2598	1.47937	0.43949E-02	2698	1.49925	0.82907E-02	2798	1.51248	0.15912E-01
2600	1.48036	0.43219E-02	2700	1.49894	0.87569E-02	2800	1.51372	0.16544E-01

Table 3. Continued

cm^{-1}	n	k	cm^{-1}	n	k	cm^{-1}	n	k
2802	1.51535	0.17328E-01	2902	1.52148	0.65147E-01	3002	1.46908	0.24744E-01
2804	1.51483	0.17929E-01	2904	1.51468	0.63658E-01	3004	1.47509	0.24353E-01
2806	1.51484	0.18535E-01	2906	1.51372	0.62154E-01	3006	1.47744	0.24273E-01
2808	1.51669	0.19156E-01	2908	1.51422	0.60977E-01	3008	1.48070	0.24347E-01
2810	1.51666	0.19766E-01	2910	1.51163	0.59861E-01	3010	1.48259	0.24714E-01
2812	1.51749	0.20151E-01	2912	1.51119	0.59075E-01	3012	1.48375	0.25033E-01
2814	1.51742	0.20720E-01	2914	1.51588	0.58606E-01	3014	1.48603	0.25342E-01
2816	1.51799	0.21260E-01	2916	1.51226	0.58308E-01	3016	1.48956	0.25794E-01
2818	1.51927	0.21982E-01	2918	1.51538	0.58397E-01	3018	1.49089	0.26196E-01
2820	1.51993	0.22682E-01	2920	1.51587	0.58524E-01	3020	1.49462	0.26779E-01
2822	1.52063	0.23472E-01	2922	1.51803	0.58785E-01	3022	1.49685	0.27445E-01
2824	1.52171	0.24464E-01	2924	1.51766	0.59074E-01	3024	1.49809	0.28164E-01
2826	1.52425	0.25621E-01	2926	1.51539	0.59456E-01	3026	1.49970	0.28581E-01
2828	1.52456	0.26827E-01	2928	1.51503	0.59606E-01	3028	1.50245	0.29352E-01
2830	1.52460	0.28043E-01	2930	1.51326	0.58897E-01	3030	1.50152	0.30241E-01
2832	1.52732	0.29450E-01	2932	1.50770	0.57137E-01	3032	1.50455	0.30940E-01
2834	1.52784	0.30979E-01	2934	1.50750	0.54728E-01	3034	1.50496	0.31967E-01
2836	1.52838	0.32427E-01	2936	1.50430	0.52398E-01	3036	1.50448	0.32618E-01
2838	1.53024	0.33948E-01	2938	1.50126	0.49785E-01	3038	1.50737	0.33246E-01
2840	1.52976	0.35501E-01	2940	1.50473	0.47311E-01	3040	1.50778	0.34386E-01
2842	1.53352	0.37402E-01	2942	1.50128	0.45169E-01	3042	1.51050	0.35357E-01
2844	1.53540	0.39099E-01	2944	1.50444	0.43390E-01	3044	1.51341	0.36411E-01
2846	1.53531	0.41024E-01	2946	1.50266	0.41380E-01	3046	1.51391	0.37348E-01
2848	1.53536	0.42930E-01	2948	1.50944	0.39946E-01	3048	1.51228	0.38177E-01
2850	1.53763	0.44676E-01	2950	1.51225	0.38668E-01	3050	1.51618	0.39407E-01
2852	1.53831	0.46582E-01	2952	1.51346	0.38427E-01	3052	1.51724	0.40447E-01
2854	1.53829	0.48128E-01	2954	1.52295	0.39175E-01	3054	1.51576	0.41571E-01
2856	1.54126	0.49765E-01	2956	1.53464	0.41566E-01	3056	1.51602	0.42732E-01
2858	1.54016	0.50815E-01	2958	1.54658	0.46303E-01	3058	1.51635	0.43738E-01
2860	1.53962	0.52217E-01	2960	1.55987	0.54674E-01	3060	1.51577	0.44874E-01
2862	1.54228	0.53610E-01	2962	1.57224	0.67711E-01	3062	1.51784	0.46154E-01
2864	1.54071	0.55462E-01	2964	1.58938	0.84170E-01	3064	1.51849	0.47774E-01
2866	1.54057	0.57425E-01	2966	1.59551	0.10143E+00	3066	1.52063	0.49325E-01
2868	1.54240	0.59473E-01	2968	1.60290	0.11651E+00	3068	1.52135	0.50407E-01
2870	1.54206	0.61230E-01	2970	1.58356	0.12702E+00	3070	1.52149	0.51782E-01
2872	1.54164	0.62368E-01	2972	1.56694	0.13088E+00	3072	1.51964	0.53146E-01
2874	1.53667	0.62964E-01	2974	1.53935	0.12811E+00	3074	1.52267	0.54589E-01
2876	1.53437	0.62663E-01	2976	1.51755	0.12036E+00	3076	1.52247	0.56305E-01
2878	1.53779	0.62641E-01	2978	1.48579	0.10928E+00	3078	1.51962	0.57819E-01
2880	1.53518	0.62566E-01	2980	1.47045	0.96716E-01	3080	1.52171	0.59330E-01
2882	1.53485	0.62849E-01	2982	1.45713	0.83080E-01	3082	1.52190	0.61198E-01
2884	1.53361	0.63588E-01	2984	1.45097	0.69932E-01	3084	1.52370	0.62469E-01
2886	1.53572	0.64409E-01	2986	1.44676	0.58575E-01	3086	1.52131	0.64027E-01
2888	1.53600	0.65547E-01	2988	1.44499	0.48967E-01	3088	1.52334	0.65810E-01
2890	1.53330	0.67056E-01	2990	1.44699	0.41300E-01	3090	1.52243	0.67334E-01
2892	1.53327	0.67684E-01	2992	1.44912	0.35643E-01	3092	1.52591	0.69040E-01
2894	1.53112	0.68457E-01	2994	1.45146	0.31387E-01	3094	1.52469	0.70202E-01
2896	1.52981	0.68421E-01	2996	1.45858	0.28547E-01	3096	1.52612	0.71638E-01
2898	1.52311	0.67427E-01	2998	1.46212	0.26716E-01	3098	1.52227	0.73792E-01
2900	1.52125	0.66384E-01	3000	1.46527	0.25388E-01	3100	1.51678	0.76091E-01

Table 3. Continued

cm^{-1}	n	k	cm^{-1}	n	k	cm^{-1}	n	k
3102	1.51935	0.77385E-01	3202	1.48439	0.16841E+00	3302	1.27521	0.16046E+00
3104	1.52259	0.79065E-01	3204	1.47985	0.17064E+00	3304	1.30139	0.16176E+00
3106	1.52421	0.80875E-01	3206	1.48746	0.17266E+00	3306	1.26327	0.15880E+00
3108	1.52180	0.83305E-01	3208	1.49828	0.17385E+00	3308	1.25000	0.15531E+00
3110	1.52391	0.84874E-01	3210	1.48794	0.17155E+00	3310	1.25222	0.15189E+00
3112	1.52291	0.86869E-01	3212	1.47750	0.17433E+00	3312	1.24213	0.14867E+00
3114	1.51868	0.88940E-01	3214	1.44682	0.17682E+00	3314	1.23153	0.14564E+00
3116	1.51795	0.90710E-01	3216	1.44749	0.17598E+00	3316	1.24724	0.14389E+00
3118	1.51515	0.92588E-01	3218	1.42849	0.17706E+00	3318	1.24688	0.14021E+00
3120	1.51792	0.94700E-01	3220	1.43111	0.17719E+00	3320	1.22547	0.13826E+00
3122	1.52301	0.96036E-01	3222	1.42861	0.17805E+00	3322	1.21716	0.13633E+00
3124	1.52019	0.97666E-01	3224	1.44311	0.17914E+00	3324	1.23427	0.13519E+00
3126	1.51787	0.98914E-01	3226	1.43194	0.17816E+00	3326	1.21633	0.13218E+00
3128	1.52265	0.10108E+00	3228	1.43556	0.17963E+00	3328	1.21344	0.12750E+00
3130	1.52728	0.10414E+00	3230	1.42260	0.18350E+00	3330	1.22105	0.12567E+00
3132	1.53023	0.10480E+00	3232	1.43210	0.18610E+00	3332	1.20736	0.12317E+00
3134	1.52721	0.10759E+00	3234	1.43086	0.18593E+00	3334	1.19661	0.12048E+00
3136	1.52494	0.10912E+00	3236	1.39207	0.18347E+00	3336	1.20689	0.11947E+00
3138	1.52701	0.11221E+00	3238	1.39718	0.18294E+00	3338	1.19505	0.11733E+00
3140	1.52012	0.11425E+00	3240	1.40325	0.18201E+00	3340	1.17122	0.11402E+00
3142	1.52391	0.11542E+00	3242	1.37662	0.18113E+00	3342	1.18356	0.11257E+00
3144	1.51535	0.11706E+00	3244	1.37564	0.18526E+00	3344	1.18909	0.10990E+00
3146	1.51992	0.11901E+00	3246	1.40996	0.18716E+00	3346	1.18105	0.10619E+00
3148	1.52546	0.12126E+00	3248	1.37388	0.18612E+00	3348	1.18712	0.10392E+00
3150	1.52532	0.12422E+00	3250	1.37501	0.18317E+00	3350	1.16610	0.10364E+00
3152	1.52309	0.12729E+00	3252	1.35219	0.18207E+00	3352	1.18307	0.10190E+00
3154	1.52318	0.12856E+00	3254	1.35467	0.18186E+00	3354	1.19808	0.98389E-01
3156	1.53528	0.13072E+00	3256	1.35982	0.18499E+00	3356	1.18619	0.95646E-01
3158	1.52372	0.13129E+00	3258	1.34865	0.18222E+00	3358	1.19588	0.94220E-01
3160	1.52638	0.13299E+00	3260	1.35222	0.18053E+00	3360	1.17193	0.92453E-01
3162	1.52969	0.13448E+00	3262	1.32313	0.18034E+00	3362	1.17802	0.89834E-01
3164	1.52264	0.13666E+00	3264	1.35120	0.18113E+00	3364	1.17926	0.88478E-01
3166	1.51835	0.13864E+00	3266	1.34138	0.18052E+00	3366	1.19463	0.87758E-01
3168	1.52832	0.14040E+00	3268	1.37250	0.18193E+00	3368	1.18099	0.85638E-01
3170	1.52770	0.14232E+00	3270	1.34109	0.18253E+00	3370	1.16738	0.83243E-01
3172	1.52146	0.14374E+00	3272	1.34178	0.18359E+00	3372	1.19056	0.81626E-01
3174	1.51916	0.14658E+00	3274	1.34127	0.18196E+00	3374	1.20646	0.79368E-01
3176	1.51897	0.14755E+00	3276	1.33593	0.18004E+00	3376	1.19160	0.77799E-01
3178	1.51806	0.15031E+00	3278	1.32014	0.17586E+00	3378	1.18992	0.75604E-01
3180	1.51134	0.15281E+00	3280	1.31310	0.17556E+00	3380	1.19717	0.74472E-01
3182	1.51859	0.15310E+00	3282	1.30479	0.17283E+00	3382	1.21631	0.72157E-01
3184	1.52015	0.15503E+00	3284	1.29222	0.17188E+00	3384	1.22012	0.70424E-01
3186	1.51998	0.15720E+00	3286	1.30484	0.17105E+00	3386	1.23132	0.69413E-01
3188	1.50683	0.15950E+00	3288	1.29793	0.17052E+00	3388	1.22849	0.67701E-01
3190	1.49941	0.16037E+00	3290	1.29719	0.17062E+00	3390	1.21399	0.65913E-01
3192	1.49868	0.16295E+00	3292	1.29568	0.17090E+00	3392	1.23551	0.64440E-01
3194	1.48756	0.16244E+00	3294	1.32206	0.16880E+00	3394	1.23661	0.62695E-01
3196	1.49298	0.16353E+00	3296	1.30546	0.16736E+00	3396	1.25221	0.61302E-01
3198	1.48053	0.16504E+00	3298	1.27356	0.16380E+00	3398	1.25551	0.59670E-01
3200	1.49899	0.16578E+00	3300	1.27039	0.16169E+00	3400	1.25918	0.58279E-01

Table 3. Continued

cm⁻¹	n	k	cm⁻¹	n	k	cm⁻¹	n	k
3402	1.26765	0.57381E-01	3502	1.35564	0.14794E-01	3602	1.39939	0.33768E-03
3404	1.26555	0.55275E-01	3504	1.35578	0.13649E-01	3604	1.39938	0.22196E-03
3406	1.28164	0.54190E-01	3506	1.35851	0.12798E-01	3606	1.40148	0.32575E-03
3408	1.28377	0.52993E-01	3508	1.35995	0.12319E-01	3608	1.40355	0.00000E+00
3410	1.29202	0.51581E-01	3510	1.36160	0.11200E-01	3610	1.40295	0.00000E+00
3412	1.28561	0.50035E-01	3512	1.36254	0.10800E-01	3612	1.40257	0.00000E+00
3414	1.29764	0.49040E-01	3514	1.36258	0.10376E-01	3614	1.40412	0.00000E+00
3416	1.30171	0.47612E-01	3516	1.36541	0.95640E-02	3616	1.40456	0.00000E+00
3418	1.30513	0.46369E-01	3518	1.36600	0.89585E-02	3618	1.40451	0.00000E+00
3420	1.30805	0.45515E-01	3520	1.36796	0.84092E-02	3620	1.40365	0.00000E+00
3422	1.31326	0.44103E-01	3522	1.36844	0.80994E-02	3622	1.40368	0.00000E+00
3424	1.31204	0.43416E-01	3524	1.36852	0.74628E-02	3624	1.40398	0.00000E+00
3426	1.31579	0.42537E-01	3526	1.37023	0.69681E-02	3626	1.40490	0.00000E+00
3428	1.30745	0.41926E-01	3528	1.37364	0.63071E-02	3628	1.41105	0.00000E+00
3430	1.31558	0.41563E-01	3530	1.37312	0.60151E-02	3630	1.40737	0.00000E+00
3432	1.32059	0.40282E-01	3532	1.37273	0.56096E-02	3632	1.40751	0.00000E+00
3434	1.31919	0.39759E-01	3534	1.37502	0.53692E-02	3634	1.40784	0.00000E+00
3436	1.32118	0.39089E-01	3536	1.37331	0.52147E-02	3636	1.40810	0.00000E+00
3438	1.32468	0.38282E-01	3538	1.37673	0.46534E-02	3638	1.40846	0.00000E+00
3440	1.32567	0.37201E-01	3540	1.37640	0.45195E-02	3640	1.40866	0.00000E+00
3442	1.32978	0.36421E-01	3542	1.37840	0.44892E-02	3642	1.40866	0.00000E+00
3444	1.32925	0.36093E-01	3544	1.37903	0.43671E-02	3644	1.40955	0.00000E+00
3446	1.33040	0.35488E-01	3546	1.37923	0.38113E-02	3646	1.41209	0.00000E+00
3448	1.33113	0.34704E-01	3548	1.37946	0.33534E-02	3648	1.41275	0.00000E+00
3450	1.33084	0.33916E-01	3550	1.38093	0.32667E-02	3650	1.41050	0.00000E+00
3452	1.33175	0.33391E-01	3552	1.38328	0.30807E-02	3652	1.41022	0.00000E+00
3454	1.33164	0.32831E-01	3554	1.38317	0.27804E-02	3654	1.41071	0.00000E+00
3456	1.33374	0.32083E-01	3556	1.38382	0.27287E-02	3656	1.41102	0.00000E+00
3458	1.33437	0.31523E-01	3558	1.38498	0.25612E-02	3658	1.41181	0.00000E+00
3460	1.33756	0.31251E-01	3560	1.38651	0.24085E-02	3660	1.41178	0.00000E+00
3462	1.33793	0.30491E-01	3562	1.38719	0.22565E-02	3662	1.41223	0.00000E+00
3464	1.33890	0.30095E-01	3564	1.38743	0.21031E-02	3664	1.41223	0.00000E+00
3466	1.33836	0.29482E-01	3566	1.38884	0.19018E-02	3666	1.41290	0.00000E+00
3468	1.33768	0.28668E-01	3568	1.38699	0.15503E-02	3668	1.41308	0.00000E+00
3470	1.34242	0.27832E-01	3570	1.38930	0.17237E-02	3670	1.41328	0.00000E+00
3472	1.34168	0.27030E-01	3572	1.39024	0.14321E-02	3672	1.41348	0.00000E+00
3474	1.34261	0.26107E-01	3574	1.39163	0.12871E-02	3674	1.41512	0.00000E+00
3476	1.34273	0.25517E-01	3576	1.39205	0.13220E-02	3676	1.41612	0.00000E+00
3478	1.34167	0.24945E-01	3578	1.39303	0.12034E-02	3678	1.41589	0.00000E+00
3480	1.34332	0.24175E-01	3580	1.39251	0.11605E-02	3680	1.41516	0.00000E+00
3482	1.34538	0.23048E-01	3582	1.39186	0.12321E-02	3682	1.41462	0.00000E+00
3484	1.34498	0.22095E-01	3584	1.39341	0.11087E-02	3684	1.41481	0.00000E+00
3486	1.34585	0.21543E-01	3586	1.39476	0.15476E-02	3686	1.41506	0.00000E+00
3488	1.34804	0.20578E-01	3588	1.39692	0.74304E-03	3688	1.41516	0.00000E+00
3490	1.34928	0.19689E-01	3590	1.39399	0.52248E-03	3690	1.41501	0.00000E+00
3492	1.34985	0.19067E-01	3592	1.39638	0.85576E-03	3692	1.41402	0.00000E+00
3494	1.35073	0.18266E-01	3594	1.39843	0.49431E-03	3694	1.41435	0.00000E+00
3496	1.35034	0.17222E-01	3596	1.39729	0.85345E-04	3696	1.41458	0.00000E+00
3498	1.35166	0.16414E-01	3598	1.39856	0.45884E-03	3698	1.41463	0.00000E+00
3500	1.35409	0.15502E-01	3600	1.39817	0.41061E-03	3700	1.41531	0.00000E+00

Table 3. Concluded

cm^{-1}	n	k	cm^{-1}	n	k	cm^{-1}	n	k
3702	1.41454	0.00000E+00	3802	1.42222	0.00000E+00	3902	1.43162	0.00000E+00
3704	1.41453	0.00000E+00	3804	1.42298	0.00000E+00	3904	1.43179	0.00000E+00
3706	1.41530	0.00000E+00	3806	1.42523	0.00000E+00	3906	1.43223	0.00000E+00
3708	1.41611	0.00000E+00	3808	1.42300	0.00000E+00	3908	1.43230	0.00000E+00
3710	1.41703	0.00000E+00	3810	1.42332	0.00000E+00	3910	1.43257	0.00000E+00
3712	1.41711	0.00000E+00	3812	1.42384	0.00000E+00	3912	1.43231	0.00000E+00
3714	1.41578	0.00000E+00	3814	1.42459	0.00000E+00	3914	1.43175	0.00000E+00
3716	1.41640	0.00000E+00	3816	1.42594	0.00000E+00	3916	1.43183	0.00000E+00
3718	1.41664	0.00000E+00	3818	1.42621	0.00000E+00	3918	1.43201	0.00000E+00
3720	1.41611	0.00000E+00	3820	1.42637	0.00000E+00	3920	1.43273	0.00000E+00
3722	1.41654	0.00000E+00	3822	1.42723	0.00000E+00	3922	1.43258	0.00000E+00
3724	1.41702	0.00000E+00	3824	1.42777	0.00000E+00	3924	1.43241	0.00000E+00
3726	1.41540	0.00000E+00	3826	1.42788	0.00000E+00	3926	1.43200	0.00000E+00
3728	1.41523	0.00000E+00	3828	1.42743	0.00000E+00	3928	1.43319	0.00000E+00
3730	1.41624	0.00000E+00	3830	1.42926	0.00000E+00	3930	1.43234	0.00000E+00
3732	1.41770	0.00000E+00	3832	1.42606	0.00000E+00	3932	1.43309	0.00000E+00
3734	1.41739	0.00000E+00	3834	1.42952	0.63039E-06	3934	1.43097	0.00000E+00
3736	1.41676	0.00000E+00	3836	1.42858	0.00000E+00	3936	1.43112	0.00000E+00
3738	1.41403	0.00000E+00	3838	1.42477	0.00000E+00	3938	1.43131	0.86806E-05
3740	1.41424	0.00000E+00	3840	1.42582	0.00000E+00	3940	1.43184	0.00000E+00
3742	1.41441	0.00000E+00	3842	1.42959	0.00000E+00	3942	1.43322	0.00000E+00
3744	1.41564	0.00000E+00	3844	1.43017	0.00000E+00	3944	1.43251	0.00000E+00
3746	1.41786	0.00000E+00	3846	1.42997	0.00000E+00	3946	1.43166	0.00000E+00
3748	1.41985	0.00000E+00	3848	1.43086	0.00000E+00	3948	1.43213	0.00000E+00
3750	1.42050	0.00000E+00	3850	1.43432	0.00000E+00	3950	1.43183	0.00000E+00
3752	1.41246	0.00000E+00	3852	1.43457	0.00000E+00	3952	1.43153	0.00000E+00
3754	1.41393	0.00000E+00	3854	1.42441	0.00000E+00	3954	1.43131	0.00000E+00
3756	1.41508	0.00000E+00	3856	1.43122	0.00000E+00	3956	1.43159	0.00000E+00
3758	1.41506	0.00000E+00	3858	1.43037	0.00000E+00	3958	1.43121	0.00000E+00
3760	1.41643	0.00000E+00	3860	1.43272	0.00000E+00	3960	1.43074	0.43029E-04
3762	1.41754	0.00000E+00	3862	1.43076	0.00000E+00	3962	1.43012	0.00000E+00
3764	1.41853	0.00000E+00	3864	1.43106	0.42718E-05	3964	1.43053	0.27431E-04
3766	1.41782	0.00000E+00	3866	1.43143	0.00000E+00	3966	1.43068	0.49585E-04
3768	1.41847	0.00000E+00	3868	1.43432	0.00000E+00	3968	1.43175	0.89829E-04
3770	1.41818	0.00000E+00	3870	1.43276	0.00000E+00	3970	1.43120	0.69974E-04
3772	1.41832	0.00000E+00	3872	1.43268	0.00000E+00	3972	1.43127	0.10458E-03
3774	1.41781	0.00000E+00	3874	1.43238	0.00000E+00	3974	1.43180	0.12671E-03
3776	1.41806	0.00000E+00	3876	1.43260	0.00000E+00	3976	1.43126	0.14087E-03
3778	1.41837	0.00000E+00	3878	1.43254	0.00000E+00	3978	1.43151	0.15120E-03
3780	1.41766	0.00000E+00	3880	1.43149	0.00000E+00	3980	1.43209	0.10794E-03
3782	1.41832	0.00000E+00	3882	1.43177	0.00000E+00	3982	1.43169	0.19380E-03
3784	1.41925	0.00000E+00	3884	1.43393	0.00000E+00	3984	1.43149	0.24609E-03
3786	1.41903	0.00000E+00	3886	1.42996	0.00000E+00	3986	1.43199	0.25805E-03
3788	1.41971	0.00000E+00	3888	1.43320	0.00000E+00	0	0.00000	0.00000E+00
3790	1.41971	0.00000E+00	3890	1.43478	0.00000E+00	0	0.00000	0.00000E+00
3792	1.41960	0.00000E+00	3892	1.43213	0.00000E+00	0	0.00000	0.00000E+00
3794	1.42014	0.00000E+00	3894	1.43192	0.00000E+00	0	0.00000	0.00000E+00
3796	1.42062	0.00000E+00	3896	1.43298	0.00000E+00	0	0.00000	0.00000E+00
3798	1.42113	0.00000E+00	3898	1.43253	0.00000E+00	0	0.00000	0.00000E+00
3800	1.42142	0.00000E+00	3900	1.43263	0.00000E+00	0	0.00000	0.00000E+00